

NASA Contractor Report 3226

NASA
CR
3226
c.1

LOAN COPY
AFW/TECHN
KIRTLAND AFB

0062028



TECH LIBRARY KAFB, NM

Dual Methods and Approximation Concepts in Structural Synthesis

Claude Fleury and Lucien A. Schmit, Jr.

GRANT NSG-1490
DECEMBER 1980

NASA



NASA Contractor Report 3226

Dual Methods and Approximation Concepts in Structural Synthesis

Claude Fleury and Lucien A. Schmit, Jr.
University of California, Los Angeles
Los Angeles, California

Prepared for
Langley Research Center
under Grant NSG-1490



National Aeronautics
and Space Administration

Scientific and Technical
Information Branch

1980

Preface

This report presents some major findings of a continuing research program entitled "Fundamental Studies of Methods for Structural Synthesis," sponsored by NASA Research Grant No. NSG-1490. The research effort reported herein was carried out in the Department of Mechanics and Structures at UCLA during the period from February 1978 to August 1979.

The ACCESS 3 computer program, which implements the new methods set forth in this report, is a research type computer program that was written by adding the dual formulation as well as the DUAL 1 and DUAL 2 maximization algorithms into the previously developed ACCESS 2 program. The ACCESS 3 computer program was delivered to the NASA Langley Research Center in June 1979. Dr. Claude Fleury carried primary responsibility for the development of ACCESS 3. Professor Lucien A. Schmit serves as principal investigator and Dr. J. Sobieski, of the NASA Langley Research Center, is the cognizant NASA Technical Officer for this research program.

The authors want to take this opportunity to express their gratitude to Dr. G.N. Vanderplaats of the NASA Ames Research Center for his cooperation and help in preparing the ACCESS 3 program for delivery to the NASA Langley Research Center. We also want to thank Deborah Haines of the Mechanics and Structures Department for her careful attention to detail in typing this report.

CONTENTS

LIST OF TABLES	viii
LIST OF FIGURES	xii
SUMMARY	1
1. INTRODUCTION.	5
2. PRIMAL AND DUAL APPROACHES TO STRUCTURAL SYNTHESIS.	9
2.1 Formulation of the Structural Synthesis Problem.	10
2.2 The Constrained Minimization Techniques.	14
2.2.1 The Primal Methods (Direct Approach).	15
2.2.2 The Penalization Methods (Transformation Approach).	16
2.2.3 The Linearization Methods (Indirect Approach)	17
2.2.4 The Multiplier Method	18
2.2.5 The Dual Methods in Convex Programming.	19
2.3 The Approximation Concepts Approach.	19
2.3.1 Reduction of the Problem Dimensionality	20
2.3.2 Linearization Process	21
2.3.3 Primal Solution Scheme.	23
2.4 Joining Approximation Concepts and Dual Formulation.	26
2.4.1 Primal and Dual Solution Schemes.	26
2.4.2 The Dual Method Formulation	29
2.5 Relations with the Optimality Criteria Approaches.	34
2.5.1 Conventional and Generalized Optimality Criteria.	35
2.5.2 The Constraint Gradients: Pseudo-Loads Versus Virtual Load Techniques	39
2.5.3 The Stress Constraints: Zero Versus First Order Approximations.	42

2.5.4	The Scaling of the Design Variables.	45
3.	DUAL METHODS FOR CONTINUOUS DESIGN VARIABLES	47
3.1	The Second Order Discontinuity Planes	47
3.2	Characteristics of the Dual Function-Continuous Case.	50
3.3	Dual 2 - Newton Type Maximizer.	51
4.	DUAL METHODS FOR DISCRETE DESIGN VARIABLES	57
4.1	The First Order Discontinuity Planes.	58
4.2	Characteristics of the Dual Function-Mixed Case	60
4.3	The Pure Discrete Case.	62
4.4	Construction of a Unique Ascent Direction	64
4.5	Dual 1 - Gradient Projection Type Maximizer	68
4.5.1	Direction Finding Process.	70
4.5.2	Restart of the Algorithm	74
4.5.3	Retrieval of the Primal Variables.	76
4.5.4	One Dimensional Maximization	80
5.	THE ACCESS 3 COMPUTER PROGRAM.	87
5.1	Scope of the ACCESS 3 Code.	88
5.2	Program Organization	93
6.	NUMERICAL EXAMPLES	97
6.1	10-Bar Truss (Problem 1).	97
6.1.1	Case A: Equality Constraints on Displacements	98
6.1.2	Case B: Pure Continuous Problem.	98
6.1.3	Case C through Case E: Assessment of DUAL 1.	100
6.1.4	Case F: Pure Discrete Problem.	100
6.2	25-Bar Truss (Problem 2).	101
6.2.1	Case A: Pure Continuous Problem	102

6.2.2	Case B through Case D: Pure Discrete Problems	103
6.3	72-Bar Truss (Problem 3)	104
6.4	63-Bar Truss (Problem 4)	105
6.5	Swept Wing Model (Problem 5)	109
6.5.1	Case A: Pure Continuous Problem	110
6.5.2	Case B: Pure Discrete Problem	112
6.6	Delta Wing Model (Problem 6)	112
6.6.1	Case A: Pure Continuous Problem	115
6.6.2	Case B: Mixed Continuous-Discrete Problem	117
7.	CONCLUSIONS	121
	REFERENCES	125
	TABLES	131
	FIGURES	185

List of Tables

Table 1	Alternate Paths After Solving ODM (Dual 1)	131
Table 2	Available Options for Natural Frequency Constraints	132
Table 3	Algorithm Options for Various Kinds of Problems	132
Table 4A	Definition of Problem 1: Planar 10-Bar Cantilever Truss (SI Units)	133
Table 4B	Definition of Problem 1: Planar 10-Bar Cantilever Truss (U.S. Customary Units)	134
Table 5A	Iteration History Data for Problem 1 (Case A) Planar 10-Bar Cantilever Truss (SI Units)	135
Table 5B	Iteration History Data for Problem 1 (Case A) Planar 10-Bar Cantilever Truss (U.S. Customary Units)	136
Table 6A	Final Designs for Problem 1 Planar 10-Bar Cantilever Truss (SI Units)	137
Table 6B	Final Designs for Problem 1 Planar 10-Bar Cantilever Truss (U.S. Customary Units)	138
Table 7A	Iteration History Data for Problem 1 (Cases B-F) Planar 10-Bar Cantilever Truss (SI Units)	139
Table 7B	Iteration History Data for Problem 1 (Cases B-F) Planar 10-Bar Cantilever Truss (U.S. Customary Units)	140
Table 8	Available Discrete Values for all Example Problems	141
Table 9A	Definition of Problem 2: 25-Bar Space Truss (SI Units)	142
Table 9B	Definition of Problem 2: 25-Bar Space Truss (U.S. Customary Units)	143
Table 10A	Iteration History Data for Problem 2 25-Bar Space Truss (SI Units)	144
Table 10B	Iteration History Data for Problem 2 25-Bar Space Truss (U.S. Customary Units)	145

List of Tables, continued

Table 11A	Final Designs for Problem 2	146
	25-Bar Space Truss (SI Units)	
Table 11B	Final Designs for Problem 2	147
	25-Bar Space Truss (U.S. Customary Units)	
Table 12A	Definition of Problem 3: 72-Bar Space Truss	148
	(SI Units)	
Table 12B	Definition of Problem 3: 72-Bar Space Truss	149
	(U.S. Customary Units)	
Table 13A	Iteration History Data for Problem 3	150
	72-Bar Space Truss (SI Units)	
Table 13B	Iteration History Data for Problem 3	151
	72-Bar Space Truss (U.S. Customary Units)	
Table 14A	Final Designs for Problem 3	152
	72-Bar Space Truss (SI Units)	
Table 14B	Final Designs for Problem 3	153
	72-Bar Space Truss (U.S. Customary Units)	
Table 15A	Definition of Problem 4: 63-Bar Space Truss	154
	(SI Units)	
Table 15B	Definition of Problem 4: 63-Bar Space Truss	155
	(U.S. Customary Units)	
Table 16A	Iteration History Data for Problem 4	156
	63-Bar Space Truss (SI Units)	
Table 16B	Iteration History Data for Problem 4	157
	63-Bar Space Truss (U.S. Customary Units)	
Table 17A	Final Designs for Problem 4	158
	63-Bar Space Truss (SI Units)	

List of Tables, continued

Table 17B	Final Designs for Problem 4	160
	63-Bar Space Truss (U.S. Customary Units)	
Table 18A	Definition of Problem 5: Swept Wing Model	162
	(SI Units)	
Table 18B	Definition of Problem 5: Swept Wing Model	163
	(U.S. Customary Units)	
Table 19A	Nodal Coordinates for Swept Wing Model (Problem 5)	164
	(SI Units)	
Table 19B	Nodal Coordinates for Swept Wing Model (Problem 5)	165
	(U.S. Customary Units)	
Table 20A	Applied Nodal Loading for Swept Wing Model (Problem 5)	166
	(SI Units)	
Table 20B	Applied Nodal Loading for Swept Wing Model (Problem 5)	167
	(U.S. Customary Units)	
Table 21A	Iteration History Data for Problem 5	168
	Swept Wing Model (SI Units)	
Table 21B	Iteration History Data for Problem 5	169
	Swept Wing Model (U.S. Customary Units)	
Table 22A	Final Designs for Problem 5	170
	Swept Wing Model (SI Units)	
Table 22B	Final Designs for Problem 5	171
	Swept Wing Model (U.S. Customary Units)	
Table 23A	Definition of Problem 6: Delta Wing Model	172
	(SI Units)	
Table 23B	Definition of Problem 6: Delta Wing Model	173
	(U.S. Customary Units)	
Table 24A	Nodal Coordinates for Delta Wing Model (Problem 6)	174
	(SI Units)	

List of Tables, continued

Table 24B	Nodal Coordinates for Delta Wing Model (Problem 6)	175
	(U.S. Customary Units)	
Table 25A	Fuel Mass Distribution for Delta Wing Model (Problem 6) . .	176
	(SI Units)	
Table 25B	Fuel Weight Distribution for Delta Wing Model (Problem 6) . .	177
	(U.S. Customary Units)	
Table 26A	Iteration History Data for Problem 6	178
	Delta Wing Model	
	(SI Units)	
Table 26B	Iteration History Data for Problem 6	179
	Delta Wing Model	
	(U.S. Customary Units)	
Table 27A	Initial and Final Designs for Problem 6	180
	Delta Wing Model	
	(SI Units)	
Table 27B	Initial and Final Designs for Problem 6	181
	Delta Wing Model	
	(U.S. Customary Units)	
Table 28A	Final Webs Thicknesses for Problem 6	182
	Delta Wing Model	
	(SI Units)	
Table 28B	Final Webs Thicknesses for Problem 6	183
	Delta Wing Model	
	(U.S. Customary Units)	
Table 29	Detailed Iteration History Data for Problem 6	184
	Delta Wing Model-Mixed Case (DUAL 1)	

UNITS

All data and results presented in this report are given in SI or SI and U.S. Customary units (see A and B Tables, respectively). Unless otherwise noted, all inputs to and outputs from ACCESS 3 were in U.S. Customary units and the computations were executed on the IBM 360/91 at CCN, UCLA using a single precision version of the program.

List of Figures

Fig. 1	Key to a Tractable Formulation	185
Fig. 2	Design Space for 3-Bar Truss	186
Fig. 3	3-Bar Truss - Trajectories in Reciprocal Space	187
Fig. 4	3-Bar Truss - Convergence of Weight.	188
Fig. 5	Zero and First Order Approximations.	189
Fig. 6	Dual 2 Algorithm - Block Diagram	190
Fig. 7	Seek Max of $\ell(\vec{\lambda})$ in Subspace M	191
Fig. 8	Simple 2D Example - Pure Discrete Problem.	192
Fig. 9	Projecting Multiple Gradients into Discontinuity Plane . . .	193
Fig. 10	Dual 1 Algorithm - Block Diagram	194
Fig. 11	One Dimensional Maximization Scheme (Dual 1)	195
Fig. 12	Basic Organization of ACCESS 3	196
Fig. 13	Planar Ten-Bar Cantilever Truss (Problem 1).	197
Fig. 14	Iteration History for Problem 1 (Case B)	198
	Ten-Bar Cantilever Truss	
Fig. 15	25-Bar Space Truss (Problem 2)	199
Fig. 16	Iteration History for Problem 2 (Case A)	200
	25-Bar Space Truss	
Fig. 17	72-Bar Space Truss (Problem 3)	201
Fig. 18	Iteration History for Problem 3.	202
	72-Bar Space Truss	
Fig. 19	63-Bar Space Truss (Problem 4)	203
Fig. 20	Iteration History for Problem 4.	204
	63-Bar Space Truss	
Fig. 21	Swept Wing Analysis Model (Problem 5).	205
Fig. 22	Swept Wing Design Model (Problem 5).	206

Fig. 23	Iteration History for Problem 5	207
	Swept Wing Model	
Fig. 24	Delta Wing Analysis Model (Problem 6)	208
Fig. 25	Delta Wing Design Model (Problem 6)	209
Fig. 26	Iteration History for Problem 6	210
	Delta Wing Model	

SUMMARY

Approximation concepts and dual method algorithms are combined to create a new method for minimum weight design of structural systems. Approximation concepts convert the basic mathematical programming statement of the structural synthesis problem into a sequence of explicit primal problems of separable form. These problems are solved by constructing explicit dual functions, which are maximized subject to nonnegativity constraints on the dual variables. It is shown that the joining together of approximation concepts and dual methods can be viewed as a generalized optimality criteria approach. The dual method is successfully extended to deal with pure discrete and mixed continuous-discrete design variable problems. The power of the method presented is illustrated with numerical results for example problems, including a metallic swept wing and a thin delta wing with fiber composite skins.

In Chapter 1, a brief literature review is presented, with an outline of the historical background of the present work, namely, the rigor of the mathematical programming approach and the efficiency of the optimality criteria approach.

In Chapter 2, the structural synthesis problem considered is stated as a nonlinear programming problem. The constrained minimization methods available to solve this problem are briefly described. It is concluded that the well established approximation concepts approach can be interpreted as a mixed primal-linearization mathematical programming method. Indeed, the initial problem is transformed into a sequence of linearized problems, however each subproblem is solved partially using a primal method that

insures generation of a sequence of steadily improved feasible designs. In view of the high quality of the approximate problem statement, it is suggested that each explicit problem can be solved exactly, rather than partially. For that purpose, dual algorithms of convex programming are seen to be especially appropriate, because the number of dual variables, which are associated with the linearized behavior constraints, is generally much smaller than the number of design variables. This dual solution scheme, which no longer produces a sequence of always feasible designs, is then related to the optimality criteria techniques, in which basically the same explicit approximate form of the constraints is achieved by neglecting internal force redistribution.

It is shown in Chapter 3 that, when all the design variables are assumed to vary continuously, there are hyperplanes in the dual space where the second partial derivatives of the dual function exhibit discontinuity. Nevertheless, a 2nd order Newton type of maximization algorithm (called DUAL 2) can be devised that is especially well suited to the solution of the dual problem in the pure continuous case.

In Chapter 4, the dual method approach is extended to deal with discrete design variables, e.g., available cross-sectional areas of bars, available gauge sizes of sheet metal, the number of plies in a laminated composite skin, etc...When the primal structural synthesis problem involves discrete design variables, there are hyperplanes in the dual space where the first partial derivatives of the dual function exhibit discontinuity. Therefore a 1st order gradient projection type of maximization algorithm (called DUAL 1) is devised, that can accommodate the local discontinuities in gradient of the dual function. The DUAL 1 algorithm can handle problems involving a

mix of discrete and continuous design variables, as well as the two limiting special cases, namely the pure discrete case and the pure continuous case.

Chapter 5 is devoted to description of the ACCESS 3 computer program, where approximation concepts and dual methods are effectively combined to produce an efficient minimum weight structural design capability. The scope and organization of the ACCESS 3 code are successively described.

Finally detailed numerical results for various structural optimization problems are presented in Chapter 6. For pure continuous variable problems, the numerical results obtained with the DUAL 2 optimizer indicate that the improved analysis/synthesis capability developed by combining approximation concepts and dual methods is remarkably efficient. Computational effort expanded in the optimization portion of the program is reduced dramatically in representative examples and the number of reanalyses required to converge the overall optimization process is reduced significantly. Results for problems involving discrete design variables show that the DUAL 1 optimizer appears to have promise as a practical design tool. The collection of examples offered is made up of several well known truss test problems, a metallic swept wing and a thin delta wing with fiber composite skins.

1. INTRODUCTION

While the coupling together of finite element methods of structural analysis and mathematical programming techniques was first suggested in 1960 [see Ref. 1], computationally efficient practical capabilities such as those represented by the WIDOWAC [e.g., Refs. 2, 3, and 4] and the ACCESS [e.g., Refs. 5, 6 and 7] codes did not begin to emerge until the 1970's. During the late 1960's and early 1970's many investigators focused their efforts on constructing automated structural design procedures based on fully stressed design and discretized optimality criteria concepts [e.g. Refs. 8 through 17]. These efforts to create practical automated design for large scale structural systems culminated in the development of the ASOP and FASTOP computer programs [Refs. 12 and 18 through 24].

The main obstacles to the implementation of efficient mathematical programming based structural synthesis methods prior to 1970 were associated with the fact that the general formulation of the basic structural design problem involves: (1) large numbers of design variables; (2) large numbers of inequality constraints; (3) many inequality constraints that are computationally burdensome implicit functions of the design variables. The introduction of approximation concepts [Ref. 25] leading to a sequence of tractable approximate problems via the use of design variable linking (and/or basis reduction), temporary constraint deletion (regionalization and truncation), and the construction of high quality explicit approximations for retained constraints (intermediate variables and Taylor series expansion), has led to the emergence of mathematical programming based structural synthesis methods that are computationally efficient [e.g., Refs. 3 through 7].

The development of discretized optimality criteria methods usually involves: (1) derivation of a set of necessary conditions that must be satisfied at the optimum design; and (2) construction of an iterative redesign procedure that drives the initial trial design toward a design which satisfies the established necessary conditions. Design procedure based on optimality criteria generally entail two distinct types of approximations: (1) those associated with identifying how many and which constraints will be critical at the optimum design; and (2) those associated with development of the iterative redesign rule. As first noted in Ref. [26], the essential difficulties involved in applying optimality criteria methods to the general structural synthesis problem are those related to identifying the correct critical constraint set and the proper corresponding set of passive members [see also Refs. 15 and 17]. These difficulties were recognized and addressed with varying degrees of success in studies such as those reported in Refs. [27, 28 and 29]. However it was only with the advent of the dual formulation set forth in Refs. [30 and 31] that these obstacles were conclusively overcome. Introduction of the dual formulation resolves the essential difficulties inherent to the optimality criteria method because determining the critical constraint set and keeping track of the status of each design variable (active or passive) becomes an intrinsic part of the algorithm used to find the maximum of the dual function subject to nonnegativity constraints. In Ref. [32], the dual formulation is interpreted as a generalized optimality criteria method and it is shown to be well suited to the efficient solution of structural design optimization problems with relatively few critical constraints. In Refs. [33 and 34], the dual method is presented as a basis for the coalescing of the

mathematical programming and optimality criteria approaches to structural synthesis.

In this work, the approximation concepts approach to structural synthesis is combined with the dual method formulation to create a powerful new method for minimum weight design of structural systems. The dual method is successfully extended to deal with pure discrete and mixed continuous-discrete design variable problems. Approximation concepts are used to convert the general structural synthesis problem into a sequence of explicit primal problems of separable algebraic form. The dual method formulation, which exploits the separable form of each approximate problem, is used to construct a sequence of explicit dual functions. These dual functions are maximized subject to nonnegativity constraints on the dual variables. The efficiency of the method is due to the fact that the dimensionality of the dual space, where most of the optimization effort is expended, is relatively low^{*} for many structural optimization problems of practical interest. Furthermore, in the dual formulation the only inequality constraints are simple nonnegativity requirements on the dual variables.

In contrast to the interior point penalty function methods used in Refs. [2-4 and 5-7], the dual methods employed in this work capitalize upon the separable form of the approximate problem at each stage and instead of seeking a partial solution to each approximate problem, they seek a complete solution for each approximate problem. Therefore, at the end

^{*}The dimensionality of the dual maximization problem is primarily dependent on the number of critical behavior constraints.

of any stage, the design may not be strictly feasible, in which case scale up is needed to obtain a feasible design. The explicit dual methods presented in this work efficiently find the "exact" solution to each of the separable approximate problems generated in sequence. For the class of problems considered herein, the approximation concepts approach generates explicit constraint functions that are identical to those employed in conventional optimality criteria techniques [see Refs. 33 and 34]. Thus, in a sense, the joining together of approximation concepts and dual methods has led to the envelopment of the optimality criteria method within the general framework of the mathematical programming approach to structural optimization.

Use of trade names or names of manufacturers in this report does not constitute an official endorsement of such products or manufacturers, either expressed or implied, by the National Aeronautics and Space Administration.

2. PRIMAL AND DUAL APPROACHES TO STRUCTURAL SYNTHESIS

The structural synthesis problem considered in this work can be briefly stated as follows: minimize the weight of a finite element model of fixed geometry with limitations on the structural response (behavioral constraints) and on the design variables (side constraints).

The most natural and rigorous way of attacking this problem is to make use of mathematical programming methods. This approach will be reviewed in this chapter, with emphasis on the practically important property of preserving the feasibility of the design. It will be shown why strict application of the available mathematical programming techniques to the structural synthesis problem has invariably failed to produce fully satisfactory results and how this led to the emergence of a powerful and now well established design procedure based on approximation concepts.

The approximation concepts approach, as applied in this work, proceeds as follows:

- (1) construct an approximate problem by linearizing the behavioral constraints with respect to the reciprocal design variables;
- (2) partially solve the current explicit problem using a primal mathematical programming algorithm;
- (3) reanalyze the structure and update the approximate problem statement.

This process facilitates generation of a sequence of steadily improved feasible designs.

Pursuing further the approximation concepts idea, it can be argued that the approximate problem statement is of such high quality that it can be solved exactly, rather than partially, at each redesign stage. Adopting

this alternative viewpoint leads naturally to consideration of dual mathematical programming algorithms for solving the explicit problem. Indeed, the number of dual variables associated with the linearized behavioral constraints is generally very small when compared to the number of design variables.

This dual solution scheme, which no longer produces a sequence of always feasible designs, will be related to the well known optimality criteria techniques, in which basically the same explicit approximate problem is constructed by neglecting the internal force redistribution. The dual method approach, which can be viewed as a generalized optimality criteria approach, can handle large numbers of inequality constraints and it intrinsically contains a rational scheme for identifying the strictly critical constraints. Finally, the virtual load technique, the stress ratio algorithm and the scaling concept, widely employed in conventional optimality criteria techniques, will be investigated for possible use in conjunction with the dual method approach.

2.1 Formulation of the Structural Synthesis Problem

The structural synthesis problem considered in this work is restricted to the weight minimization of a finite element model with fixed geometry and material properties. The transverse sizes of the structural members (e.g. bar areas, shear panel and membrane thicknesses, etc...) are the design variables D_i . They are subjected to the side constraints

$$D_i^{(L)} \leq D_i \leq D_i^{(U)} ; \quad i = 1, 2, \dots, I \quad (2.1)$$

where $D_i^{(L)}$ and $D_i^{(U)}$ are lower and upper limits that reflect fabrication and analysis validity considerations. For the moment, all the design variables are assumed to be continuous, but later in this work, treatment of discrete

design variables will be included in the structural synthesis problem (see Chapter 4). The behavioral constraints impose limitations on quantities describing the structural response, for example, the stresses and the displacements under multiple static loading cases, the natural frequencies, etc... They can be written as nonlinear inequality constraints:

$$g_q(\vec{D}) \geq 0 ; q = 1, 2, \dots, Q \quad (2.2)$$

The number of inequality constraints Q is large since usually one behavioral constraint is associated with each failure mode (e.g. upper limit on deflection) in each load condition. The objective function to be minimized is the structural weight. It is a linear function of the design variables:

$$M(\vec{D}) = \sum_i^I m_i D_i \quad (2.3)$$

where m_i denotes the weight of the i^{th} member when $D_i = 1$ (i.e., specific weight times length of a bar truss member; specific weight times area of a membrane element).

In equations (2.1) through (2.3), it has been assumed that the vector of design variables \vec{D} contains one scalar component for each finite element in an idealized structural representation involving I finite elements. However it is neither necessary nor desirable for each finite element in the structural analysis model to have its own independent design variable. Design variable linking can be used to reduce the number of variables. As implemented in the ACCESS programs (see Refs. 5, 6 and 7), design variable linking simply fixes the relative size of some preselected group of finite elements, so that one independent design variable controls the size of all finite elements in that linking group. Hence the element sizes D_i (e.g., bar areas and sheet thicknesses) are linked to the independent reciprocal

variables α_b by the relation:

$$D_i = T_{ib(i)} \frac{1}{\alpha_{b(i)}} ; i = 1, 2, \dots, I \quad (2.4)$$

where $T_{ib(i)}$ is the linking table constant and $b(i)$ denotes an integer element of a pointer vector \vec{b} which, given the integer i , identifies the variable b to which the size of the element i is linked.

Reciprocal variables $\{\alpha_b; b = 1, 2, \dots, B\}$ are used as the independent variables after linking, because the behavior constraints are much more shallow in the space of the reciprocal variables. Indeed it is well known that the stresses and the displacements are strictly linear functions of the reciprocal design variables for a statically determinate structure. Therefore it is reasonable to expect that they remain nearly linear in case of redundancy. Linear approximation in terms of the α_b is the key idea of both the approximation concepts method and the optimality criteria techniques (see Sections 2.3 and 2.5).

Design variable linking reduces the number of design variables while facilitating the imposition of constraints that make the final design more realistic. Linking makes it possible to introduce constraints based on symmetry, prior design experience, fabrication and cost considerations associated with the number of parts to be assembled. Taking account of the linking relations given by Eq. (2.4), the weight objective function defined in Eq. (2.3) is written as follows in terms of the independent reciprocal variables α_b :

$$W = \sum_{i=1}^I m_i D_i = \sum_{b=1}^B \frac{w_b}{\alpha_b} \quad (2.5)$$

where the constant weight coefficients w_b are given by

$$w_b = \sum_{i \in b} m_i^T i_b(i) \quad (2.6)$$

Keeping in mind the linking relations, the structural synthesis problem, originally defined by Eqs. (2.1 through 2.3), can be concisely stated as a nonlinear mathematical programming problem of the following form:

Find the vector of independent reciprocal variables $\vec{\alpha}$ such that

$$w(\vec{\alpha}) = \sum_{b=1}^B \frac{w_b}{\alpha_b} \rightarrow \text{Min} \quad (2.7)$$

subject to behavioral constraints

$$h_q(\vec{\alpha}) \geq 0 \quad ; \quad q = 1, 2, \dots, Q \quad (2.8)$$

and side constraints

$$\alpha_b^{(L)} \leq \alpha_b \leq \alpha_b^{(U)} \quad ; \quad b = 1, 2, \dots, B \quad (2.9)$$

Standard minimization techniques have been applied with varying degrees of success to the nonlinear programming problem embodied in Eqs. (2.7 through 2.9). However this problem exhibits some characteristics that make it complicated when practical structural design applications are considered. The main difficulty arises from the fact that the $h_q(\vec{\alpha})$ appearing in Eq. (2.8) are in general implicit functions of the design variables and their precise numerical evaluation for a particular design $\vec{\alpha}$ requires a complete finite element analysis. Since the solution scheme is essentially iterative, it involves a large number of structural reanalyses. Therefore the computational cost often becomes prohibitive when large structural systems are dealt with.

2.2 The Constrained Minimization Techniques

The structural synthesis problem stated in Section 2.1 is a nonlinear mathematical programming problem for which a wide variety of solution methods are available. Before describing briefly these various constrained minimization techniques, it is worthwhile mentioning that all of them seek a local optimum, which must necessarily satisfy the following first order KUHN-TUCKER conditions [see Ref. 35]:

$$\frac{\partial W}{\partial \alpha_b} - \sum_{q=1}^Q \lambda_q \frac{\partial h_q}{\partial \alpha_b} - \mu_b + v_b = 0 \quad ; \quad b = 1, B \quad (2.10)$$

$$\lambda_q h_q = 0 \quad \lambda_q \geq 0 \quad ; \quad q = 1, Q \quad (2.11)$$

$$\mu_b (\alpha_b - \alpha_b^{(L)}) = 0 \quad \mu_b \geq 0 \quad ; \quad b = 1, B \quad (2.12)$$

$$v_b (\alpha_b^{(U)} - \alpha_b) = 0 \quad v_b \geq 0 \quad ; \quad b = 1, B \quad (2.13)$$

The quantities $\{\lambda_q; q=1, Q\}$, associated with the behavioral constraints (Eq. 2.8), and $\{\mu_b, v_b; b=1, B\}$, associated with the side constraints (Eq. 2.9), are called dual variables. They have the meaning of Lagrangian multipliers conjugated to the constraints. Depending upon whether a given constraint becomes an equality or not at the optimum (i.e., is active or inactive), the corresponding dual variable is positive or equal to zero. The KUHN-TUCKER relations embodied in Eqs. (2.10 - 2.13) are in general necessary conditions for local optimality. In the special case of a convex problem, they become sufficient conditions for global optimality. They can then be used to relate the primal variables - i.e., design variables - to the dual variables - i.e., Lagrangian multipliers -.

The classification of the constrained minimization techniques given

in the sequel is of course not the only one possible. However it is convenient for organizing the discussion of the solution algorithms that have been applied to the structural optimization problem stated in Eqs. (2.7 - 2.9). This classification also shows clearly why the strategy recommended in the present work - combination of approximation concepts and dual methods - emerges as one of the best approaches available at this time.

2.2.1 The Primal Methods (Direct Approach)

The well known and widely used direct constrained minimization techniques employ a sequence of search directions in the space of the primal variables, such that the constraints remain satisfied and that the objective function is minimized along each search direction. They are thus very similar to the unconstrained minimization techniques such as steepest descent, conjugate gradient etc..., where a sequence of one dimensional minimizations are carried out. Essentially two kinds of algorithms belong in this category: the feasible direction methods and the projection methods. They have been very popular in the structural synthesis field [see Refs. 36-39], mainly because they generate a sequence of feasible designs with decreasing structural weight. Even when the optimization process is terminated before convergence has been achieved, a practical and meaningful design, better than the initial one, is generally obtained.

Since the direct constrained minimization techniques start from a feasible design and gradually improve it by working on the primal variables, they are often referred to as "primal" methods [see Ref. 40]. Although this appellation could sometimes be ambiguous, it is very convenient, and throughout this work, a primal solution scheme will denote one in which the design is continuously improved while remaining feasible. It will be seen subse-

quently that not only the direct constrained minimization methods - feasible direction and projection algorithms - enjoy this important "primal" property.

2.2.2 The Penalty Function Methods (Transformation Approach)

The main drawback of the primal methods arises from the special treatment of the constraints they require. Except in the simple case where the constraints are linear, keeping them satisfied is an arduous task which always demands a sophisticated algorithm.

In an attempt to circumvent these difficulties, penalty function methods have been introduced that transform the original problem in a sequence of unconstrained problems, by adding to the objective function a penalty term reflecting the degree of non-satisfaction of the constraints. The exterior point penalty function formulation leads to generation of a sequence of infeasible designs and therefore it has received relatively little attention in structural synthesis applications [see Ref. 41]. The interior point penalty function methods - or barrier methods - are especially attractive since they yield a sequence of feasible points corresponding to decreasing values of the objective function. Such a formulation clearly adheres to a primal philosophy. The only difference is that strict primal methods - projection and feasible direction algorithms - produce boundary points (critical designs), while barrier methods generate interior points (noncritical designs). In the context of structural synthesis, this kind of method was used in Refs. [42-44].

It is worth mentioning that the primal and penalty methods have exhibited rather poor convergence properties when applied to structural optimization problems. They require a large number of iterations, each involving at least one reanalysis of the structure. Moreover the number

of iterations grows with the number of design variables. That troublesome trend led many investigators to believe that the mathematical programming approach to structural synthesis would not work for large practical systems [see Ref. 45]. This viewpoint fails to recognize that the primal and penalty methods are only a subset of the mathematical programming techniques available.

2.2.3 The Linearization Methods (Indirect Approach)

Probably the simplest approach to a nonlinear programming problem is to transform it into a sequence of linear programming problems. Each iteration consists of linearizing the objective function and the constraints at the current design point and solving the resulting linear problem. Applied as such this technique usually fails because it tends to converge to a vertex in the design space or indefinitely oscillate between two vertices [see Refs. 46 and 47]. By introducing move limits, which restrain the range of the design variables to the neighborhood around the point where the linearization is made, the method of approximation programming is able to overcome these drawbacks and, though very simple, constitutes one of the most powerful and versatile optimization techniques currently available [see Refs. 48 and 49].

In contrast with the primal and barrier methods, the linearization methods do not maintain the feasibility of the design point at each iteration[†]. On the other hand, their convergence properties are not related to the number of design variables, but to the degree of nonlinearity of the problem. This is a much more attractive dependence for structural synthesis

[†]An exception is the method of inscribed hyperspheres [see Refs. 25]. This special linearization technique usually generates a sequence of feasible designs.

applications.

2.2.4 The Multiplier Method

The multiplier method, which has enjoyed considerable popularity in recent years, has not yet been extensively applied to structural synthesis and it is mentioned in this classification only for the sake of completeness [see Ref. 50 for more details]. The multiplier method is a general purpose mathematical programming method whose algorithmic philosophy is similar to the usual exterior quadratic penalty function formulation, in that a constrained nonlinear programming problem is transformed into a sequence of unconstrained minimization problems. The penalty term is added to the Lagrangian function, rather than simply to the objective function, so that the multiplier method is sometimes referred to as the "augmented Lagrangian function method." The updated Lagrangian multiplier estimates at each stage are used to accelerate the overall optimization process. An attractive feature of the multiplier method is that each unconstrained minimization problem tends to be well behaved, which is a significant improvement over conventional penalty function methods. When the Lagrangian multipliers are regarded as the dual variables, the method can be viewed as seeking a saddle point by working alternatively in the primal and dual spaces. Therefore the multiplier method is also called a "primal-dual method." In its usual implementation the algorithm tends to generate a sequence of infeasible designs, like the regular exterior penalty function method.

The method was applied in Ref. [50] to optimum design of truss structures considering both configuration and sizing type design variables.

2.2.5 The Dual Methods in Convex Programming

All the previously mentioned methods are quite general and they can be applied to obtain a local optimum for any nonlinear programming problem. In the special but important case of a convex problem, it is well known that every local optimum is also global. Furthermore the Lagrangian multipliers associated with the constraints have the meaning of dual variables in terms of which an auxiliary and equivalent problem can be stated. Under some unrestrictive conditions, this dual problem can be reduced to the maximization of the Lagrangian functional with simple nonnegativity requirements on the dual variables. If, in addition, the problem is separable, the dual formulation leads to a very efficient solution scheme since each primal variable can be independently expressed in terms of the dual variables.

As the present work seeks to point out, dual methods should play an important role in the structural synthesis field. Used in conjunction with a special linearization technique - the approximation concepts approach reviewed in the next section - they facilitate creation of a powerful structural synthesis method. This method is, in its own right, a mathematical programming approach, as usually defined, but it can also be viewed as a generalized optimality criteria approach.

2.3 The Approximation Concepts Approach

As described in the previous section the use of primal and barrier methods had only a limited success in structural synthesis due to their prohibitive cost when large numbers of design variables were considered [see for example Refs. 36 and 37]. On the other hand, recourse to pure linearization methods, with or without move limits, failed to be efficient

because the behavioral constraints, expressed in terms of direct sizing variables, exhibit a rather high degree of nonlinearity.

It is then not surprising that the combined use of a primal philosophy and of linearization techniques (using reciprocal variables) has finally led to a very efficient method, known as the "approximation concepts approach" (see Refs. 5,6,7 and 25). Briefly stated this approach replaces the initial problem with a sequence of approximate - but explicit and tractable - problems while retaining the important features of the primary problem. This is achieved through the coordinated use of various approximation concepts:

- (1) design variable linking;
- (2) temporary deletion of unimportant constraints;
- (3) generation of high quality explicit approximations
for the surviving behavioral constraints.

2.3.1 Reduction of the Problem Dimensionality

Design variable linking, previously described in Section 2.1, leads to a significant reduction in the number of independent variables, which helps make the initial structural synthesis problem described by Eqs. (2.1 through 2.3) more tractable. Similarly, constraint deletion techniques are used to decrease the large number of behavioral constraints usually embodied in Eqs. (2.8) (see Ref. 5, Sections 2.4.1, 2.4.2, and 2.4.3.). These constraint deletion techniques are nothing more than the computer implementation of traditional design practice. At the beginning of each stage in the iterative design procedure a complete finite element structural analysis is executed and all of the constraints (see Eq. 2.8) are evaluated.

Constraint deletion techniques are then used to temporarily ignore redundant and unimportant constraints. Let the relatively small set of surviving constraints for the p^{th} stage be denoted by $Q_R^{(p)} \in Q$. The constraints retained during the p^{th} stage of the design procedure, as a function of the independent reciprocal design variables after linking (α_b), are represented by

$$h_q(\vec{\alpha}) \geq 0 ; \quad q \in Q_R^{(p)} \in Q \quad (2.14)$$

As a result of constraint deletion only the critical and potential critical constraints (design drivers) are considered during the p^{th} stage of the iterative design process. It is important to understand that at the beginning of each stage in the design process, the status of all of the constraints in the set Q is assessed and the subset of constraints to be retained is re-established. Thus constraints that are ignored during an early stage may appear during a later stage if they become design drivers.

It is worth noticing that, while design variable linking leads to reducing the number of primal variables in the structural synthesis problem, constraint deletion techniques result in a decrease in the number of dual variables. The net result is to reduce the dimensionality of the problem in both its primal and dual forms.

2.3.2 Linearization Process

The most important feature of the approximation concepts approach lies in the construction of simple explicit expressions for the set of constraints retained during each stage. This is achieved by using linearization of these constraints with respect to the linked reciprocal design variables α_b . At each stage p , the following explicit approximate problem - referred to as the "linearized problem" - is thus generated:

✓ The notations Q (or Q_R) are used to represent either the number of behavioral constraints (retained) or the set of indexes q corresponding to these constraints.

Find $\vec{\alpha}$ such that

$$W(\vec{\alpha}) = \sum_{b=1}^B \frac{w_b}{\alpha_b} \rightarrow \text{Min} \quad (2.15)$$

subject to

$$\tilde{h}_q^{(p)}(\vec{\alpha}) \geq 0 \quad ; \quad q \in Q_R^{(p)} \quad (2.16)$$

$$\alpha_{bp}^{(L)} \leq \alpha_b \leq \alpha_{bp}^{(U)} \quad ; \quad b = 1, B \quad (2.17)$$

where $W(\vec{\alpha})$ is the weight objective function, $\tilde{h}_q^{(p)}(\vec{\alpha})$ represents the linearized form of the q^{th} constraint function constructed at the beginning of the p^{th} stage, $Q_R^{(p)}$ denotes the reduced set of constraints to be retained during the p^{th} stage, $\alpha_{bp}^{(L)}$ and $\alpha_{bp}^{(U)}$, respectively, represent the lower and upper move limits for the p^{th} stage.

The objective function (Eq. 2.15) does not need to be linearized, since it is an exact explicit function of the α_b . The linearized behavior constraints (Eq. 2.16) are obtained using a first order Taylor series expansion in terms of the reciprocal variables[†]:

$$h_q(\vec{\alpha}) \approx \tilde{h}_q^{(p)}(\vec{\alpha}) = h_q(\vec{\alpha}_p) + \sum_{b=1}^B (\alpha_b - \alpha_b^{(p)}) \frac{\partial h_q}{\partial \alpha_b}(\vec{\alpha}_p) \quad ; \quad q \in Q_R^{(p)} \quad (2.18)$$

where $\vec{\alpha}_p$ and $\alpha_b^{(p)}$ denote the design at the beginning of the p^{th} stage in vector and scalar form respectively. The side constraints defined by Eqs. (2.17) arise from the original side constraints expressed in

[†]Note that the finite element analysis must include auxiliary sensitivity analyses, which evaluate first partial derivatives of approximate response quantities.

Eq. (2.9), but they can be modified at each stage p to include move limits which restrict the design modifications, during the p^{th} stage, to a region in the $\vec{\alpha}$ space over which the linearized expressions of the constraint functions in Eq. (2.18) are accurate enough to guide the design improvement process.

In summary, then, design variable linking, constraint deletion techniques and linearization of the behavior constraints retained are used to generate a sequence of relatively small explicit mathematical programming problems which retain the essential features of the primary structural synthesis problem stated in equations (2.1), (2.2) and (2.3). This use of approximation concepts as the key to generating tractable approximate problems is summarized schematically in Fig. 1. In the p^{th} stage, the original problem, expressed in terms of the linked reciprocal design variables (see Eqs. 2.7, 2.8 and 2.9), is replaced with its linearized form at the current design point $\vec{\alpha}_p$ (Eqs. 2.15 through 2.18). Except for the fact that the explicit objective function is not linearized, the approximation concepts approach proceeds therefore as a classical linearization method in mathematical programming (see Section 2.2.3). It should be recognized that while recourse to the reciprocal variables α_p is initially motivated by the observation that the linearized forms of static stress and displacement constraints are exact for a statically determinate structures, a more analytic justification is also available (see Section 2.5.4 and Fig. 5).

2.3.3 Primal Solution Scheme

The linearized problem stated in Eqs. (2.15 through 2.18) is still a nonlinear mathematical programming problem, because of the nonlinear

objective function, but it is now explicit and easily treated by standard minimization techniques. In order to maintain a primal philosophy (sequence of steadily improved feasible designs), the approximation concepts approach, as initially proposed in Ref. [5], employed either a feasible direction method or an interior penalty function method to solve the linearized problem. In this way, it was possible to solve it only partially and to preserve, at each stage of the process, the feasibility of the design point with respect to the primary problem (Eqs. 2.7-2.9). In addition, the minimization algorithms were designed to permit introduction, in the approximate problem statement, of more sophisticated explicit constraints than the simple linear constraints of Eq. (2.18), such as spherical displacement constraints, second order Taylor series expansions, etc.

In the ACCESS-1 computer program [Ref. 5], two distinct optimizer options were available: (1) CONMIN - a general purpose optimizer based on a modified feasible direction method [see Ref. 51] and (2) NEWSUMT 1 - a sequence of unconstrained minimization techniques based on the linear extended interior penalty function formulation of Ref. [43] and a modified Newton method minimizer introduced in Ref. [2]. Subsequently the ACCESS-2 program [see Ref. 7] employed an improved optimization scheme called NEWSUMT 2, based on the quadratic extended penalty function set forth in Ref. [3]. NEWSUMT 2 uses a rational method for determining a suitable transition parameter [see Ref. 52]. This new optimizer is capable, for moderately infeasible designs, of guiding the design back to the feasible region. It is worth noticing that, when starting from a feasible interior point, the NEWSUMT optimizers tend to generate a sequence of designs that "funnel down the middle" of the feasible region. This represents an

attractive feature in the context of approximation concepts and from an engineering point of view.

On the other hand, starting from an optimality criteria approach, a method similar to the approximation concepts approach was independently initiated in Ref. [53]. Using virtual load considerations, a first order approximate problem is generated, which is identical to the linearized problem posed by Eqs. (2.15 - 2.18). This problem is also solved partially using a primal solution scheme, with the aim of preserving the design feasibility, as in the approximation concepts approach. However, the method is less general since it relies on first or second order projection algorithms restricted to the case of linear constraints. The first order algorithm is very similar to the well known gradient projection method. The second order algorithm uses a weighed projection operator to generate a sequence of Newton's search directions that are constrained to reside in the subspace defined by the set of active constraint hyperplanes. A partial solution of the linearized problem is obtained by prescribing an upper limit on the number of one dimensional minimizations performed before updating the explicit problem statement [see Refs. 54 and 55].

In summary, the approximation concepts approach can be classified as a mixed primal-linearization method. The initial problem is transformed into a sequence of linearized problems, which is classical in the mathematical programming linearization methods. However each subproblem is solved using a primal solution scheme that insures feasibility of the intermediate designs at each stage.

2.4 Joining Approximation Concepts and Dual Formulation

2.4.1 Primal and Dual Solution Schemes

A partial solution of the current explicit problem (Eqs. 2.15 - 2.18) reduces the weight while maintaining feasibility with respect to the constraints. An exact solution of the current explicit problem finds the minimum weight, subject to the constraints, recognizing that one or more of the constraints will be critical at the solution.

So far a primal philosophy has been adopted that leads only to partial solution of the linearized problem (Eqs. 2.15 through 2.18), using for example an interior point penalty function formulation with only a small number of response surfaces (typically 1 or 2) and a rather high response factor decrease ratio (typically 0.5). A structural reanalysis is then performed, the linearized problem is reformed and again solved partially. This primal solution scheme produces a sequence of feasible designs with decreasing values of the structural weight, an attractive feature of practical interest to the designer.

An alternative viewpoint is to recognize that the approximation made by linearizing the constraints with respect to the reciprocal design variables is of such high quality that the current explicit problem can be solved exactly, and not partially, after each structural reanalysis. This idea leads to abandoning the primal philosophy in favor of a pure linearization approach.[†]

In order to illustrate this concept consider the classical 3 bar truss shown in Fig. 2. By symmetry only 2 design variables define the

[†]It should be noted that in conventional linearization methods the objective function is also linearized. This is not the case in the present work.

problem which therefore admits the simple geometrical representation shown in Fig. 2 in the space of the direct design variables. The behavioral constraints consist of tensile and compressive stress limits and the side constraints reduce to non-negativity of the bar cross-sectional areas. At the optimum only one constraint is active (tensile stress in member 1); the associated constraint surface is tangent to a constant weight plane ($W = 0.074$ kg). This problem has been solved using the approximation concepts approach with a penalty function formulation using the ACCESS 3 program. Three different couples of values have been successively adopted for the response factor decrease ratio and the number of response surfaces: (0.5×1) , (0.3×2) and (0.1×3) . Thus increasingly exact solutions are generated for each linearized problem and the approximation concepts approach gradually changes from a pure primal method, with partial solution of the explicit problem, to a pure linearization technique, with complete solution of the explicit problem. The trajectory of the design point toward the optimum is shown for each case in Fig. 3, the space of the reciprocal variables, where the constraints are linearized. The approximation concepts approach, as initially formulated, leads to a sequence of interior points; the trajectory "funnels down the middle" of the feasible region. On the other hand, forgetting the primal philosophy by solving almost exactly each explicit approximate problem produces a trajectory very close to the boundary of the feasible region (see Fig. 3). The convergence curves of the weight with respect to the number of structural reanalyses are represented on Fig. 4 for the three previously mentioned cases. The benefit gained from a complete solution of each linearized problem is clearly illustrated.

Once a primal philosophy is abandoned in favor of a pure linearization approach, any minimization algorithm can be chosen to solve the explicit approximate problem posed by Eqs. (2.15-2.18) since only its final exact solution needs to be known at each redesign stage. In order to improve the computational efficiency it is advisable to select a specialized nonlinear programming algorithm, well suited to the particular mathematical structure of the explicit problem. The objective function is strictly convex and all the constraints are linear, so that the problem is a convex programming problem. Moreover all the functions involved in this problem are explicit and separable. In such a case the dual method formulation is attractive, because the dual problem presents a much simpler form than the primal problem (see Section 2.2.5).

Numerical experiments and engineering practice indicate that the number of strictly critical behavioral constraints is most often small when compared to the number of independent design variables. That is the reason why the convex, separable problem stated in Eqs. (2.15-2.18) can be very efficiently handled with the dual methods of convex programming, in which the variables become the Lagrangian multipliers (or dual variables) associated with the linearized constraints (Eq. 2.16). Therefore the dimensionality of the dual problem is much lower than that of the original - or primal - problem. The dual methods are thus likely to provide the most efficient solution scheme to the linearized problem, provided the original behavioral constraints are not too nonlinear in the reciprocal variables. This is actually true for most problems involving stress, displacement, frequency and buckling constraints [see Ref. 56]. The extension to more sophisticated constraints - such as flutter and time parametric

dynamic responses - remains to be proven feasible.

Another important advantage of the dual methods is that they allow, without weakening the efficiency of the optimization process, the introduction of discrete design variables, e.g., available cross-sectional areas of bars, available gage sizes of sheet metal, the number of plies in a laminated composite skin, etc.. (see Chapter 4). Finally a philosophically important feature of the dual formulation lies in its interpretation as a generalized optimality criteria approach (see Section 2.5).

2.4.2 The Dual Method Formulation

For the purpose of forming the explicit dual function it will be convenient to restate the primal problem at the p^{th} stage as follows (see Eqs. 2.15-2.18):

Find $\vec{\alpha}$ such that

$$W(\vec{\alpha}) = \sum_{b=1}^B \frac{w_b}{\alpha_b} \rightarrow \text{Min} \quad (2.19)$$

subject to linear constraints

$$\tilde{h}_q(\vec{\alpha}) = \bar{u}_q - u_q(\vec{\alpha}) \geq 0 \quad ; \quad q \in Q_R \quad (2.20)$$

where

$$u_q(\vec{\alpha}) = \sum_{b=1}^B c_{bq} \alpha_b \quad ; \quad q \in Q_R \quad (2.21)$$

and the side constraints are written separately:

$$\alpha_b^{(L)} \leq \alpha_b \leq \alpha_b^{(U)} \quad ; \quad b = 1, B \quad (2.22)$$

The w_b in Eq. (2.19) are positive fixed constants (see Eq. 2.6) corresponding to the weight of the set of elements in the b^{th} linking group when $\alpha_b = 1$. Equations (2.20) represent the current linearized approximations

of the retained behavior constraints, in which the C_{bq} are constant. The $\alpha_b^{(L)}$ and $\alpha_b^{(U)}$ respectively denote lower and upper limits on the independent reciprocal design variables. Q_R is the set of retained behavioral constraints for the current stage. For convenience, the index p denoting the stage in the iterative design process has been dropped in Eqs. (2.20-2.22). However it should be kept in mind that Eqs. (2.19-2.22) represent only the approximate^{*} primal problem for the p^{th} stage of the overall iterative design process.

Let a Lagrangian function corresponding to the foregoing primal problem be defined as follows:

$$L(\vec{\alpha}, \vec{\lambda}) = \sum_{b=1}^B \frac{w_b}{\alpha_b} - \sum_{q \in Q_R} \lambda_q (\bar{u}_q - \sum_{b=1}^B C_{bq} \alpha_b) \quad (2.23)$$

with the understanding that the nonnegativity conditions

$$\lambda_q \geq 0 ; \quad q \in Q_R \quad (2.24)$$

must be satisfied. In view of the separability of each function involved in the primal problem, the Lagrangian function $L(\vec{\alpha}, \vec{\lambda})$ is also separable. By regrouping terms, $L(\vec{\alpha}, \vec{\lambda})$ can be put in the following form:

$$L(\vec{\alpha}, \vec{\lambda}) = \sum_{b=1}^B \left[\frac{w_b}{\alpha_b} + \alpha_b \sum_{q \in Q_R} \lambda_q C_{bq} \right] - \sum_{q \in Q_R} \lambda_q \bar{u}_q \quad (2.25)$$

Let Λ denote the set of all dual points satisfying the nonnegativity conditions expressed by Eq. (2.24) and let A define the set of all primal points satisfying the side constraints embodied in Eq. (2.22). Now $(\vec{\alpha}^*, \vec{\lambda}^*)$ is

^{*}Note that for statically determinate structures subject to static stress and displacement constraints, the primal formulation given by Eqs. (2.20 and 2.21) is exact.

said to be a saddle point of $L(\vec{\alpha}, \vec{\lambda})$ if

$$L(\vec{\alpha}^*, \vec{\lambda}^*) \leq L(\vec{\alpha}, \vec{\lambda}^*) \text{ for all } \vec{\alpha} \in A$$

and

$$L(\vec{\alpha}^*, \vec{\lambda}^*) \geq L(\vec{\alpha}^*, \vec{\lambda}) \text{ for all } \vec{\lambda} \in \Lambda$$

It is known that if $(\vec{\alpha}^*, \vec{\lambda}^*)$ is a saddle point of $L(\vec{\alpha}, \vec{\lambda})$, then $\vec{\alpha}^*$ is a solution of the primal problem [see pages 83-91 of Ref. 57]. Furthermore the existence of a unique saddle point of $L(\vec{\alpha}, \vec{\lambda})$ can be proven because the approximate primal problem posed by Eqs. (2.19-2.22) is demonstrably convex (since the w_b are positive and all the constraints are linear).

The saddle point of $L(\vec{\alpha}, \vec{\lambda})$ can be obtained by a two phase procedure as follows:

$$\vec{\lambda} \in \Lambda \quad \text{Max} \quad \vec{\alpha} \in A \quad \text{Min} \quad L(\vec{\alpha}, \vec{\lambda}) \quad (2.26)$$

or, alternatively,

$$\vec{\lambda} \in \Lambda \quad \text{Max} \quad \ell(\vec{\lambda}) \quad (2.27)$$

where

$$\ell(\vec{\lambda}) = \vec{\alpha} \in A \quad \text{Min} \quad L(\vec{\alpha}, \vec{\lambda}) \quad (2.28)$$

is defined as the dual function. Substituting Eq. (2.25) into Eq. (2.28) leads to the following expression of the dual function:

$$\ell(\vec{\lambda}) = \vec{\alpha} \in A \quad \text{Min} \quad \left\{ \sum_{b=1}^B \left[\frac{w_b}{\alpha_b} + \alpha_b \sum_{q \in Q_R} \lambda_q c_{bq} \right] - \sum_{q \in Q_R} \lambda_q \bar{u}_q \right\} \quad (2.29)$$

Since the last term in this equation is a constant and the set A is separable, the minimum value of the sum of B single variable functions is equal to the sum of the minimum values of each single variable function. Therefore

Eq. (2.29) can be written in the alternative form:

$$\ell(\vec{\lambda}) = \sum_{b=1}^B \left\{ \alpha_b^{(L)} \text{Min}_{\alpha_b^{(L)} \leq \alpha_b \leq \alpha_b^{(U)}} \left[\frac{w_b}{\alpha_b} + \alpha_b \sum_{q \in Q_R} \lambda_q C_{bq} \right] \right\} - \sum_{q \in Q_R} \lambda_q \bar{u}_q \quad (2.30)$$

Focusing attention on the single variable minimization problems

$$\alpha_b^{(L)} \text{Min}_{\alpha_b^{(L)} \leq \alpha_b \leq \alpha_b^{(U)}} \left[\frac{w_b}{\alpha_b} + \alpha_b \sum_{q \in Q_R} \lambda_q C_{bq} \right]; \quad b = 1, 2, \dots, B \quad (2.31)$$

let

$$f(\alpha_b) = \frac{w_b}{\alpha_b} + \alpha_b \sum_{q \in Q_R} \lambda_q C_{bq} \quad (2.32)$$

Taking the first derivative and setting it equal to zero yields

$$\frac{df}{d\alpha_b} = -\frac{w_b}{\alpha_b^2} + \sum_{q \in Q_R} \lambda_q C_{bq} = 0 \quad (2.33)$$

Solving Eq. (2.33) for α_b locates the extremum point $\tilde{\alpha}_b$

$$\tilde{\alpha}_b^2 = \frac{w_b}{\sum_{q \in Q_R} \lambda_q C_{bq}} \quad (2.34)$$

which is the minimum point of $f(\alpha_b)$, since, for $\tilde{\alpha}_b > 0$,

$$\frac{d^2 f}{d\alpha_b^2} = \frac{2w_b}{\alpha_b^3} > 0 \quad (2.35)$$

because w_b is known to be positive. Since α_b is subjected to side constraints, the minimum of $f(\alpha_b)$ is given by $\alpha_b = \tilde{\alpha}_b$ in Eq. (2.34) provided it resides in the acceptable interval $\alpha_b^{(L)} < \tilde{\alpha}_b < \alpha_b^{(U)}$. If $\tilde{\alpha}_b \leq \alpha_b^{(L)}$, then $\alpha_b = \alpha_b^{(L)}$ or if $\tilde{\alpha}_b \geq \alpha_b^{(U)}$, then $\alpha_b = \alpha_b^{(U)}$. Note also that in view of Eq. (2.35), $f(\alpha_b)$ has positive curvature for any $\alpha_b > 0$ and is consequently

unimodal.

From the foregoing development, it can be concluded that the dual problem has the following explicit form:

Find $\vec{\lambda}$ such that the explicit dual function

$$\ell(\vec{\lambda}) = \sum_{b=1}^B \frac{w_b}{\alpha_b} + \sum_{q \in Q_R} \lambda_q [u_q(\vec{\alpha}) - \bar{u}_q] \rightarrow \text{Max} \quad (2.36)$$

subject to nonnegativity constraints

$$\lambda_q \geq 0 ; \quad q \in Q_R \quad (2.37)$$

where

$$u_q(\vec{\alpha}) = \sum_{b=1}^B C_{bq} \alpha_b \quad (2.38)$$

and the primal variables α_b are given explicitly in terms of the dual variables λ_q by:

$$\alpha_b = \left[\frac{w_b}{\sum_{q \in Q_R} \lambda_q C_{bq}} \right]^{1/2} \quad \text{if} \quad [\alpha_b^{(L)}]^2 < \left[\frac{w_b}{\sum_{q \in Q_R} \lambda_q C_{bq}} \right] < [\alpha_b^{(U)}]^2 \quad (2.39)$$

$$\alpha_b = \alpha_b^{(L)} \quad \text{if} \quad \frac{w_b}{\sum_{q \in Q_R} \lambda_q C_{bq}} \leq [\alpha_b^{(L)}]^2 \quad (2.40)$$

$$\alpha_b = \alpha_b^{(U)} \quad \text{if} \quad \frac{w_b}{\sum_{q \in Q_R} \lambda_q C_{bq}} \geq [\alpha_b^{(U)}]^2 \quad (2.41)$$

The key to being able to construct this explicit dual problem resides in the convexity and separability of the approximate primal problem (i.e., Eqs. 2.19 - 2.22) and the simplicity of the single variable minimization problems embodied in Eq. (2.31).

An attractive feature of the dual problem is that it is a quasi-unconstrained problem, because taking care of the nonnegativity constraints (Eq. 2.37) is straightforward. Two maximization methods will be subsequently described in this work: a second order Newton type algorithm (DUAL2; see Chapter 3) and a first order conjugate gradient type algorithm (DUAL1; see Chapter 4). In addition the dual method formulation will be extended to deal with pure discrete and mixed continuous-discrete problems, and a specially devised gradient projection type of algorithm will be developed (see Chapter 4).

2.5 Relations with the Optimality Criteria Approaches

Most of the earlier optimality criteria techniques are based on the consideration of a statically determinate truss subject to stress and displacement constraints. In such a case, the behavior constraints take on explicit forms which can be expressed using virtual load techniques and/or stress ratio formulas (see Sections 2.5.2 and 2.5.3 respectively). As a result, the minimum weight design can be defined analytically, provided an appropriate algorithm is available for selecting the critical constraints. In the case of a statically indeterminate structure, the explicit redesign relations must be employed recursively, by constructing new explicit forms of the behavior constraints after each structural reanalysis. Therefore, the basic assumption is that the amount of force redistribution induced when the design variables are modified will generally be moderate enough to insure the convergence of the redesign process. This is the central idea of the optimality criteria approach and, not too surprisingly, it is also the main reason for the success of

the mathematical programming approach using approximation concepts.

In fact, as shown in Ref. [32], the whole process of combining the linearization of the behavioral constraints with respect to the reciprocal design variables and a dual solution scheme can be viewed as a generalization of the optimality criteria approach. In other words, a generalized optimality criteria approach can be defined as a special form of the linearization methods in mathematical programming. It amounts to replacing the original problem with a sequence of explicit approximate problems where the behavior constraints are linearized with respect to the reciprocal design variables.

Conversely the joining together of approximation concepts and dual methods (see Section 2.4) can be interpreted as a powerful mathematical programming approach that contains and generalizes the conventional optimality criteria techniques.

2.5.1 Conventional and Generalized Optimality Criteria

The generalized optimality criteria approach set forth in Ref. [32] consists in solving exactly, after each structural reanalysis, the linearized problem stated in Eqs. (2.15 - 2.18), which can be recast as follows in terms of the direct design variables D_i (assuming no linking nor constraint deletion and dropping the stage index p , for sake of simplicity):

$$\text{minimize} \quad W = \sum_i^I m_i D_i \quad (2.42)$$

$$\text{subject to} \quad \bar{u}_q - \sum_i^I \frac{C_{iq}}{D_i} \geq 0 \quad q \in Q \quad (2.43)$$

$$D_i^{(U)} \geq D_i \geq D_i^{(L)} \quad (2.44)$$

Instead of employing primal or dual mathematical programming methods, an alternative approach, which is typical of the optimality criteria philosophy, is to use the explicit character of the approximate problem embodied in Eqs. (2.42 - 2.44) in order to express analytically the optimal design variables. This can be achieved through the use of the KUHN-TUCKER conditions (see Eqs. 2.10 - 2.13) which, in view of the convexity of the linearized problem, are sufficient for global optimality. These conditions lead to a generalized optimality criterion yielding explicitly the design variables:

active design variables:

$$\text{if } [D_i^{(L)}]_{m_i}^2 < \sum_{q \in Q} C_{iq} \lambda_q < [D_i^{(U)}]_{m_i}^2 \rightarrow D_i = \left[\frac{1}{m_i} \sum_{q \in Q} C_{iq} \lambda_q \right]^{\frac{1}{2}} \quad (2.45)$$

passive design variables:

$$\text{if } \sum_{q \in Q} C_{iq} \lambda_q \leq [D_i^{(L)}]_{m_i}^2 \rightarrow D_i = D_i^{(L)} \quad (2.46)$$

$$\text{if } \sum_{q \in Q} C_{iq} \lambda_q \geq [D_i^{(U)}]_{m_i}^2 \rightarrow D_i = D_i^{(U)} \quad (2.47)$$

In these expressions, the Lagrangian multipliers λ_q are associated with the linearized behavior constraints (Eq. 2.43). They must satisfy the complementary conditions given in Eqs. (2.11), namely:

critical constraint:

$$\lambda_q \geq 0 \quad \text{if} \quad \sum_{i=1}^I \frac{C_{iq}}{D_i} = \bar{u}_q \quad (2.48)$$

non critical constraint

$$\lambda_q = 0 \quad \text{if} \quad \sum_{i=1}^I \frac{C_{iq}}{D_i} < \bar{u}_q \quad (2.49)$$

The Eqs. (2.45 - 2.47) relating the design variables D_i to the Lagrangian multipliers λ_q provide a basis for separating the design variables in two groups. The passive variables are those that are fixed to a lower or an upper limit (see Eqs. 2.46 and 2.47) while the active variables are explicitly given in terms of the Lagrangian multipliers using Eq. (2.45). This subdivision of the design variables into active and passive groups is classical in the optimality criteria approaches [see Refs. 13-17 and 26-29].

When the Lagrangian multipliers satisfying Eqs. (2.48 and 2.49) are known, the optimal design variables can be easily computed using the explicit optimality criterion stated in Eqs. (2.45 - 2.47). Therefore the problem has been replaced with a new one, which is defined in terms of the Lagrangian multipliers only. To solve this new problem, the conventional optimality criteria techniques usually make the assumption that the behavior constraints critical at the optimum are known a priori, avoiding thus the inequality constraints on the Lagrangian multipliers appearing in Eqs. (2.48, 2.49). An update procedure for the retained Lagrangian multipliers is then employed, so that the optimal design variables can be sought in an iterative fashion by coupling the update procedure and the explicit optimality criterion defined by Eqs. (2.45 - 2.47).

As first noted in Ref. [26], the essential difficulties involved in applying these optimality criteria methods to the general structural synthesis problem are those associated with identifying the correct critical constraint set and the proper corresponding set of passive members [see

also Ref. 17]. These difficulties were recognized and addressed with varying degrees of success in studies such as those reported in Refs. [27-29]. However, it was only with the advent of the dual formulation set forth in Refs. [30 and 31] that these obstacles were conclusively overcome.

The dual method approach inherently contains a mechanism for iteratively seeking the optimal Lagrangian multipliers satisfying the generalized optimality criterion embodied in Eqs. (2.45 - 2.49). In fact, the equivalence between this generalized optimality criterion and the Eqs. (2.39 - 2.41) derived in the dual method formulation is straightforward (the only difference is the change from direct to reciprocal variables). Therefore it is apparent that the dual method formulation, which consists in maximizing the Lagrangian function subject to nonnegativity constraints on the Lagrangian multipliers, can be viewed as an update procedure for the Lagrangian multipliers. After the update procedure is completed, the primal design variables can be evaluated using the optimality criteria equations (2.45 - 2.47).

The main difference between the conventional and the generalized optimality criteria approaches can now be identified as lying in the iterative process used to seek the dual variables (or Lagrangian multipliers). The conventional optimality criteria techniques replace the inequality relations (2.43) with equalities, postponing the selection of the active constraints to a subsequent part of the iterative process (or simply assuming that the active constraint set is known a priori). Consequently, simple recursive relations can be derived. The low computational cost of these recursive relations is the attractive feature of the conventional optimality criteria approaches. On the other hand, the dual

method formulation employed in the generalized optimality criterion method demands, at least formally, solution of an auxiliary mathematical programming problem (see Eqs. 2.36 - 2.41). However this maximization problem is remarkably simple and its exact solution can be generated at a low computational cost, which is comparable to that required by the recursive techniques of conventional optimality criteria. The dual algorithms can handle a large number of inequality constraints. They intrinsically contain a rational scheme for identifying the critical constraints through the nonnegativity constraints on the dual variables. They also automatically sort out the active and passive design variable groups using the explicit relations between primal and dual variables.

In conclusion, while the coupling together of approximation concepts and the dual method formulation represents a pure mathematical programming approach, it can also be viewed as a generalized optimality criteria approach.

2.5.2 The Constraint Gradients: Pseudo-loads Versus Virtual Load Techniques

So far, no attention has been given, in this work, to the way the constraint gradients are evaluated. In the approximation concepts method, which has its genesis in the mathematical programming approach to structural synthesis, the pseudo-loads technique is used to compute the gradients of the nodal displacements under a given set of load conditions [see Ref. 58, page 242]. The stress and displacement constraint gradients are then readily evaluated. This procedure requires that a certain number of additional loading cases be treated in the structural analysis phase. Introducing the pseudo-load vectors

$$\vec{V}_{bk} = - \left[\frac{\partial K}{\partial \alpha_b} \right] \vec{u}_k \quad (2.50)$$

the gradients of the nodal displacements are computed by solving the systems of linear equations

$$[K] \frac{\partial \vec{u}_k}{\partial \alpha_b} = \vec{V}_{bk} \quad \begin{cases} b = 1, B \\ k = 1, K \end{cases} \quad (2.51)$$

where \vec{u}_k is the displacement vector for the kth load condition and $[K]$ is the system stiffness matrix [see Ref. 5 page 83]. The number of pseudo-load vectors is directly related to the number of load conditions and the number of independent design variables after linking and it is independent of the number of behavior constraints.

On the other hand, the generalized optimality criterion reported in Ref. [30] uses, as do most of the conventional optimality criteria approaches, the virtual load technique to generate first order explicit approximations of the stress and displacement constraints:

$$u_{jk} = \sum_{i=1}^I \frac{C_{ijk}}{D_i} \leq \bar{u}_j \quad (2.52)$$

with

$$C_{ijk} = (\vec{u}_j^T [K_i] \vec{u}_k) D_i \quad (2.53)$$

In these expressions, \vec{u}_k denotes the displacement vector for the k^{th} load condition, $[K_i]$ represents contribution to system stiffness matrix of the i^{th} element and \vec{u}_j is the displacement vector due to a virtual loading case conjugated to the j^{th} behavior constraint. As shown in Ref. [30], the coefficients C_{ijk} , which have the meaning of energy densities in an optimality criteria context, are also the gradients of the constraints with respect to the reciprocal design variables $\delta_i = 1/D_i$:

$$C_{ijk} = \frac{\partial u_{jk}}{\partial \delta_i} = \frac{1}{\delta_i} (\vec{u}_j^T [K_i] \vec{u}_k) \quad (2.54)$$

Consequently, the explicit expressions defined in Eq. (2.52) are first order approximations of the behavior constraints. Recast in terms of the linked reciprocal variables α_b , they turn out to be identical to the first order Taylor series expansions used in the approximation concepts approach.

The virtual load technique is widely used in conventional optimality criteria approaches [see Refs. 13-17]. It employs a few additional unit loads to generate first order explicit approximations for preselected displacement constraints. In Ref. [30], this technique has been extended to stress constraints, for which the virtual loading cases are no longer represented by unit loads. Introducing virtual load vectors \vec{V}_j conjugated to the behavior constraints, the corresponding virtual displacement vectors are evaluated by solving the systems of linear equations

$$[K] \vec{u}_j = \vec{V}_j \quad j = 1, Q_R \quad (2.55)$$

The coefficients C_{ijk} are then computed using Eq. (2.53), and the explicit forms of the behavior constraints defined by Eq. (2.52) are available.

This alternative approach to the evaluation of the constraint gradients requires as many additional virtual loading cases as the number of stress and displacement constraints retained, regardless of the number of design variables and of the number of real loading conditions.

The decision as to which procedure should be selected to compute the constraint gradients can be based on a comparison of the total number of additional loading cases introduced into the structural reanalysis at each

given stage:

- (1) if the pseudo-loads technique is used, the number of additional loading cases is equal to the number of independent design variables after linking times the number of applied loading conditions;
- (2) if the virtual load technique is adopted, the number of additional loading cases is equal to the number of potentially active stress and displacement constraints retained for the current stage (provided each stress constraint involves only one stress component; see Ref. [30]).

It is worthwhile noticing that a primal versus dual opposition appears in the number of additional loading cases, which, on one hand, ("optimality criteria"), is equal to the number Q_R of dual variables, while, on the other hand ("mathematical programming"), it is proportional to the number B of primal variables.

2.5.3 The Stress Constraints: Zero Versus First Order Approximations

In the approximation concepts approach that is adopted in this work, as well as in the generalized optimality criteria approach proposed in Ref. [30], all the behavior constraints are replaced by first order explicit approximations. In many conventional optimality criteria techniques, such as those reported in Refs. [13-17], only the displacement constraints are approximated by first order expansions, while the stress constraints are treated using the classical "Fully Stressed Design" (FSD) concept. In this approach, the implicit nonlinear stress constraints

$$\sigma_{ik}(\vec{D}) \leq \sigma_i^{(U)} \quad \begin{array}{l} i = 1, 2, \dots, I \\ k = 1, 2, \dots, K \end{array} \quad (2.56)$$

(where σ_{ik} denotes a suitable reference stress in the i^{th} element for the k^{th} loading condition and $\sigma_i^{(U)}$ is the corresponding allowable stress limit) are transformed, at each stage p , into simple side constraints:

$$\alpha_b \leq \tilde{\alpha}^{(p)} \quad (2.57)$$

by using the well known stress ratio formula:

$$\tilde{\alpha}_b^{(p)} = \frac{\alpha_b^{(p)}}{\max_{i \in b} \left\{ \max_{k=1, K} \left[\frac{\sigma_{ik}^{(\vec{D}_p)}}{\sigma_i^{(U)}} \right] \right\}} \quad (2.58)$$

As shown in Ref. [33], this FSD procedure can be interpreted as using zero order approximation of the stress constraints, because it relies on explicit expressions that preserve only the value of the stress constraints, and not of their derivatives.

The zero order approximation of stress constraints offers two important advantages. First when the virtual load technique is used to compute the constraint gradients, the number of additional loading cases is significantly reduced because no virtual load cases have to be associated with the stress constraints. Secondly, the number of behavior constraints retained in each explicit approximate problem (see Eq. 2.20) is also substantially reduced, since all the stress constraints are now transformed into side constraints. This feature is especially beneficial when dual methods are employed to solve the explicit problem, because the dimensionality of the dual problem corresponds to the number Q_R of first order approximated constraints embodied in Eq. (2.20).

On the other hand, it is well known that the FSD procedure, because it employs a zero order approximation of the stress constraints, does not

always converge to the true optimum and sometimes is the source of instability or divergence of the optimization process. In practical structures, it is observed that many of the stress constraints can be approximated with sufficient accuracy by the FSD procedure, while others require a more sophisticated approximation using, for example, first order Taylor series expansion with respect to the reciprocal design variables.

The selection of constraints requiring first order approximation can be made automatically on the basis of the following criterion [see Ref. 32]. A retained potentially critical stress constraint must be linearized with respect to the reciprocal variables if,

$$\frac{\partial \sigma_b}{\partial \alpha_b} (\vec{\alpha}_p) < \frac{\sigma_b(\vec{\alpha}_p)}{\alpha_b} \quad (2.59)$$

where σ_b denotes the appropriate reference stress in an element whose size is controlled by the b^{th} independent design variable. That condition arises from the fact that, in a statically determinate structure, zero and first order approximations of the stress constraints coalesce, since then:

$$\frac{\partial \sigma_b}{\partial \alpha_a} = 0 \quad \text{for } a \neq b \quad (2.60)$$

It should be clearly recognized that the selection criterion stated in Eq. (2.59) must be repeated at each design stage of the overall optimization process, exactly like the well known truncation procedure for deleting temporarily redundant and unimportant constraints (see Section 2.3.1).

Mixing the FSD criterion and the virtual load procedure for generating accurate representation of the stress constraints has been presented in Ref. [32] as a hybrid optimality criterion. It can be interpreted in

the present work as replacing some of the high quality, first order approximations of the constraints with computationally inexpensive, zero order approximations.

2.5.4 Scaling of the Design Variables

To close this section, it is worthwhile giving a geometrical interpretation of the approximation concepts approach. This interpretation is based upon the concept of scaling, which is classically used in optimality criteria approaches. Scaling simple sizing type design variables (e.g., bar areas and sheet thickness) does not lead to any force distribution. That is, when all the member sizes are multiplied by the same factor, the stresses and the displacements are simply divided by the scaling factor (assuming the applied loads do not depend on the design variables). Therefore scaling is a convenient procedure for bringing the design point back to the boundary of the feasible region (see Refs. 54 and 55).

In the design space, scaling corresponds to a move along a straight line joining the origin to the point where the structural analysis is made. Along a scaling line, the gradients of the stress and displacement constraints with respect to the reciprocal variables remain constant (see Ref. 33). Therefore the linearized forms of the constraints embodied in Eq. (2.18) furnish the exact values of the constraints and of their gradients all along the scaling line passing through the design point $\vec{\alpha}_p$ where the linearization is accomplished. Consequently, in the space of the reciprocal variables, the approximation concepts approach can be interpreted as replacing each real constraint surface by its tangent plane at its point of intersection with the scaling line (see Fig. 5).

When zero order approximation is used, the stress constraints are transformed into the simple side constraints embodied in Eq. (2.57). It can be shown [see Ref. 34] that each approximate constraint surface $\alpha_b = \tilde{\alpha}_b^{(p)}$ is again represented by a plane passing through the point of intersection of the corresponding real constraint surface with the scaling line. However it is no longer the tangent plane, but the plane perpendicular to the b^{th} axis of the design space (see Fig. 5).

Finally, the criterion for automatic selection of zero or first order approximation can be geometrically interpreted as follows: the condition posed by Eq. (2.59) is satisfied when the relevant stress constraint for the b^{th} independent design variable is represented in the design space by a surface that is roughly parallel to the b^{th} base plane.

3. DUAL METHODS FOR CONTINUOUS DESIGN VARIABLES

In this chapter, solution methods for the dual problem formulated in Section 2.4.2 are examined. All the design variables are assumed to vary continuously and the dual problem posed by Eqs. (2.36 - 2.41) corresponds to the primal problem stated in Eqs. (2.19 - 2.22). It will be shown that, although there are hyperplanes in the dual space where the second partial derivatives of the dual function exhibit discontinuity, a second order Newton type of maximization algorithm can be devised that is especially well suited to the solution of the dual problem in the pure continuous case.

3.1 The Second Order Discontinuity Planes

An attractive feature of the dual method formulation is that the first derivatives of the dual function are readily available, because they are given by the primal constraints (Eq. 2.20):

$$\frac{\partial \ell}{\partial \lambda_q}(\vec{\lambda}) = u_q(\vec{\alpha}) - \bar{u}_q \quad q \in Q_R \quad (3.1)$$

This is a well known theorem in convex programming [see, for instance, Ref. 35, 40 and 57] which, for the explicit dual problem considered here, can be easily demonstrated. Taking the first derivatives of the dual function embodied in Eq. (2.36) yields:

$$\frac{\partial \ell}{\partial \lambda_q} = - \sum_{b=1}^B \frac{w_b}{\alpha_b} \frac{\partial \alpha_b}{\partial \lambda_q} + \sum_{k \in Q_R} \lambda_k \frac{\partial u_k}{\partial \lambda_q} + u_q - \bar{u}_q \quad (3.2)$$

From Eqs. (2.39 - 2.41), it follows that:

$$\frac{\partial \alpha_b}{\partial \lambda_q} = \begin{cases} -\frac{\alpha_b^3 C_{bq}}{2w_b} & \text{if } [\alpha_b^{(L)}]^2 < \frac{w_b}{\sum_{q \in Q_R} \lambda_q C_{bq}} < [\alpha_b^{(U)}]^2 \\ 0 & \text{otherwise} \end{cases} \quad (3.3)$$

Substituting Eq. (3.3) into the first term of Eq. (3.2) gives

$$-\sum_{b=1}^B \frac{w_b}{\alpha_b^2} \frac{\partial \alpha_b}{\partial \lambda_q} = \frac{1}{2} \sum_{b \in \tilde{B}} C_{bq} \alpha_b \quad (3.4)$$

where the summation on the index b is over the set of free primal variables[†]

$$\tilde{B} = \{b \mid \alpha_b^{(L)} < \alpha_b < \alpha_b^{(U)}\} \quad (3.5)$$

On the other hand, using the explicit definition of $u_q(\vec{\alpha})$ (Eq. 2.38)

yields

$$\frac{\partial u_k}{\partial \lambda_q} = \sum_{b=1}^B C_{bk} \frac{\partial \alpha_b}{\partial \lambda_q} \quad (3.6)$$

so that, taking successively account of Eq. (3.3) and Eqs. (2.39 - 2.41),

and rearranging the terms under summation, the second term in Eq. (3.2)

becomes:

$$\sum_{k \in Q_R} \lambda_k \frac{\partial u_k}{\partial \lambda_q} = -\frac{1}{2} \sum_{b \in \tilde{B}} \frac{\alpha_b^3 C_{bq}}{w_b} \sum_{k \in Q_R} \lambda_k C_{bk} = -\frac{1}{2} \sum_{b \in \tilde{B}} C_{bq} \alpha_b \quad (3.7)$$

Finally, comparing Eq. (3.4) and Eq. (3.7), it is seen that the first and

second terms in Eq. (3.2) cancel and the first derivatives of the dual

function are given by Eq. (3.1). The simplicity of Eq. (3.1) is a com-

[†] A primal variable is said to be "free" if it has not taken on its upper or lower bound value ($\alpha_b^{(U)}$ or $\alpha_b^{(L)}$), that is if it is given by Eq. (2.39) rather than Eq. (2.40) or Eq. (2.41).

putationally important property of the dual method formulation. When a numerical maximization scheme is employed to solve the dual problem, the evaluation of the dual function (Eq. 2.36) requires the determination of the primal constraint values $(u_q - \bar{u}_q)$, so that the first derivatives given by Eq. (3.1) are available without additional computation.

In the DUAL 2 algorithm described subsequently, the Newton method is used to maximize the dual function and therefore the second partial derivatives of $\ell(\vec{\lambda})$ must be evaluated. Let the elements of the Hessian matrix associated with $\ell(\vec{\lambda})$ be represented by the notation F_{qk} , then, from Eq. (3.1):

$$F_{qk} = \frac{\partial^2 \ell}{\partial \lambda_q \partial \lambda_k}(\vec{\lambda}) = \frac{\partial u_q}{\partial \lambda_k}(\vec{\lambda}) \quad (3.8)$$

Interchanging the indices k and q in Eq. (3.6), it follows that

$$F_{qk} = \sum_{b=1}^B c_{bq} \frac{\partial \alpha_b}{\partial \lambda_k} \quad (3.9)$$

Changing the index q to k in Eq. (3.3) and substituting Eq. (3.3) into Eq. (3.9) gives the explicit form of the second derivatives:

$$F_{qk} = -\frac{1}{2} \sum_{b \in \tilde{B}} \frac{c_{bq} c_{bk}}{w_b} \alpha_b^3 \quad (3.10)$$

where the summation on the index b is over the set of free primal variables (see Eq. 3.5).

From Eq. (3.10), it can be concluded that the second derivatives of the dual function are discontinuous, because the F_{qk} elements jump to other values each time the set \tilde{B} of free primal variables is modified. Now, the explicit relationships between primal and dual variables (see Eqs. 2.39 - 2.41) indicate that changes in the status of primal variables (from free to bound), which signal discontinuities in the second deriva-

tives, occur on hyperplanes in the dual space given by

$$\sum_{q \in Q_R} \lambda_q C_{bq} = \frac{w_b}{[\alpha_b^{(L)}]^2} \quad (3.11)$$

and

$$\sum_{q \in Q_R} \lambda_q C_{bq} = \frac{w_b}{[\alpha_b^{(U)}]^2} \quad (3.12)$$

The hyperplane defined by Eq. (3.11) subdivides the dual space into a half-space where $\alpha_b = \alpha_b^{(L)}$ (bounded primal variable) and another half-space where $\alpha_b > \alpha_b^{(L)}$ (free primal variable). Clearly, the same argument holds for Eq. (3.12), with $\alpha_b^{(L)}$ replaced by $\alpha_b^{(U)}$. Consequently the dual space is partitioned into several domains separated by the second order discontinuity planes embodied in Eqs. (3.11 and 3.12). In each domain, the set \tilde{B} of free primal variables remains constant. However when passing from one domain to another, across a second order discontinuity plane, the set \tilde{B} is modified and the second derivatives of the dual function change abruptly (see Eq. 3.10).

3.2 Characteristics of the Dual Function - Continuous Case

The explicit dual function for the pure continuous variable case, defined by Eqs. (2.36 - 2.41), has several interesting and computationally important properties, which are summarized as follows:

- (1) it is a concave function and the search region in dual space is a convex set defined by Eq. (2.37);
- (2) it is continuous and it has continuous first derivatives with respect to λ_q over the entire region defined by Eq. (2.37);
- (3) the first derivatives of $\ell(\vec{\lambda})$ are easily available because

they are given by the primal constraints, that is:

$$\frac{\partial \ell}{\partial \lambda_q}(\vec{\lambda}) = u_q(\vec{\alpha}) - \bar{u}_q = \sum_{b=1}^B c_{bq} \alpha_b - \bar{u}_q \quad (3.13)$$

(4) the second derivatives of $\ell(\vec{\lambda})$ are given explicitly by:

$$\frac{\partial^2 \ell}{\partial \lambda_q \partial \lambda_k}(\vec{\lambda}) = -\frac{1}{2} \sum_{b \in \tilde{B}} \frac{c_{bq} c_{bk}}{w_b} \alpha_b^3 \quad (3.14)$$

where \tilde{B} denotes the set of free primal variables (see Eq. 3.5);

(5) discontinuities of the second derivatives exist on hyperplanes in the dual space defined by Eqs. (3.11 and 3.12), which locate points where there is a change in status of the b^{th} design variable from "free" to "bound".

3.3 DUAL 2 - Newton Type Maximizer

In this section, a second order Newton type algorithm for finding the maximum of the dual function (see Eqs. 2.36, 2.38, 2.39, 2.40 and 2.41), subject to nonnegativity constraints (see Eq. 2.37), is described. The method has been found to be very efficient in practice, even though there are hyperplanes in the dual space where the second partial derivatives are not unique (see Eqs. 3.11 and 3.12). The algorithm involves iterative modification of the dual variable vector as follows:

$$\vec{\lambda}_{t+1} = \vec{\lambda}_t + d_t \vec{S}_t \quad (3.15)$$

where \vec{S}_t denotes the modification direction in dual space and d_t represents the distance of travel along that direction. Alternatively, in scalar form, the modification is given by

$$\lambda_{q,t+1} = \lambda_{qt} + d_t s_{qt} ; \quad q \in Q_R \quad (3.16)$$

In the DUAL 2 algorithm, the Newton method is used to seek the maximum of the dual function in various dual subspaces

$$M = \{q | \lambda_{qt} > 0 ; q \in Q_R\} \quad (3.17)$$

which exclude those λ_q components that are not currently positive. The move direction in such a dual subspace is given by

$$\vec{s}_t = -[F(\vec{\lambda}_t)]^{-1} \nabla \ell(\vec{\lambda}_t) \quad (3.18)$$

where $F(\vec{\lambda}_t)$ denotes the Hessian matrix of the dual function evaluated at $\vec{\lambda}_t$ (see Eq. 3.10) and the subscript \sim indicates that the collapsed vector (matrix) includes only those components (elements) corresponding to strictly positive values of the dual variables at $\vec{\lambda}_t$ (i.e., entries for $\lambda_{qt} > 0$ only).

If the initial starting point in dual space is such that the Hessian matrix (see Eq. 3.18) is non-singular, and additional non-zero components $\lambda_q > 0$ are added one at a time, each subsequent Hessian $[F(\vec{\lambda}_t)]$ will be non-singular [see Ref. 30, page 50]. In the first stage ($p=1$), it is convenient to select the starting point so that the only non-zero dual variable corresponds to the most critical constraint (based on the structural analysis of the primal design used to generate the current approximate primal problem). For subsequent stages ($p>1$), the starting point is given by the dual variable values at the end of the dual function maximization in the previous stage. This procedure is employed in DUAL 2 and therefore the dimensionality of the maximization problem generally does not exceed the number of strictly critical constraints excluding side constraints (see Eq. 2.22).

The DUAL 2 algorithm is outlined in the block diagrams shown in

Figs. 6 and 7. Given a set of values for the dual variables $\lambda_{qt}; q \in Q_R$ (see block 1) attention is directed to identifying the set of non-zero dual variables M (block 2). The integers in the set M define a dual subspace and in that subspace the maximum of the dual function $\ell(\vec{\lambda})$ is sought subject to nonnegativity constraints (see block 3; Fig. 6 and Fig. 7). Let the maximum of $\ell(\vec{\lambda})$ in the subspace defined by the set M be denoted as $\vec{\lambda}_M$. At $\vec{\lambda}_M$ evaluate the first partial derivatives of $\ell(\vec{\lambda})$ with respect to those λ_q not included in the subspace defined by the set M (block 4, Fig. 6). Test to see if the maximum of $\ell(\vec{\lambda})$ in the dual space ($q \in Q_R$) has been obtained (block 5), if so store the primal variables corresponding to the current dual variables $\vec{\lambda}_M$, end the stage and go to the overall design process convergence test. If any of the first partial derivatives $\frac{\partial \ell}{\partial \lambda_q}(\vec{\lambda}_M); q \in Q_R$ are positive find the largest one, denote the corresponding index as q^+ (see block 6, Fig. 6), add this component to the set M (increasing the dimensionality of the dual subspace), and continue to seek the maximum of the dual function $\ell(\vec{\lambda})$ associated with the current stage.

The procedure followed in order to find the maximum of $\ell(\vec{\lambda})$ in a dual subspace M (see block 3, Fig. 6) is elaborated on in Fig. 7. The START block in Fig. 7 is entered from block 3 of Fig. 6. Given the initial values of the non-zero dual variables $\lambda_{qt} > 0; q \in M$ (block 1, Fig. 7), evaluate the partial derivatives $\frac{\partial \ell}{\partial \lambda_q}(\vec{\lambda}_t); q \in M$ (block 2, Fig. 7), and then test to see if the maximum point in the subspace defined by $q \in M$ has been found (block 3, Fig. 7). If the absolute value of the gradient $|\nabla \ell(\vec{\lambda}_t)|$ is equal to or less than ϵ , the maximum of $\ell(\vec{\lambda})$ in the subspace defined by $q \in M$ has been found. Let $\vec{\lambda}_t$ replace $\vec{\lambda}_M$ (block 4, Fig. 7) and go to point G on Fig. 6.

On the other hand, if $|\nabla \ell(\vec{\lambda})|$ is greater than ϵ , the maximum of $\ell(\vec{\lambda})$ in the subspace defined by $q \in M$ has not been found and the search for the maximum is continued by using Eq. (3.18) to generate a new search direction \vec{s}_t (see block 5, Fig. 7).

The next step is to determine the maximum step length (d_{\max}) along the direction \vec{s}_t such that none of the $\lambda_{q,t+1}$ become negative. Setting the $\lambda_{q,t+1}$ to zero in Eq. (3.16) and focusing attention on only the negative components ($s_{qt} < 0$) it follows that the maximum step length is given by

$$d_{\max} = \min_{s_{qt} < 0} \left| \frac{\lambda_{qt}}{s_{qt}} \right| ; \quad q \in M \quad (3.19)$$

Determine d_{\max} and let the value of q which gives d_{\max} be denoted by the symbol q^- (see block 6 of Fig. 7). Test d_{\max} to see if it is less than unity, if so then the move distance d_t is replaced by d_{\max} (block 7a, Fig. 7), otherwise the move distance is set equal to unity (block 7b, Fig. 7). The dual variables are now updated using the move direction generated in block 5 and the move distance d_t generated in either block 7a or block 7b. Also the primal variables ($\alpha_{b,t+1}$; $b = 1, 2, \dots, B$) (corresponding to the $\lambda_{q,t+1}$; $q \in M$) are evaluated using Eqs. (2.39, 2.40 and 2.41) (see block 8, Fig. 7). The next step is to determine whether or not the move from $\vec{\lambda}_t$ to $\vec{\lambda}_{t+1}$ has involved passing through any discontinuity planes (see Eqs. 3.11 and 3.12). This is accomplished by comparing the set of free primal variables at design point $\vec{\alpha}_t$ with those at $\vec{\alpha}_{t+1}$. If there is no change in the set of free primal variables, then it follows that none of the hyperplanes defined by Eqs. (3.11 and 3.12) have been traversed in moving from $\vec{\lambda}_t$ to $\vec{\lambda}_{t+1}$ in dual space. Now if $\vec{\lambda}_t$ and $\vec{\lambda}_{t+1}$ are in the same domain (i.e., the move from $\vec{\lambda}_t$ to $\vec{\lambda}_{t+1}$ has not involved passing through any

discontinuity planes) and $d_t \neq d_{\max}$ (see block 10 -False; Fig. 7), then the scheme behaves like a regular Newton method taking a unit step in the \vec{S}_t direction and going to block 2 to continue the iteration. When $\vec{\lambda}_t$ and $\vec{\lambda}_{t+1}$ are in the same domain and $d_t = d_{\max}$ (see block 10 -True; Fig. 7), evaluate the directional derivative at $\vec{\lambda}_{t+1}$ (block 11, Fig. 7), using the following well known relation

$$\ell'(d_t) = \vec{S}_t^T \nabla \ell(\vec{\lambda}_{t+1}) = \sum_{q \in M} S_{qt} \frac{\partial \ell}{\partial \lambda_q}(\vec{\lambda}_{t+1}) \quad (3.20)$$

Note that the partial derivatives $\frac{\partial \ell}{\partial \lambda_q}(\vec{\lambda}_{t+1})$ are easily evaluated using Eq. (3.13) since the primal variables $\vec{\alpha}_{t+1}$ were previously computed and stored. When $\vec{\lambda}_t$ and $\vec{\lambda}_{t+1}$ are not in the same domain (block 9 -False; Fig. 7) the directional derivative at $\vec{\lambda}_{t+1}$ should also be evaluated (block 11, Fig. 7). If in block 12, $\ell'(d_t)$ is positive and d_t does not equal d_{\max} (block 13 -False), move the distance d_t along the direction \vec{S}_t and go to block 2 to continue the iteration. If in block 12, $\ell'(d_t)$ is positive and $d_t = d_{\max}$ then go to H (i.e., return to H in Fig. 6) and delete the component q^- tagged in block 6 of Fig. 7 when d_{\max} was evaluated. Finally, if $\ell'(d_t)$ is not positive then cut d_t in half (block 14, Fig. 7) and go to block 8.

The scheme for determining the step length along a direction \vec{S}_t described by blocks 6 through 14 of Fig. 7 does not seek the maximum of the dual function along the direction \vec{S}_t , rather it is designed to assure that either: (a) a regular Newton unit step is taken without any change in the set of free primal variables; or (b) the move distance is selected so that the value of the dual function increases. Note that in contrast to the DUAL 1 algorithm, which will be described subsequently, the move distance selection scheme employed in the DUAL 2 algorithm does not calculate dis-

tances along \vec{S}_t locating the intercepts with the 2nd order discontinuity planes defined by Eqs. (3.11 and 3.12).

4. DUAL METHODS FOR DISCRETE DESIGN VARIABLES

Attention is now directed toward extending the explicit dual formulation to problems involving discrete design variables. There are many occasions in structural optimization where the design variables describing the member sizes must be selected from a list of discrete values. For example, conventional metal alloy sheets are commercially available in standard gauge sizes and cross-sectional areas for truss members may, in practice, have to be chosen from a list of commercially available member sizes. Furthermore the growing use of fiber composite materials in aerospace structures also underscores the importance of being able to treat structural synthesis problems where some or even all of the design variables are discrete.

In the structural optimization literature, relatively little attention has been given to dealing with discrete variables. Those efforts that have been reported [see Ref. 59 for a review of this literature] generally attack the discrete design variable optimization problem by employing integer programming algorithms to treat the problem directly in the primal variable space. In this chapter it will be shown that the combined use of approximation concepts and dual methods, set forth in chapters 2 and 3 for continuous sizing type design variables, can be extended to structural synthesis problems involving a mix of discrete and continuous sizing type design variables. The mixed case formulation and the implementing algorithm DUAL 1, described in the sequel, can also handle the two limiting special cases, namely, the pure discrete and the pure continuous variable cases.

It is worthwhile noticing that when discrete design variables are

introduced, the approximate primal problem is no longer convex and therefore, the dual formulation presented in this chapter does not necessarily yield the exact solution of the approximate primal problem (duality gap). However the computational experience reported in Chapter 6 shows that useful and plausible discrete designs are readily generated using the DUAL 1 algorithm. These numerical results confirm the observation made in Refs. [57 and 60] to the effect that although the extension of the dual formulation to discrete variables lacks rigor, it frequently gives good results.

4.1 The First Order Discontinuity Planes

The explicit dual method previously described can be extended to mixed continuous-discrete variable primal problems of the form given by Eqs. (2.19 - 2.21), with the side constraints of Eq. (2.22) replaced by

$$\alpha_b^{(L)} \leq \alpha_b \leq \alpha_b^{(U)} \quad \text{for continuous } \alpha_b \quad (4.1)$$

and

$$\alpha_b \in A_b^{(D)} \quad \text{for discrete } \alpha_b \quad (4.2)$$

where

$$A_b^{(D)} = \{\alpha_b^{(k)}; \quad k = 1, 2, \dots, n_b\} \quad (4.3)$$

represents the set of available discrete values for the design variable α_b , listed in ascending order. For convenience the index p denoting the stage in the iterative design process has been dropped from Eqs. (4.1 - 4.3) as well as from Eqs. (2.19 - 2.21). However, it should be kept in mind that in general Eqs. (2.19 - 2.21) and Eqs. (4.1 - 4.3) represent only the approximate primal problem for the p^{th} stage of the overall iterative design process.

The primal variables in terms of the dual variables are given implicitly by (see Eqs. 2.31):

$$\alpha_b^{(L)} \leq \alpha_b \leq \alpha_b^{(U)} \quad \left\{ \frac{w_b}{\alpha_b} + \alpha_b \sum_{q \in Q_R} \lambda_q C_{bq} \right\} \quad (4.4)$$

and explicitly by Eqs. (2.39 - 2.41) for continuous α_b . In an analogous manner, for discrete α_b it is assumed that

$$\alpha_b \in A_b^{(D)} \quad \left\{ \frac{w_b}{\alpha_b} + \alpha_b \sum_{q \in Q_R} \lambda_q C_{bq} \right\} \quad (4.5)$$

relates the continuous dual variables to the discrete primal variables α_b .

The dual function $\ell(\vec{\lambda})$ is still given by Eq. (2.36) and the first derivatives $\frac{\partial \ell}{\partial \lambda_q}(\vec{\lambda})$ are still given by Eq. (3.13). It is apparent from Eq. (3.13) that discrete values for some of the primal variables α_b will cause discontinuities in the first derivatives of the dual function to arise. When the solution of Eq. (4.5) shifts from one value of $\alpha_b^{(k)}$ to the next $\alpha_b^{(k+1)}$ the following identity maintains continuity of the dual function

$$\frac{w_b}{\alpha_b^{(k)}} + \alpha_b^{(k)} \sum_{q \in Q_R} \lambda_q C_{bq} = \frac{w_b}{\alpha_b^{(k+1)}} + \alpha_b^{(k+1)} \sum_{q \in Q_R} \lambda_q C_{bq} \quad (4.6)$$

Equation (4.6) can be reduced to the following form

$$\sum_{q \in Q_R} \lambda_q C_{bq} = \frac{w_b}{\alpha_b^{(k)} \alpha_b^{(k+1)}} \quad (4.7A)$$

which defines hyperplanes in the dual space where the dual function $\ell(\vec{\lambda})$ exhibits first order discontinuities. The hyperplane defined by Eq. (4.7) subdivides the dual space into a half-space where $\alpha_b = \alpha_b^{(k)}$ and another half-space where $\alpha_b = \alpha_b^{(k+1)}$. Similarly the hyperplane defined by

$$\sum_{q \in Q_R} \lambda_q C_{bq} = \frac{w_b}{\alpha_b^{(k-1)} \alpha_b^{(k)}} \quad (4.7B)$$

is associated with a shift in the solution of Eq. (4.5) from $\alpha_b^{(k-1)}$ to $\alpha_b^{(k)}$ and it subdivides the dual space into a region where $\alpha_b = \alpha_b^{(k-1)}$ and another region where $\alpha_b = \alpha_b^{(k)}$.

It is apparent from the foregoing interpretation of Eq. (4.7), that the discrete primal variables α_b are explicitly related to the continuous dual variables λ_q as follows:

$$\alpha_b = \alpha_b^{(k)} \text{ if } \frac{w_b}{\alpha_b^{(k)} \alpha_b^{(k-1)}} < \sum_{q \in Q_R} \lambda_q C_{bq} < \frac{w_b}{\alpha_b^{(k)} \alpha_b^{(k+1)}} \quad (4.8)$$

In summary, the dual problem corresponding to the mixed continuous-discrete primal problem posed by Eqs. (2.19 - 2.21) and Eqs. (4.1 - 4.3) is taken to have the form: find $\vec{\lambda}$ such that $\ell(\vec{\lambda}) \rightarrow \text{Max}$ (see Eq. 2.36), subject to the nonnegativity constraints embodied in Eq. (2.37), where the continuous α_b are given in terms of the dual variables λ_q by Eqs. (2.39 - 2.41) and the discrete α_b are given explicitly by Eq. (4.8).

4.2 Characteristics of the Dual Function-Mixed Case

The explicit dual function for the mixed continuous-discrete variable case, defined by Eqs. (2.36) through (2.41) and Eq. (4.8) has the following

interesting and computationally important properties:

- (1) it is a concave function and the search region in dual space is a convex set defined by Eq. (2.37);
- (2) it is a continuous function and it has continuous first derivatives with respect to λ_q over the region defined by Eq. (2.37) except for points located in hyperplanes defined by Eq. (4.7) - these first order discontinuities are associated with shifts in the discrete variable solution of the one dimensional minimization problem represented by Eq. (4.5);
- (3) the first derivatives of $\ell(\vec{\lambda})$ are easily available because they are given by the primal constraints

$$\frac{\partial \ell}{\partial \lambda_q}(\vec{\lambda}) = u_q(\vec{\alpha}) - \bar{u}_q = \sum_{b=1}^B c_{bq} \alpha_b - \bar{u}_q \quad (4.9)$$

and on the first order discontinuity planes two distinct values of the first derivative arise, because at such a point there is a shift in the discrete value of a particular primal variable, say α_b , from $\alpha_b^{(k)}$ to $\alpha_b^{(k+1)}$ which gives

$$\frac{\partial \ell}{\partial \lambda_q}^{(k)}(\vec{\lambda}) = \sum_{j \neq b}^B c_{jq} \alpha_j + c_{bq} \alpha_b^{(k)} - \bar{u}_q \quad (4.10)$$

and

$$\frac{\partial \ell}{\partial \lambda_q}^{(k+1)}(\vec{\lambda}) = \sum_{j \neq b}^B c_{jq} \alpha_j + c_{bq} \alpha_b^{(k+1)} - \bar{u}_q \quad (4.11)$$

- (4) discontinuities of the second derivatives $\frac{\partial^2 \ell}{\partial \lambda_q \partial \lambda_k}(\vec{\lambda})$ exist

on hyperplanes in the dual space defined by Eqs. (3.11 and 3.12) for continuous α_b variables - these second order discontinuity planes locate points in the dual space where there is a change in status of the b^{th} continuous primal variable from "free" to bound.

4.3 The Pure Discrete Case

In the pure discrete variable case, the explicit dual function is piecewise linear, that is, its contours are sections of intersecting hyperplanes. The dual space is partitioned into several domains, each of which corresponds to a distinct combination of available discrete values of the primal variables. The following simple two dimensional example may help to clarify the foregoing points.

The example illustrated in Fig. 8 concerns a 2-bar truss subjected to a single horizontal load [see Ref. 30, page 59]. The vertical and horizontal displacements are limited and the problem takes the explicit form:

find α_1, α_2 such that

$$\frac{1}{\alpha_1} + \frac{1}{\alpha_2} \rightarrow \text{Min} \quad [\text{weight}] \quad (4.12)$$

and

$$\alpha_1 + \alpha_2 \leq \frac{3}{2} \quad [\text{horiz. displ.}] \quad (4.13)$$

$$\alpha_1 - \alpha_2 \leq \frac{1}{2} \quad [\text{vert. displ.}] \quad (4.14)$$

In the space of the reciprocal variables (α_1, α_2) , the continuous optimum occurs at the point $(\frac{3}{4}, \frac{3}{4})$. Only one constraint is active (horizontal displacement; see Fig. 8A). A pure discrete problem has been constructed

by restricting the cross-sectional areas of both bars to the discrete values 1, 1.5 and 2 corresponding to $\alpha_1, \alpha_2 \in \{\frac{1}{2}, \frac{2}{3}, 1\}$.

The formulation of the dual problem involves 2 dual variables associated with the two displacement constraints (4.13) and (4.14). The first order discontinuity planes are given explicitly by the equations

$$\begin{cases} \lambda_1 + \lambda_2 = \frac{3}{2} \\ \lambda_1 + \lambda_2 = 3 \end{cases} \quad \begin{cases} \lambda_1 - \lambda_2 = \frac{3}{2} \\ \lambda_1 - \lambda_2 = 3 \end{cases} \quad (4.15)$$

They subdivide the dual space in 9 regions each corresponding to a different primal point (see Fig. 8.B). The dual objective function is written

$$\ell(\lambda_1, \lambda_2) = \frac{1}{\alpha_1} + \frac{1}{\alpha_2} + \lambda_1(\alpha_1 + \alpha_2 - \frac{3}{2}) + \lambda_2(\alpha_1 - \alpha_2 - \frac{1}{2}). \quad (4.16)$$

where the primal variables α_1 and α_2 are given in terms of the dual variables λ_1 and λ_2 according to the explicit inequalities (see Eq. 4.8):

$$\begin{aligned} \alpha_1 &= 1 \quad \text{if} \quad \lambda_1 + \lambda_2 < \frac{3}{2} \\ \alpha_1 &= \frac{2}{3} \quad \text{if} \quad \frac{3}{2} < \lambda_1 + \lambda_2 < 3 \\ \alpha_1 &= \frac{1}{2} \quad \text{if} \quad 3 < \lambda_1 + \lambda_2 \end{aligned} \quad (4.17.A)$$

and

$$\begin{aligned} \alpha_2 &= 1 \quad \text{if} \quad \lambda_1 - \lambda_2 < \frac{3}{2} \\ \alpha_2 &= \frac{2}{3} \quad \text{if} \quad \frac{3}{2} < \lambda_1 - \lambda_2 < 3 \\ \alpha_2 &= \frac{1}{2} \quad \text{if} \quad 3 < \lambda_1 - \lambda_2 \end{aligned} \quad (4.17.B)$$

The contours of the dual function are represented in Fig. 8.C. The maximum of the dual problem lies at the dual point $(\frac{3}{2}, 0)$ where the dual function value is 2.75. The optimal subdomain is cross hatched in Fig. 8.B. It corresponds to the primal point $(\frac{2}{3}, \frac{2}{3})$, with the weight equal to 3.

4.4 Construction of a Unique Ascent Direction

The main difficulty associated with the explicit dual formulation of the mixed continuous-discrete variable case is linked to the existence of hyperplanes in the dual space, where the gradient of the dual function $\nabla \ell(\vec{\lambda})$ is not uniquely defined, because of the previously described first order discontinuities (see Eqs. 4.10 and 4.11). The existence of these first order discontinuity hyperplanes in dual space complicates the task of devising a computational algorithm for finding the maximum of the explicit dual function. Fortunately, it turns out that at points in the dual space where the gradient $\nabla \ell(\vec{\lambda})$ is multivalued, the orthogonal projection of each distinct gradient into the subspace defined by the set of pertinent discontinuity hyperplanes, yields a single move direction \vec{Z} and furthermore the directional derivative $(\frac{d\ell}{d\vec{Z}})$ of the dual function along the move direction \vec{Z} is unique and positive.

An intuitive understanding of the basic scheme used to cope with the existence of first order discontinuity planes can be gained by examining a simple example, with a single discontinuity hyperplane, such as that depicted schematically in Fig. 9. Let the equation of the first order discontinuity plane (line a-a in Fig. 9) be represented by (see Eq. 4.7A with $k = 1$)

$$f_b(\vec{\lambda}) \equiv \vec{\lambda}^T \vec{C}_b - \frac{w_b}{\alpha_b^{(1)} \alpha_b^{(2)}} = 0 \quad (4.18)$$

then the normal to the discontinuity plane is

$$\nabla f_b = \vec{C}_b \quad (4.19)$$

Let \vec{g}_1 and \vec{g}_2 denote the two distinct values of the gradient at point t on the first order discontinuity plane (see Fig. 9). Components of the vectors \vec{g}_1 and \vec{g}_2 are given by Eqs. (4.10) and (4.11) with $k = 1$, that is

$$g_q^{(1)} = \frac{\partial \ell^{(1)}}{\partial \lambda_q} (\vec{\lambda}_t) = h_q + c_{bq} \alpha_b^{(1)} \quad (4.20)$$

and

$$g_q^{(2)} = \frac{\partial \ell^{(2)}}{\partial \lambda_q} (\vec{\lambda}_t) = h_q + c_{bq} \alpha_b^{(2)} \quad (4.21)$$

where

$$h_q = \sum_{j \neq b}^B c_{jb} \alpha_j - \bar{u}_q \quad (4.22)$$

Rewriting Eqs. (4.20) and (4.21) in vector form gives

$$\vec{g}_1 = \vec{h} + \alpha_b^{(1)} \vec{C}_b \quad (4.23)$$

and

$$\vec{g}_2 = \vec{h} + \alpha_b^{(2)} \vec{C}_b \quad (4.24)$$

The projections of \vec{g}_1 and \vec{g}_2 into the discontinuity plane are given by

$$\vec{z} = \vec{g}_1 - \frac{\vec{C}_b^T \vec{g}_1}{\vec{C}_b^T \vec{C}_b} \vec{C}_b \quad (4.25)$$

and

$$\vec{z} = \vec{g}_2 - \frac{\vec{C}_b^T \vec{g}_2}{\vec{C}_b^T \vec{C}_b} \vec{C}_b \quad (4.26)$$

To confirm that the move direction given by Eqs. (4.25 and 4.26) is unique, simply substitute Eq. (4.23) into (4.25) or Eq. (4.24) into (4.26) to find

$$\vec{Z} = \vec{h} - \frac{\vec{C}_b^T \vec{h}}{\vec{C}_b^T \vec{C}_b} \vec{C}_b = [I - \frac{\vec{C}_b \vec{C}_b^T}{\vec{C}_b^T \vec{C}_b}] \vec{h} \quad (4.27)$$

in either case.

To show that the directional derivative along \vec{Z} is unique and positive use Eq. (4.27) and (4.23) to show that

$$\frac{d\ell}{dz} = \vec{Z}^T \vec{g}_1 = \vec{h}^T \vec{h} - \frac{(\vec{C}_b^T \vec{h})^2}{\vec{C}_b^T \vec{C}_b} \quad (4.28)$$

and use Eqs. (4.27) and (4.24) to show that

$$\frac{d\ell}{dz} = \vec{Z}^T \vec{g}_2 = \vec{h}^T \vec{h} - \frac{(\vec{C}_b^T \vec{h})^2}{\vec{C}_b^T \vec{C}_b} \quad (4.29)$$

Furthermore, since it follows from Eq. (4.27) that

$$\vec{Z}^T \vec{Z} = \vec{h}^T \vec{h} - \frac{(\vec{C}_b^T \vec{h})^2}{\vec{C}_b^T \vec{C}_b} \quad (4.30)$$

also, it is apparent that

$$\vec{Z}^T \vec{g}_1 = \vec{Z}^T \vec{g}_2 = \vec{Z}^T \vec{Z} > 0 \quad \text{if } \vec{Z} \neq \vec{0} \quad (4.31)$$

and therefore, provided $\vec{Z} \neq \vec{0}$, the directional derivative along \vec{Z} is unique and positive.

The foregoing development can be generalized to the case where the current point in the dual space $\vec{\lambda}_t$ resides in the subspace defined by P first order discontinuity planes (see Eq. 4.7). For convenience assume that the primal variables are numbered so that the first P variables are

those associated with the discontinuity planes pertinent to the current point in dual space $\vec{\lambda}_t$. The equations of these P first order discontinuity planes are

$$f_b(\vec{\lambda}) \equiv \vec{\lambda}^T \vec{C}_b - \frac{w_b}{\alpha_b^{(k)} \alpha_b^{(k+1)}} = 0; \quad b = 1, 2, \dots, P \quad (4.32)$$

At such a point in dual space there are 2^P different gradients (denote them as $\vec{g}^{(\ell)}$; $\ell = 1, 2, \dots, 2^P$) corresponding to the 2^P possible combinations of the values $\alpha_b^{(k)}$ or $\alpha_b^{(k+1)}$ for $b = 1, 2, \dots, P$ and they can be represented as follows

$$\vec{g}^{(\ell)} = \vec{h} + \sum_{b=1}^P \alpha_b^{(\ell)} \vec{C}_b; \quad \ell = 1, 2, \dots, 2^P \quad (4.33)$$

where the components of \vec{h} are given by

$$h_q = \sum_{b=P+1}^B C_{bq} \alpha_b - \bar{u}_q \quad (4.34)$$

Now the orthogonal projection operator, which will yield the projection of any vector into the subspace defined by the set of discontinuity planes, is given by [see p. 177, Ref. 58]

$$[P] = [I - N(N^T N)^{-1} N^T] \quad (4.35)$$

where I is a $Q_R \times Q_R$ identity matrix and N denotes a $Q_R \times P$ matrix with columns corresponding to the vectors $\vec{C}_1, \vec{C}_2, \dots, \vec{C}_b, \dots, \vec{C}_P$ appearing in Eq. (4.32), that is

$$[N]_{Q_R \times P} = [\vec{C}_1, \vec{C}_2, \dots, \vec{C}_b, \dots, \vec{C}_P] \quad (4.36)$$

To show that the projection of the 2^P distinct gradients (see Eq. 4.33), into the subspace defined by the P discontinuity hyperplanes (see Eq. 4.32),

yields a unique direction of travel \vec{Z} , write

$$\vec{Z} = [P]\vec{g}^{(\ell)} \quad (4.37)$$

and substitute in for $\vec{g}^{(\ell)}$ from Eq. (4.33), then

$$\vec{Z} = [P]\vec{h} + [P] \left(\sum_{b=1}^P \alpha_b^{(\ell)} \vec{C}_b \right) = [P]\vec{h} \quad (4.38)$$

$$\text{since } [P]\vec{C}_b = \vec{0} ; b = 1, 2, \dots, P \quad (4.39)$$

Furthermore it can also be shown that the directional derivative along the move direction \vec{Z} given by Eq. (4.38) is unique and positive, that is

$$\frac{d\ell}{dz} = \vec{Z}^T \vec{g}^{(\ell)} = \vec{Z}^T \vec{h} = \vec{h}^T [P]\vec{h} = ([P]\vec{h})^T [P]\vec{h} = \vec{Z}^T \vec{Z} > 0 \quad \text{if } \vec{Z} \neq 0 \quad (4.40)$$

In the DUAL 1 algorithm described in the next section, direction vectors are generated using the projection matrix, whenever the current point $\vec{\lambda}_t$ resides in one or more first order discontinuity planes. However, for computational efficiency the $[P]$ matrix is actually generated by employing update formulas rather than by using Eq. (4.35).

4.5 DUAL 1 - Gradient Projection Type Maximizer

In this section a first order gradient projection type algorithm for finding the maximum of the explicit dual function $\ell(\vec{\lambda})$ (defined by Eqs. 2.36 through 2.41 and Eq. 4.8) for mixed continuous-discrete variable problems, subject to the nonnegativity constraints of Eq. (2.37), is described. The existence of hyperplanes in the dual space (see Eq. 4.7) where the dual function $\ell(\vec{\lambda})$ exhibits first-order discontinuities, for pure discrete and mixed continuous-discrete variable problems, requires the use of a specially devised first order algorithm akin to the well known gradient

projection method. For each stage P of the overall design process, the DUAL 1 algorithm seeks $\vec{\lambda}$ such that $\ell(\vec{\lambda}) \rightarrow \text{Max}$ subject to $\lambda_q \geq 0; q \in Q_R^{(P)}$. The dual variable vector is modified iteratively as follows

$$\vec{\lambda}_{t+1} = \vec{\lambda}_t + d_t \vec{S}_t \quad (4.41)$$

The maximization algorithm consists of a sequence of one dimensional maximizations (ODM's) executed along ascent directions \vec{S}_t obtained by projecting the dual function gradient into an appropriate subspace.

To help fix ideas consider the pure discrete variable case where each ODM necessarily terminates on either a discontinuity plane or a boundary plane where some λ_q becomes zero. In either case it is possible to construct a new projection matrix by updating the old one, avoiding the costly matrix inversion which would be required if the projection matrix was obtained from Eq. (4.35). The authors are not aware of a comparably efficient scheme for directly updating the projection matrix itself when a first order discontinuity plane must be dropped from the current set, or when a zero dual variable must re-enter the set of nonzero dual variables. Since the foregoing scheme does not provide for the selection and release of discontinuity or base plane equality constraints, the maximization process can terminate at a "vertex" of the dual space [number of discontinuity planes equal to the number of nonzero ($\lambda_q > 0$) dual variables] that is not necessarily the optimum. The DUAL 1 algorithm copes with this difficulty by restarting the maximization procedure releasing all or all but one of the previously accumulated equality constraints[‡].

[‡]If the last ODM executed prior to the restart test terminated on either a discontinuity plane or a base plane, that corresponding single equality constraint is retained.

Now if the previous maximum of the dual function was really the true dual maximum, then the new updating sequence will generate the same projection matrix and the dual function maximum point will be located in the same subspace as before. On the other hand, if the previous maximum of the dual functional (just prior to the restart test) was not the true dual maximum, then the algorithm will sequentially accumulate a new set of discontinuity and boundary planes and terminate at a different vertex with a higher dual function value.

4.5.1 Direction Finding Process

Turning attention to the general mixed continuous-discrete variable case, the DUAL 1 algorithm is described using the schematic block diagram shown in Fig. 10. At each step the direction \vec{S}_t is taken as the gradient $\nabla \ell(\vec{\lambda}_t)$ or a projection of the gradient into an appropriate subspace. The scheme for generating the next search direction depends upon the nature of the previous ODM's termination point.

Initially [block 1], or when the dual point $\vec{\lambda}_t$ does not reside in any of the discontinuity planes, the move direction \vec{S}_t is taken as the gradient at $\vec{\lambda}_t$ modified so as to avoid violation of the nonnegativity constraints $\lambda_q \geq 0$; $q \in Q_R$, that is [block 2]

$$S_{qt} = 0 \quad \text{if} \quad \lambda_{qt} = 0 \quad \text{and} \quad \frac{\partial \ell}{\partial \lambda_q}(\vec{\lambda}_t) = u_q(\vec{\alpha}_t) - \bar{u}_q \leq 0 \quad (4.42.A)$$

otherwise

$$S_{qt} = \frac{\partial \ell}{\partial \lambda_q}(\vec{\lambda}_t) = u_q(\vec{\alpha}_t) - \bar{u}_q \quad (4.42.B)$$

The foregoing procedure for generating the move vector is equivalent to

projecting the gradient vector into the subspace represented by the set of base planes $\{\lambda_q = 0; q \in N\}$ where

$$N = \{q | \lambda_{qt} = 0; \frac{\partial \ell}{\partial \lambda_q} (\vec{\lambda}_t) \leq 0; q \in Q_R\} \quad (4.43)$$

Typically, at this point, the convergence test $|\vec{S}_t| < \epsilon$ [block 3] will not be satisfied, therefore go to block 4 and determine whether or not the conjugate direction modification is appropriate.

Whenever it makes sense successive move directions are conjugated to each other using the well known Fletcher-Reeves formula [see Ref. 58 p. 87]

$$\vec{S}_t \leftarrow \vec{S}_t + \beta_t \vec{S}_{t-1} \quad (4.44)$$

where

$$\beta_t = \frac{\vec{S}_t^T \vec{S}_t}{\vec{S}_{t-1}^T \vec{S}_{t-1}} \quad (4.45)$$

The second and subsequent move directions within a subspace are generated using Eqs. (4.44 and 4.45) [block 5]. In the DUAL 1 algorithm several ODM's can take place without a change in subspace, provided these ODM's do not terminate on either a new first order discontinuity plane or a new base plane. In any event the conjugacy modification is reinitialized ($\beta_t = 0$) if the number of ODM's executed within a single subspace becomes equal to the dimensionality of the subspace. The dimensionality of a subspace is equal to Q_R , less the number of zero dual variables N , less the number of first-order discontinuity planes encountered so far.

With the move direction \vec{S}_t established in block 4 or 5 go to block 6 and solve the one dimensional maximization (ODM) problem. The scheme employed to solve the ODM problem in DUAL 1 will be described subsequently,

however it should be clearly recognized that in contrast to the DUAL 2 line search scheme, which simply assures an increase in $\ell(\vec{\lambda})$, the DUAL 1 ODM accurately locates the maximum of $\ell(\vec{\lambda})$ along the direction \vec{S}_t . After solving the current ODM [block 6] there are six possible paths leading to the calculation of a new move direction \vec{S}_t in either block 15 or block 2 of Fig. 10. The six paths are summarized in Table 1 and each of them will be briefly described in the sequel:

Path 1: The updated $\vec{\lambda}_t$ emerging from block 6 does not reside in either a new discontinuity plane [block 7 \rightarrow F] nor a new base plane [block 8 \rightarrow F], but at least one first order discontinuity plane has been previously encountered [block 9 \rightarrow F]^{FOD} leading via point B to block 15, where the move direction is calculated without updating the projection matrix according to the relation

$$\vec{S}_t + \vec{Z} = [P]\vec{h} \quad (4.46)$$

which is based on Eq. (4.38).

Path 2: The updated $\vec{\lambda}_t$ emerging from block 6 does not reside in either a new discontinuity plane [block 7 \rightarrow F] nor a new base plane [block 8 \rightarrow F] and it is true that no discontinuity planes have been previously encountered [block 9 \rightarrow T] leading to block 2, where the next move direction is calculated using Eqs. (4.42.A and 4.42.B).

Path 3: The updated $\vec{\lambda}_t$ emerging from block 6 does not lie on a new discontinuity plane [block 7 \rightarrow F], but it does reside on a new

^{FOD} denotes a Boolean variable which is zero when no first order discontinuity planes have been encountered.

base plane [block 8 \rightarrow T] and no discontinuity planes have been previously encountered [block 10 \rightarrow T], leading to block 2 where the next move direction is calculated using Eqs. (4.42.A and B).

Path 4: The updated $\vec{\lambda}_t$ emerging from block 6 does not reside on a new discontinuity plane [block 7 \rightarrow F], but it does reside on a new base plane [block 8 \rightarrow T] and one or more discontinuity planes have been previously encountered [block 10 \rightarrow F], leading to block 14 where the [P] matrix is updated by letting

$$\vec{Y} \leftarrow [P]\vec{e}_q \quad (4.47)$$

where \vec{e}_q is a unit vector normal to the newly encountered base plane, and then modifying the projection matrix as follows

$$[P] \leftarrow [P] - \frac{\vec{Y}\vec{Y}^T}{\vec{Y}^T\vec{Y}} \quad (4.48)$$

The next move direction is calculated in block 15 using the updated [P] matrix from Eq. (4.48).

Path 5: The updated $\vec{\lambda}_t$ emerging from block 6 resides on a new discontinuity plane [block 7 \rightarrow T] and it is the first discontinuity plane encountered [block 11 \rightarrow T] leading to block 12 where the projection matrix is initialized according to the following procedure. Let \vec{C}_b denote the gradient to the first discontinuity plane encountered. Construct a trial projection matrix as follows

$$[P] = [I] - \frac{\vec{C}_b \vec{C}_b^T}{\vec{C}_b^T \vec{C}_b} \quad (4.49)$$

and project either value of the gradient at $\vec{\lambda}_t$ into the subspace defined by the first discontinuity plane using Eq. (4.27), that is

$$\vec{Z}_t = [P]\vec{h} \quad (4.50)$$

If $Z_{qt} < 0$ for $\lambda_{qt} = 0$ set the corresponding elements of the vector \vec{C}_b to zero ($C_{bq} = 0$) and recalculate $[P]$ and \vec{Z}_t . When $Z_{qt} \geq 0$ for all $\lambda_{qt} = 0$ the initial projection matrix has been obtained. The end result of this iteration is to generate a $[P]$ matrix that projects any vector into the subspace defined by the first discontinuity plane and the appropriate current set of $\lambda_q = 0$ base planes. The next move direction is calculated in block 15.

Path 6: The updated $\vec{\lambda}_t$ emerging from block 6 lies on a new discontinuity plane [block 7 \rightarrow T] but it is not the first discontinuity plane encountered [block 11 \rightarrow F] leading to block 13. The projection matrix is updated as follows:

$$\vec{Y} \leftarrow [P]\vec{C}_b \quad (4.51)$$

where \vec{C}_b is understood to denote the gradient to the new discontinuity plane and

$$[P] \leftarrow [P] - \frac{\vec{Y} \vec{Y}^T}{\vec{Y}^T \vec{Y}} \quad (4.52)$$

The next move direction is calculated in block 15.

4.5.2 Restart of the Algorithm

At the end of each of the six paths that may be followed after solving the ODM and updating $\vec{\lambda}_t$ [block 6] the result is a new move direction \vec{S}_t

If the new move direction has an absolute value equal to or greater than ϵ [block 3 \rightarrow F] the search for the maximum of the dual function in the current subspace continues (i.e., go to block 4). On the other hand if $|\vec{s}_t| < \epsilon$ or if the subspace defined by the set of base planes $\lambda_q = 0$; $q \in N$ and the set of P first order discontinuity planes has collapsed to a single point (i.e., $Q_R = N + P$) go to block 16. If no first order discontinuity planes have been encountered (i.e. FOD = 0 \rightarrow T] then the maximum of the dual function, subject to the nonnegativity constraints $\lambda_q \geq 0$; $q \in Q_R$, has been obtained, the stage is complete, and the values of the primal variables are stored.

On the other hand, if one or more first order discontinuity planes have been encountered [block 16 \rightarrow F], go to block 17 and make the following restart tests:

- (1) if the current value of the dual function $\ell(\vec{\lambda}_t)$ is equal to or greater than the upper bound weight[#] associated with the current $\vec{\lambda}_t$ restart and go to block 18;
- (2) if the current value of the dual function $\ell(\vec{\lambda}_t)$ is less than the upper bound weight[#] associated with the current $\vec{\lambda}_t$, compare $\ell(\vec{\lambda}_t)$ with its value when the restart block 17 was previously entered, and if the difference is small go to block 21, otherwise go to block 18.

It should be noted that unless the stage ends without encountering

[#] upper bound weight is given by selecting the smaller of the two candidate values ($\alpha_b^{(k)}$, $\alpha_b^{(k+1)}$) for each discrete primal variable (associated with a first order discontinuity plane) in calculating the weight (n.b. the primal variables α_b are reciprocal variables).

any discontinuity planes [block 16 \rightarrow T] there will always be at least one restart. Once it is determined that the maximum of $\ell(\vec{\lambda})$ subject to $\lambda_q \geq 0$; $q \in Q_R$ may not have been obtained yet, the algorithm is restarted releasing all of the previously accumulated equality constraints. However if the last ODM prior to restart terminated on either a discontinuity plane [block 18 \rightarrow T] or a new base plane [block 19 \rightarrow T] this single constraint is retained while all the others are dropped. This scheme guards against the possibility of two successive restarts leading to traversal of exactly the same sequence of subspaces. If the last ODM prior to restart is on a discontinuity plane, retention of that constraint is handled by going to block 12 and initializing the projection matrix. If the last ODM prior to restart is on a new base plane, retention of that constraint is handled by modifying Eq. (4.42.A) to read [see block 20]

$$s_{qt} = 0 \quad \text{if} \quad \lambda_{qt} = 0 \quad (4.42.A')$$

where q is associated with the base plane encountered by the last ODM prior to restart. Finally, if the last ODM prior to restart does not reside on either a discontinuity plane or a new base plane, go to block 1 and restart dropping all the previously accumulated base and discontinuity plane constraints.

4.5.3 Retrieval of the Primal Variables

For mixed continuous-discrete problems, a stage usually ends by exiting block 17 \rightarrow F and entering block 21 with a dual point $\vec{\lambda}_t$ that resides on one or more first order discontinuity planes (see Eq. 4.7). For each of these P discontinuity planes the corresponding primal variable α_b has

two candidate values denoted $\alpha_b^{(k)}$ and $\alpha_b^{(k+1)}$. The upper bound solution is obtained by selecting the smaller discrete value for each such discrete variable. If the upper bound design is feasible^{*}, the lowest weight feasible design is selected from the set of 2^P possibilities that exist. On the other hand, if the upper bound solution is not feasible, then a feasible design, or by default the design which is most nearly feasible, is selected from the set of 2^P possibilities. This is done by finding the design for which the most seriously violated constraint exhibits the smallest infeasibility. Computational experience indicates that when the upper bound design is infeasible, none of the other $(2^P - 1)$ designs are feasible.

The foregoing discrete search through 2^P possible designs is organized in such a way that, when passing from one primal candidate to the next, only one design variable changes. As a consequence, the new weight and the associated constraint values can be computed very efficiently as follows. When the b^{th} design variable changes from a discrete value $\alpha_b^{(k)}$ to the next available discrete value $\alpha_b^{(k+1)}$ [with $\alpha_b^{(k)} < \alpha_b^{(k+1)}$], the weight becomes

$$w^{(k+1)} = w^{(k)} + w_b \left[\frac{1}{\alpha_b^{(k+1)}} - \frac{1}{\alpha_b^{(k)}} \right] \quad (4.53)$$

and the corresponding constraint values are:

$$u_q^{(k+1)} = u_q^{(k)} + C_{bq} [\alpha_b^{(k+1)} - \alpha_b^{(k)}]; \quad q \in Q_R \quad (4.54)$$

The second term on the right hand side of both equations (4.53) and (4.54) can be computed and stored once and for all prior to starting the search

^{*}With respect to the approximate constraints for the p^{th} stage.

through the 2^P possible combinations of discrete primal points. Hence subsequent calculations involve only $(Q_R + 1)$ additions [or subtractions if the design variable α_b changes from $\alpha_b^{(k+1)}$ to $\alpha_b^{(k)}$] for each new candidate optimum. It is worth mentioning that, as soon as it is known that a feasible primal solution exists, all the design points for which the weight is lower than the maximum dual function value can be disregarded, because the final optimal weight must satisfy the following relation:

$$W^* = \ell^* - \sum_{q \in Q_R} \lambda_q^* (u_q^* - \bar{u}_q) \geq \ell^* \quad (4.55)$$

since

$$\lambda_q^* \geq 0 ; u_q^* - \bar{u}_q \leq 0 ; q \in Q_R \quad (4.56)$$

[Note that in Eqs. (4.55, 4.56), the superscript * is associated with optimal quantities]. As a result, if the weight computed using Eq. (4.53) turns out to be lower than ℓ^* , it is superfluous to evaluate the constraint values (Eq. 4.54) to check design feasibility and the next discrete point can be treated.

In the DUAL 1 algorithm, the discrete search through 2^P possible primal points is based on a sequence of integer numbers, each of which corresponds to a distinct discrete solution. To help understand the procedure followed, it is useful to represent each possible discrete solution as a point in a P-dimensional integer space where only two different values exist along each axis. Such a point can be described using binary coding, 0 corresponding to one discrete value and 1, to the other. This binary representation facilitates creation, in the P-dimensional integer space, of a sequence of discrete points such that, when passing from a point to

the next, only one component (0 or 1) changes (to 1 or 0). This can be achieved as follows, depending upon the value of P:

	binary coding	decimal equivalent
<u>P = 1</u>	0	0
	1	1
<u>P = 2</u>	0 0	0
	0 1	1
	<hr/> 1 1	3 (= 1+2)
	1 0	2 (= 0+2)
<u>P = 3</u>	0 0 0	0
	0 0 1	1
	0 1 1	3
	0 1 0	2
	<hr/> 1 1 0	6 (= 2+4)
	1 1 1	7 (= 3+4)
	1 0 1	5 (= 1+4)
	1 0 0	4 (= 0+4)

The foregoing developments permit construction of a computational procedure for automatically defining the sequence of discrete points to be successively processed. For example, it is easily verified that, for $P = 4$, the following sequence of integer numbers is generated:

P = 4 0 1 3 2 6 7 5 4 12 13 15 14 10 11 9 8

The difference between two successive integers in the foregoing sequence gives all information about the next discrete primal point to be processed.

The absolute value of this difference indicates the discrete number to be changed, according to the following prescription:

difference	→	discrete variable number
± 1		1
± 2		2
± 4		3
± 8		4
$\pm \dots$		\dots
$\pm 2^{P-1}$		P

If the difference is positive, then the corresponding discrete variable shifts to a smaller value. If the difference is negative, then the discrete variable changes to a larger value. With this process, all the 2^P possible primal points are taken into account without repetition and in such a way that only one design variable is modified each time.

It is important to recall that the number P of first order discontinuity planes cannot be larger than the number $(Q_R - N)$ of nonzero dual variables. In other words, the number of ambiguous design variables, for which one out of two candidate values must be selected, never exceeds the number of strictly critical behavioral constraints, which is precisely the effective dimensionality of the dual space. This number is usually small for practical problems and therefore dual methods retain their attractiveness when discrete variables are introduced.

4.5.4 One Dimensional Maximization

In the DUAL 1 algorithm, once a move direction is established (see blocks 2, 15, 4 and 5; Fig. 10), it is necessary to find the maximum of the

explicit dual function $\ell(\vec{\lambda})$ along the direction \vec{S}_t emanating from the point $\vec{\lambda}_t$, using Eq. (4.41). It follows that $\ell(\vec{\lambda})$ becomes a function of the scalar move distance d along the direction \vec{S}_t . The one dimensional maximization (ODM) of this concave function $\ell(d)$ is equivalent to seeking the vanishing point of the directional derivative (see Eq. 3.20):

$$\ell'(d) = \vec{S}_t^T \nabla \ell(\vec{\lambda}) = \sum_{b=1}^B z_{bt} \alpha_b(d) - x_t \quad (4.57)$$

where

$$z_{bt} = \sum_{q \in Q_R} s_{qt} c_{bq} \quad (4.58)$$

and

$$x_t = \sum_{q \in Q_R} s_{qt} \bar{u}_q \quad (4.59)$$

The primal variables $\alpha_b(d)$ are known explicit functions of d along the direction \vec{S}_t in dual space (by using Eqs. 2.39, 2.40 and 2.41 for the continuous variables and Eq. 4.8 for the discrete variables), except for the indices b related to the current P discontinuity planes (see Eq. 4.7) in which the gradients are projected. For these indices the discrete primal variables $\alpha_b(d)$ can take on either of two distinct values. Fortunately the corresponding values of z_{bt} happen to vanish, since the direction \vec{S}_t lies in the discontinuity planes (see Eq. 4.32), so that:

$$z_{bt} = \vec{S}_t^T \vec{C}_b = 0 ; b \in P \quad (4.60)$$

With this remark the ODM problem is uniquely defined and consists of seeking the vanishing point of $\ell'(d)$ over the interval $0 < d < d_{\max}$.

The maximum allowable step length d_{\max} is selected so that none of the dual variables can become negative. The computation of d_{\max} is accomplished employing the same scheme as in Dual 2 (see Eq. 3.19), namely

$$d_{\max} = \min_{s_{qt} < 0} \left| \frac{\lambda_{qt}}{s_{qt}} \right| \quad (4.61)$$

It should be recognized that the dual space is subdivided into several domains separated by first and second order discontinuity planes defined in Eq. (4.7) and Eqs. (3.11, 3.12), respectively. Typically the move vector \vec{S}_t will intersect the discontinuity planes at several values of d which fall in the interval $0 < d < d_{\max}$ and therefore the ODM search is subdivided into several distinct intervals within which the function $\ell'(d)$ and $\ell''(d)$ remain continuous.

Substituting Eq. (4.41) into Eqs. (3.11 and 3.12), it is easily shown that the vector \vec{S}_t intersects the second order discontinuity planes at values of d given by

$$d_b^{(L)} = \frac{w_b}{z_{bt}} \left\{ \frac{1}{[\alpha_b^{(L)}]^2} - y_{bt} \right\} ; \quad b = 1, 2, \dots, B \quad (4.62)$$

and

$$d_b^{(U)} = \frac{w_b}{z_{bt}} \left\{ \frac{1}{[\alpha_b^{(U)}]^2} - y_{bt} \right\} ; \quad b = 1, 2, \dots, B \quad (4.63)$$

where

$$y_{bt} = \sum_{q \in Q_R} \lambda_{qt} c_{bq} \quad (4.64)$$

and z_{bt} is defined by Eq. (4.58). The function $\ell'(d)$ exhibits slope discontinuities for values of d equal to the intercept distances $d_b^{(L)}$ and

$d_b^{(U)}$ (i.e., $\ell''(d)$ is discontinuous). In a similar way, the intercept distances to the first order discontinuity planes are obtained by substituting Eq. (4.41) into Eq. (4.7):

$$d_b^{(k)} = \frac{w_b}{z_{bt}} \left\{ \frac{1}{\alpha_b^{(k)} \alpha_b^{(k+1)}} - y_{bt} \right\} ; \quad \begin{matrix} b = 1, 2, \dots, B \\ k = 1, 2, \dots, n_b \end{matrix} \quad (4.65)$$

The function $\ell'(d)$ is discontinuous for values of d equal to the intercept distances $d_b^{(k)}$.

The key idea of the ODM procedure employed in DUAL 1 is that the intercept distances to first and second order discontinuity planes (see Eqs. 4.62, 4.63 and 4.65) are evaluated and used to locate either the one dimensional maximum or an appropriate uncertainty interval within which $\ell'(d)$ vanishes and both $\ell'(d)$ and $\ell''(d)$ are continuous. The procedure will be described qualitatively using Fig. 11 to help clarify the basic approach followed. It will be convenient to consider the pure continuous, pure discrete and mixed continuous-discrete cases separately.

- (1) Pure Continuous Variable Case. A hypothetical plot of the dual function versus d along the direction \vec{S}_t is shown in Fig. 11.A. With d_{\max} already known from Eq. (4.61), the intercept distances $d_b^{(L)}$ and $d_b^{(U)}$ to second order discontinuity planes (see Eqs. 4.62 and 4.63) that intersect \vec{S}_t between 0 and d_{\max} are computed and stored in ascending order (i.e., $0 < d_j < d_{\max}$; $j = 1, 2, \dots$). The slope of dual function (see Eq. 4.57) along the direction \vec{S}_t is then evaluated at each intercept location until the sign of $\ell'(d)$ changes from plus to minus [$\ell'(d_j) > 0$ and $\ell'(d_{j+1}) < 0$]. Once it is known that the maximum of $\ell(d)$ resides in the interval

$d_j < d < d_{j+1}$, in which $\ell''(d)$ is continuous, the Newton Raphson method is used to refine the location of the maximum point;

$$d^{(v+1)} = d^{(v)} - \frac{\ell'(d^{(v)})}{\ell''(d^{(v)})} \quad (4.66)$$

Referring to Eq. (4.57), it is easily verified that

$$\ell''(d) = -\frac{1}{2} \sum_{b \in \tilde{B}} \frac{z_{bt}^2 \alpha_b^3}{w_b} \quad (4.67)$$

where the set \tilde{B} is that associated with the free primal variables (see Eq. 3.5). The free primal variables are known explicit functions of d :

$$\alpha_b = \left[\frac{y_{bt} + dz_{bt}}{w_b} \right]^{-\frac{1}{2}}; \quad b \in \tilde{B} \quad (4.68)$$

The Newton-Raphson iteration described in Eq. (4.66) furnishes the point d^* where $\ell'(d^*) = 0$, which corresponds to the maximum point of $\ell(d)$ and this distance is selected as the solution of the ODM (i.e. $d_t \leftarrow d^*$).

- (2) Pure Discrete Variable Case. A representative one-dimensional plot of the dual function versus d along the direction \vec{S}_t is shown in Fig. 11.B. This plot consists of a sequence of linear segments with discontinuous first derivatives at distances $d_b^{(k)}$ locating the points where the vector \vec{S}_t intersects first-order discontinuity planes (see Eq. 4.65). With d_{\max} already known from Eq. (4.61), the intercept distances $d_b^{(k)}$ between 0 and d_{\max} are computed and stored in ascending order (i.e., $0 < d_j < d_{\max}$; $j = 1, 2, \dots$). The slopes of the dual function along the direction

\vec{S}_t are evaluated at each intercept location until the sign of $\ell'(d)$ changes from plus to minus [$\ell'(d_j^-) > 0$ and $\ell'(d_j^+) < 0$], indicating that the maximum is at d_j (i.e. $d_t \leftarrow d_j$).

- (3) Mixed Continuous-Discrete Variable Case. A representative plot of the dual function versus d is shown in Fig. 11.C. With d_{\max} already known from Eq. (4.61), the intercept distances to both first (Eq. 4.65) and second order (Eqs. 4.62 and 4.63) discontinuity planes that reside between 0 and d_{\max} are computed and stored in ascending order (i.e. $0 < d_j < d_{\max}$; $j = 1, 2, \dots$). The slope(s) of the dual function along \vec{S}_t is then evaluated at each intercept location until a sign change signals the location (see Fig. 11.C1) or trapping (see Fig. 11.C2) of the maximum. In the first case, the maximum has been located at d_j since $\ell'(d_j^-) > 0$ and $\ell'(d_j^+) < 0$ (Fig. 11.C1). In the second case, the maximum has been trapped in the interval $d_j < d < d_{j+1}$, since $\ell'(d_j^+) > 0$ and $\ell'(d_{j+1}^-) < 0$. The Newton-Raphson method (see Eq. 4.66) is then used to locate the point d^* where $\ell'(d^*) = 0$ and this distance is taken as the solution of the ODM (i.e. $d_t \leftarrow d^*$).

It is important to notice that, with this ODM procedure, the discrete primal variables do not need to be explicitly computed from Eq. (4.8), where a lot of tests have to be completed before finding the right discrete values. They are directly deduced from "status" vectors identifying the design variable (index b) and the discrete value (index k) to which each intercept distance $d_b^{(k)}$ corresponds (see Eq. 4.65). The status vectors are constructed, stored and reordered when the intercept distances

$(0 < d_j < d_{\max})$ are evaluated and put in ascending order. As a result, it is only in block 1 in Fig. 10 that the discrete primal variables are evaluated using Eq. (4.8) (i.e., in order to start or restart the maximization procedure). Subsequently, the primal variables are always determined in the ODM part of the algorithm using the intercept values and corresponding "status" vectors.

5. THE ACCESS 3 COMPUTER PROGRAM

The ACCESS^f computer programs have been developed to demonstrate the effectiveness of an automated structural synthesis capability formed by combining finite element analysis techniques and mathematical programming algorithms. The ACCESS 1 program demonstrated the efficiency of the coordinated use of approximation concepts on problems of relatively small scale, subject to simple static constraints [see Refs. 5 and 6]. Subsequently the ACCESS 2 program was developed to permit consideration of more complicated constraints than those treated in ACCESS 1 and to build a body of experience that can be used to set sound guidelines for future developments of large scale industrial application problems [see Refs. 7 and 61].

The basic ideas set forth in this work, which combine approximation concepts and the dual method formulation, have been implemented in a further improved computer program called ACCESS 3. In contrast to its predecessors ACCESS 1 and ACCESS 2, which employed feasible direction and/or interior penalty function algorithms without exploiting the special algebraic form of the explicit approximate problem (see Eqs. 2.19 - 2.22), the new ACCESS 3 program uses the dual formulation as the basis for adding two powerful optimization algorithms into the ACCESS framework (namely, DUAL 1 and DUAL 2). ACCESS 3 retains all of the ACCESS 2 capabilities as a subset and the data preparation formats are fully compatible [see Ref. 62].

^fApproximation Concepts Code for Efficient Structural Synthesis

5.1 Scope of the ACCESS 3 Code

The ACCESS 3 program assumes that the structural topology, configuration and material are preassigned parameters given by the user. The topology is specified via element-node connectivity data, the configuration is established by giving nodal positions (for the undeformed system) relative to a fixed reference coordinate system, and the given material is represented by its specific weight, stiffness, strength and thermal expansion properties. The program treats sizing quantities (i.e., truss cross-sectional areas and thicknesses of shear panel or membrane elements) as design variables. The design variables can be continuous or discrete variables. In the case of discrete variables, the user supplies the set of available values in ascending order. The ACCESS 3 code accepts user supplied side constraints on continuous design variables and a rather general capability for design variable linking is also built into the program. Move limits can also be specified restricting the percentage change in the design variables within a given stage of the overall iterative design process.

Four distinct optimization algorithms are available in the ACCESS 3 program. The user can select a specific optimizer, depending upon the nature of the constraints, the expected number of strictly critical first order approximated constraints, the number of design variables, and their continuous or discrete character. The four optimization algorithms are as follows:

- (1) the NEWSUMT optimizer implements a sequence of unconstrained minimizations technique using a quadratic extended penalty function feature [see Ref. 7];

- (2) the PRIMAL 2 optimizer uses a second order projection algorithm to generate a sequence of feasible search directions [see Ref. 30];
- (3) the DUAL 2 optimizer employs a second order Newton type of algorithm to find the maximum of the dual function when all the design variables are continuous (see Chapter 3); since it has been found to be very efficient in practice, it is the recommended option for pure continuous variable problems (see Chapter 6);
- (4) the DUAL 1 optimizer employs a gradient projection type of algorithm to maximize the dual function when the design variables are all discrete or mixed continuous-discrete (see Chapter 4); when all the design variables are continuous, the DUAL 1 algorithm reduces to a special form of the conjugate gradient method; however it is generally less efficient than the DUAL 2 optimizer for pure continuous variable problems.

The two primal optimizers (i.e., NEWSUMT and PRIMAL 2) tend to generate a sequence of steadily improved feasible designs, because they are employed to solve only partially each explicit approximate problem. This feature can be used to control the convergence of the overall optimization process when the constraints of the primary problem are highly nonlinear. On the other hand, the two dual optimizers (i.e., DUAL 1 and DUAL 2) produce a sequence of not necessarily feasible designs, because they find the "exact" solution to each of the separable approximate problems generated in sequence. However it has been observed that the design infeasibility, if any, is usually small and it decreases stage by stage.

The program includes provision for guarding against a variety of failure modes including strength, deflection, slope (relative deflections) and natural frequency limits. For truss members independent tension and compression allowables can be specified. In shear panels and isotropic membrane elements, where multiaxial stress states exist, strength constraints are introduced by limiting the value of an equivalent stress based on the distortion energy criterion. In the orthotropic membrane elements used to model fiber composite lamina at a preassigned orientation, three separate strength failure criteria options are available: the maximum strain criteria, stress interaction formulas or the Tsai-Azzi criterion [see Refs. 7 and 61]. These strength failure criteria for fiber composite lamina take into account differences in the longitudinal, transverse and shear allowables as well as differences in the tension and compression allowables. When the explicit problem is formed at each stage, all the stress and strain constraints can be replaced with either first order approximations or with zero order ones. The zero order explicit approximations are obtained using classical stress ratio formulas (see Eq. 2.58). They can be expressed as simple side constraints, which is especially beneficial when dual methods are employed. A selection criterion permits automatic subdivision of the stress and strain constraints in two categories: those requiring first order approximation (full linear Taylor series expansion) and those for which zero order approximation (side constraint) is sufficiently accurate (see Section 2.5.3).

The program also contains provisions for placing lower and upper limits on the first several natural frequencies. In addition to the structural mass, which varies as the sizing design variables change, fixed nodal

masses can also be prescribed. For example, these fixed nodal masses can be used to simulate fuel inertia or engine masses in wing problems. There are three distinct approximation options available for frequency constraints in ACCESS 3, namely, the $\lambda = \omega^2$ are approximated by: (1) a first order Taylor series in terms of the independent reciprocal sizing variables after linking; (2) a first order Taylor series in terms of the direct independent sizing variables after linking; (3) a full second order Taylor series expansion in terms of direct independent sizing variables after linking [see Ref. 63]. It should be noted that only option 1 above can be used with any one of the four optimization algorithms options (NEWSUMT, PRIMAL 2, DUAL 2, DUAL 1) available in ACCESS 3. On the other hand the NEWSUMT optimization algorithm can be used with any one of the three $\lambda = \omega^2$ approximation options. The available combinations of $\lambda = \omega^2$ approximation and optimization algorithm are shown in Table 2.

It is also important to recognize that while ACCESS 3 can handle three distinct kinds of sizing type structural optimization problems [(1) pure continuous variable problem, (2) pure discrete variable problems, and (3) mixed continuous-discrete variable problems], only the DUAL 1 optimization algorithm is applicable to pure discrete and mixed continuous-discrete problems. For the case of pure continuous design variable problems all four optimization algorithm options (NEWSUMT, PRIMAL 2, DUAL 2 and DUAL 1) are applicable and DUAL 2 is the preferred choice[†], because it will generally be the most efficient. The algorithm options available for various kinds

[†] Unless the approximation selected for the frequency constraints requires the use of NEWSUMT (See Table 2).

of problems are summarized in Table 3.

The set of finite element types available in ACCESS 3 is the same as that in its precursor program ACCESS 2. They include uniform bar (TRUSS), isotropic constant strain triangle (CSTIS), orthotropic constant strain triangle (CSTOR), isotropic symmetric shear panel (SSP), pure shear panel (PSP) and thermal shear panel (TSP) element types. The program data structure can accommodate four additional finite element types. A detailed description of the basic characteristics of the six element types currently included will be found in Appendix A of Refs [61 and 62]. All finite element types include provisions for representing thermal and body force loads. For each of several distinct loading conditions temperature changes and gravity field loads may be specified. These design variable dependent loads are included in addition to specified external applied loading conditions. The external applied loads may take the form of specified pressure loadings and/or given nodal forces for each loading condition. The objective function in ACCESS 3 is taken to be the total weight of the idealized finite element representation of the structural system.

The ACCESS 3 computer program is a research type program, however, it is capable of treating example problems that are large enough to clearly demonstrate the generality and efficiency that can be achieved by combining approximation concepts and dual methods. Such research programs provide a knowledge and experience base on which to build full scale analysis/synthesis capabilities for widespread use by industry. The current version of ACCESS 3 has a data structure which permits it to handle problems with up to 1000 finite elements, 600 displacement degrees-of-freedom, 200 independent design variables and 20 distinct load conditions. The current problem size limits

are due primarily to the restriction that the compact vector form of the system stiffness and mass matrices must fit in core simultaneously. A further discussion of restrictions and limitations applicable to both[†] ACCESS 2 and 3 will be found in Section 2.3 of Ref. [62].

In summary, the main feature of ACCESS 3 lies in the joining together of approximation concepts and dual methods. This solution scheme can be interpreted as a generalized optimality criteria method. Another new capability is the zero order approximation of the stress constraints based on the conventional "Fully Stressed Design" optimality criterion. Therefore the ACCESS 3 program can be regarded as an advanced research tool where mathematical programming and optimality criteria approaches coalesce to provide an efficient and reliable structural weight minimization method.

5.2 Program Organization

The organization of the ACCESS 3 computer program is, in principle, similar to that of its precursor ACCESS 2. The function of the "preprocessor" (see Fig. 12) is to compute and store all necessary information that is independent of the design variables after linking. A typical stage in the overall iterative design process begins with the control block supplying a "primal trial design" to the "approximate problem generator" block (see Fig. 12). This primal trial design is subjected to a detailed finite element structural analysis and the results are used to evaluate all of the constraints. Deletion techniques are employed to temporarily drop unimportant constraints. This is followed by calculation of partial derivatives

[†]The only additional limitations on problem size for ACCESS 3 arise from storage requirements for discrete variable data sets.

(sensitivity analysis) and construction of first or zero order explicit approximations for the constraints that survived the deletion process.

The approximate primal problem for the p^{th} stage is passed back through the design process control block and this primal problem plus a set of initial trial values for the dual variables (if the DUAL 1 or DUAL 2 option has been selected) or the primal variables (if the NEWSUMT or PRIMAL 2 option has been selected) are handed off to the optimization algorithm block. In the case of dual methods, which are of primary interest herein, the explicit dual function is formed and its maximum is then sought (subject to nonnegativity constraints on the dual variables). If all the design variables in the primal problem are continuous, either algorithm (DUAL 1 or DUAL 2) may be used, but the second order Newton type maximizer of DUAL 2 is recommended because it is usually more efficient. For problems where the design variables are all discrete or mixed continuous-discrete, the DUAL 1 algorithm must be used, because it can accommodate the local discontinuities in gradient of the dual function which arise in such problems. It should be emphasized that when dual methods are used, a precise solution to the approximate problem posed at each stage p is sought while when interior point penalty function methods (i.e., NEWSUMT optimizer) or projection methods (i.e., PRIMAL 2 optimizer) are used in primal space, the goal of each stage is to produce an improved noncritical design (as in ACCESS 1 and 2).

Once the set of dual variable values corresponding to the maximum of the dual function for the p^{th} stage has been found, the corresponding set of primal variables is stored. This improved set of primal variables is then subject to an overall design process convergence test and if con-

vergence has not been achieved, the improved set of primal variables (as well as the associated dual variables⁷) are passed back to the design process control block and another stage begins. It should be clearly recognized that only one detailed finite element structural analysis is executed per stage and none of the constraints included in the original problem statement are permanently deleted (unless they are strictly redundant).

In summary, one stage of iteration includes one finite element structural analysis, one constraint deletion process, one sensitivity evaluation for retained constraints, and one optimization of an approximate problem using either primal or dual algorithms. Since the final design is subjected to a detailed finite element analysis, the total number of structural analyses equal the number of iteration stages plus one. The iterative design process is terminated when one of the specified convergence criteria is satisfied, which will be typically after about 10 redesign stages.

⁷The dual variables generated at the end of a stage are used as a starting point for the next maximization problem.

6. NUMERICAL EXAMPLES

In this chapter, detailed results for various structural optimization problems are presented. For pure continuous variable problems, attention is focused on results obtained with the DUAL 2 optimizer and efficiency is assessed using comparable results obtained with the previously available [Refs. 5-7] NEWSUMT algorithm. The numerical results reported here indicate that the improved analysis/synthesis capability developed by combining dual methods and approximation concepts is remarkably efficient. Computational effort expended in the optimization portion of the program is reduced dramatically in representative examples (by at least a factor of ten) and the total computer time required to converge the overall optimization process is also reduced significantly. Results for pure discrete and mixed continuous-discrete variable problems show that although the extension of dual methods represented by the DUAL 1 optimizer is lacking in mathematical rigor, it appears to have promise as a practical design tool (see Chapter 4). Unless otherwise specified, all problems have been run using a single precision version of ACCESS 3 on the IBM 360/91 at CCN, UCLA.

6.1 10-Bar Truss (Problem 1)

In this section, consideration is given to the planar 10-bar cantilever truss shown on Fig. 13. The structure is subject to a single load condition consisting of 444.8 kN (100 kip) downward loads applied at nodes 2 and 4 (see Fig. 13). The truss element material properties, as well as initial cross-sectional area, minimum member size and displacement limits, are summarized in Table-4. Detailed tabular input data can be found in Ref. [5], where this

example was designated as problem 3. Note that only lower limit side constraints are imposed on the member sizes and uniform stress limits are prescribed. No design variable linking is specified and therefore this problem has ten independent design variables. Several cases will be considered; they include pure continuous, pure discrete and mixed continuous-discrete variable cases.

6.1.1 Case A: Equality Constraints on Displacements

An interesting feature of the dual algorithms implemented in ACCESS 3 is that they permit treatment of equality constraints (simply by assigning the same value to the lower and upper limits). As an example, the previously described ten bar truss problem is considered with equality constraints on the vertical displacements at nodes 1 [-5.08 cm (-2.0 in)] and 3 [-2.54 cm (-1.0 in)], in addition to the usual stress limitations and side constraints (see Table 4; Case A). The iteration history presented in Table 5 shows that the DUAL 2 algorithm generates the optimal design after only 9 reanalyses, despite the difficulty of the problem. Table 5 also gives for each stage, the values of the constrained displacements and of the stress in member 6, which reaches the allowable limit [$172,375 \text{ kN/m}^2$ (25,000 psi)] at the optimal design. The final design presented in Table 6 is identical to that given in Ref. [30], where this problem was first solved.

6.1.2 Case B: Pure Continuous Problem

The ten-bar truss problem will now be discussed in its conventional form, namely with inequality constraints imposed on the displacements in the Y direction for all nodes [$\pm 5.08 \text{ cm}$ ($\pm 2.0 \text{ in}$)]. Stress limitations [$\pm 172,375 \text{ kN/m}^2$ ($\pm 25,000 \text{ psi}$)] and minimum area [0.6452 cm^2 (0.1 in^2)] constraints are also taken into account. The final designs presented in Table 6

and the iteration history data given in Table 7 and plotted in Fig. 14 permit comparison of the results generated by ACCESS 3 using the NEWSUMT and DUAL 2 optimizers for the pure continuous variable case. It can be seen that when compared to NEWSUMT, DUAL 2 leads to a significant improvement in the rate of convergence, a lower final mass and a dramatic reduction in the amount of computer time required by the optimizer (see Table 7). For comparison with previously published results for this now classical problem, Refs. [5 and 30] can be consulted, where various mathematical programming and optimality criteria techniques are discussed.

It is well known that the 10-bar truss problem presents at least two distinct local optima [2302.78 kg (5076.67 lbm) and 2295.60 kg (5060.85 lbm); see Refs. 30, 34 and 64]. The present approach, combining approximation concepts and dual methods, leads to the lowest mass design [2296 kg (5061 lbm)] in 13 reanalyses. The optimal design with mass 2296 kg (5061 lbm) exhibits the interesting property that member 5 is simultaneously constrained by stress and minimum size limitations. Only one displacement constraint is strictly critical (node 2), while the displacement constraint at node 1 is almost critical [$5.057 \text{ cm} < 5.080 \text{ cm}$ ($1.991 \text{ in} < 2.0 \text{ in}$)]. With regard to the final design generated by NEWSUMT [2309 kg (5090 lbm)], the downward vertical deflections at nodes 1 and 2 both attain the limiting value and no stress constraint is critical.

It should be noted that the iteration history data given in Table 7 for this example (Case B; pure continuous case) contains both the unscaled and scaled mass (feasible, strictly critical) for each iteration using DUAL 2. The iteration history for NEWSUMT contains the unscaled mass only since NEWSUMT generates a sequence of feasible, noncritical designs.

6.1.3 Case C through Case E: Assessment of DUAL 1

In order to validate the DUAL 1 optimizer, several simple discrete problems have been derived from the foregoing 10 bar truss example. The data are the same as in the previous case, except that for all or some members, the cross-sectional areas can only take on the available discrete values given in Table 8. These values have been selected as follows: they are the numbers $\{6.452 \text{ cm}^2, 12.904 \text{ cm}^2, 19.356 \text{ cm}^2, \dots, 25.08 \text{ cm}^2\}$, that is the integer sequence $\{1 \text{ in}^2, 2 \text{ in}^2, 3 \text{ in}^2, \dots, 40 \text{ in}^2\}$ in which the optimal values of the design variables obtained in the pure continuous case have been inserted. In each of the test cases to be discussed subsequently (pure discrete and mixed continuous-discrete), the DUAL 1 optimizer should be capable of retrieving the previously generated continuous variable optimum design with a mass of 2296 kg (5061 lbm). The results are summarized in Table 7 under the headings Case B through Case E. Case B is the pure continuous problem, previously described. Case C is the pure discrete problem, where all the cross-sectional areas can only take on the available discrete values given in Table 8. Case D is a mixed discrete-continuous problem, where only the design variables 1, 3, 6, 8 and 10 are discrete. Case E is also a mixed discrete-continuous problem, where now the only discrete variables are those numbered 2, 4, 5, 7 and 9. The iteration histories given in Table 7 illustrate the efficiency of DUAL 1. In all cases, the expected optimal solution is retrieved [2296 kg (5061 lbm)], within 13 to 15 iterations.

6.1.4 Case F: Pure Discrete Problem

Finally, Case F is another pure discrete variable problem where the set of available discrete values is $\{0.6452 \text{ cm}^2, 3.226 \text{ cm}^2, 6.452 \text{ cm}^2, 9.678 \text{ cm}^2, 12.904 \text{ cm}^2, 16.130 \text{ cm}^2, \dots\}$, that is the sequence $\{0.1 \text{ in}^2, 0.5 \text{ in}^2, 1.0 \text{ in}^2, 1.5 \text{ in}^2, 2.0 \text{ in}^2, 2.5 \text{ in}^2, \dots\}$. Unlike Cases C

through E, this set no longer contains the optimal continuous solution values of the design variables. The iteration history is given in Table 7 and it is not very different from the iteration history for the pure continuous variable case (i.e., case B). The final design given in Table 6 is slightly infeasible (0.04%), which explains why the mass for this pure discrete case [2295 kg (5060 lbm)] is lower than the mass obtained in the pure continuous case [2296 kg (5061 lbm)]. It should be noted that the design generated at iteration 11 [2303 kg (5078 lbm)] is feasible and it could be chosen as the final design (see Table 7, case F and Table 6).

It is worth mentioning that all the masses given in Table 7 do not correspond to a feasible design. This is because a dual solution scheme is used, yielding the exact solution to each explicit approximate problem (see Eqs. 2.19 - 2.22). Furthermore, when discrete variables are involved scaling cannot be used to produce a feasible critical design after each full structural analysis.

6.2 25-Bar Truss (Problem 2)

Attention is now focused on the 25-bar space truss represented in Fig. 15. The structure is assumed to be symmetric with respect to both the X-Z and Y-Z planes and therefore the problem involves eight independent design variables after linking in order to impose symmetry (see Table 11 for the linking scheme). Material properties and other data sufficient to fully describe the problem are given in Table 9. Constraints are placed on member sizes [0.06452 cm^2 (0.01 in^2) minimum area], displacements in X, y and Z directions for the two upper nodes [$\pm 0.889 \text{ cm}$ ($\pm 0.35 \text{ in.}$)], tensile stresses [$275,800 \text{ kN/m}^2$ (40,000 psi)] and compressive stresses (reduced

stress limits based on the Euler buckling formula; see Ref. 5, Problem 5). Two distinct loading conditions are applied to the structure. Several cases will be considered, including pure continuous and pure discrete variable problems.

6.2.1 Case A: Pure Continuous Problem

The NEWSUMT and DUAL 2 options of the ACCESS 3 program have been employed to solve the 25-bar truss problem with all continuous design variables. Detailed numerical results are given in Tables 10 and 11, while Fig. 16 presents the iteration histories graphically. Again the use of the DUAL 2 algorithm dramatically reduces the computer time expended in the optimizer portion of the program and improves the convergence properties of the overall optimization process. Only 3 reanalyses are sufficient to produce a nearly optimal design (within 0.4% of the final mass) and convergence is achieved after 6 reanalyses (see Table 10). For this problem, the truncation procedure used in ACCESS 3 [see Refs. 5-7] does not significantly reduce the number of potentially active constraints retained at each stage. In the last iteration, 13 constraints are still retained, which is larger than the number of independent design variables (eight). However, the efficiency of the DUAL 2 optimizer is not adversely affected, because the effective dimensionality of the dual problem does not exceed the number of strictly active, linearly independent constraints (three). At the optimum design, the critical constraints are the Y components of displacements at nodes 1 and 2 under both load conditions as well as the compressive stress in member 19 and 20 (both in linking group 7) under load condition 2.

In this particular example the dual method approach generates a sequence of feasible, noncritical designs despite the fact that the explicit approximate problem is solved completely, rather than partially (NEWSUMT), during each redesign stage. As a result, scaling down the design variables to generate a critical design leads to further reduction in the structural mass (see Table 10; DUAL 2 scaled and unscaled mass). It can also be observed that the iteration history produced by the DUAL 2 algorithm is the same as the one generated by the generalized optimality criterion [Ref. 30] and it is also very similar to the iteration history of the conventional optimality criteria technique reported in Ref. [13]. These results offer numerical confirmation of the fact that the general (mathematical programming based) capability represented by ACCESS 3 generates, with comparable efficiency, iteration histories and final designs that are very similar to those produced by conventional optimality criteria techniques. This parallel performance is observed and can be expected for those problems where conventional optimality criteria techniques are found to be adequate.

6.2.2 Case B through Case D: Pure Discrete Problems

The 25-bar truss is one of the few discrete problems for which a reference solution is available in the literature [see Ref. 65]. Therefore, it offers an opportunity to relate the present work to past experience on discrete variable problems. The data are the same as for the pure continuous case (Case A). The available discrete values for the cross-sectional areas are given in Table 8 for the three cases under consideration. The differences between two successive values are $[0.6452 \text{ cm}^2 \text{ (} 0.1 \text{ in}^2 \text{)} \text{ Case B}]$, $[2.5808 \text{ cm}^2 \text{ (} 0.4 \text{ in}^2 \text{)} \text{ Case C}]$ and $[5.1616 \text{ cm}^2 \text{ (} 0.8 \text{ in}^2 \text{)} \text{ Case D}]$. Case A is the pure

continuous case. The iteration histories generated by DUAL 1 are given in Table 10 while the final designs are compared in Table 11 with solutions reported in Ref. [65] for Cases C and D. In all cases, ACCESS 3 produces very good results. It leads to plausible designs (when compared with the continuous solution), which are superior to those given in Ref. [65]. It is interesting to note that all designs presented in Table 11 are feasible. Comparison of the minimum mass achieved in Cases B, C and D gives a quantitative measure of the increasing mass penalty (1.4%, 5.5%, 14.6%) associated with larger increments between available discrete member sizes.

6.3 72-Bar Truss (Problem 3)

In this section, attention is directed to the 72-bar four level skeletal tower depicted in Fig. 17. Definition data for this widely studied example are summarized in Table 12. In addition to stress [$\pm 172,375 \text{ kN/m}^2$ ($\pm 25,000 \text{ psi}$)] and minimum area [0.6452 cm^2 (0.1 in^2)] constraints, displacement limits [$\pm 0.635 \text{ cm}$ ($\pm 0.25 \text{ in}$)] are imposed on the four uppermost nodes in the X and Y directions. Two distinct loading conditions are applied (see Table 12). By symmetry the problem involves 16 independent design variables after linking (see Table 14 for the linking scheme). In this example, the capability available in ACCESS 3 of treating the stress constraints by using zero order explicit approximations is exploited (see Section 2.5.3). The program automatically finds out that none of the stress constraints has to be first order approximated, so that, at each stage, all stress constraints are replaced with simple side constraints.

The numerical experiment conducted in Section 2.4.1 with a three bar truss example was reproduced with the 72 bar truss problem. Namely, the problem was solved using the NEWSUMT option of ACCESS 3, with different values

for the control parameters, in such a way that increasingly exact solutions are generated for each explicit approximate problem. The iteration history data given in Table 13 and plotted in Fig. 18 clearly show that the more precise solutions of the explicit problems lead to faster convergence of the mass, with respect to the number of structural reanalyses. In the limiting case where the explicit problems are solved exactly at each stage, the NEWSUMT optimizer would of course generate the same sequence of design points as the DUAL 2 optimizer. In addition to the iteration history data corresponding to NEWSUMT and DUAL 2, Table 13 and Fig. 18 also contain results produced by conventional optimality criteria techniques. The close similarity between the results from ACCESS 3 [NEWSUMT (0.1x3) or DUAL 2 options] and those of Refs. [15, 17 and 30] numerically confirms the interpretation of the dual method approach as a generalized optimality criteria method (see Section 2.5).

For the final design obtained with ACCESS 3 [as well as with the methods of Refs. 15, 17 and 30], the critical constraints are the compressive stress in members 1 through 4 (linking group 1) under load condition 2, the X and Y displacements of node 1 under load condition 1 and the minimum member size requirements for the members of linking groups 7, 8, 11, 12, 15 and 16. The member sizes corresponding to this design are given in Table 14.

6.4 63-Bar Truss (Problem 4)

The next example involves a 63 bar-truss idealization of the wing carry through box for a large swing wing aircraft subject to two distinct loading conditions (see Fig. 19). Detailed data defining this problem are given in Table 15 (see Table 17 for element-node connectivity data). Minimum mass

design is sought considering stress and minimum size constraints [$\pm 689,500$ kN/m^2 (100,000 psi) and 0.06452 cm^2 (0.01 in^2) limits, respectively], as well as a torsional rotation limit. The torsional rotation constraint is introduced by imposing an upper bound [2.54 cm (1.0 in)] on a relative displacement of nodes 1 and 2 in the x direction. Since design variable linking is not used, the problem involves 63 independent design variables. The problem was first proposed in Ref. [17] and it has been studied further in Refs. [5, 6, 7, 30, & 32].

In Table 16, the iteration history data reported in these references are compared with the results generated by ACCESS 3. The NEWSUMT option leads to a sequence of noncritical feasible designs with monotonically decreasing mass, which corresponds well to the primal philosophy of this solution scheme. Once again, when the explicit approximate problem is solved with more accuracy at each stage, the convergence of the mass becomes faster, but the computational cost increases substantially [when passing from NEWSUMT (0.5x1) to NEWSUMT (0.5x2) in Table 16]. Solving each explicit approximate problem exactly using the DUAL 2 optimizer yields a sequence of infeasible designs (unscaled masses in Table 16). Consequently scaling produces feasible mass from one iteration to the next (scaled masses in Table 16). A graphical comparison of NEWSUMT and DUAL 2 performance is shown in the convergence curves of Fig. 20. The net result is that DUAL 2 furnishes an optimal design after a smaller number of structural reanalyses than NEWSUMT, at a much lower computational cost (60 sec for DUAL 2 and 163 sec for NEWSUMT). It is worthwhile noticing that the computer time expended in the optimizer portion of the program remains small when DUAL 2 is employed, despite the relatively large dimensionality of the dual problem at each stage (25 strictly

active behavior constraints at the optimum design).

The final design generated by ACCESS 3 (DUAL 2 option) is compared in Table 17 to those reported in Refs. [5, 17, and 30]. Except for the design of Ref. [17], all the other designs are very close to each other and they exhibit essentially the same set of critical constraints, namely: torsional rotation limit under load condition 2; minimum member size for elements 19, 20, 23, 24, 25, 29, 58, 59, 60, 61, 62, and 63; tension stress under load condition 1 for members 2, 4, 6, 8, 10, 12, 14, 16, 17, 21, 28, and 29; and compression stress under load condition 1 for members 1, 3, 5, 7, 9, 11, 13, 15, 18, 22[†], 50, and 51.

Looking at the results produced by the optimality criteria technique of Ref. [17] (see Tables 16 and 17), it appears that these results, without being as good as those generated by DUAL 2, are nevertheless acceptable for practical purposes. Since the approach of Ref. [17] employs the computationally inexpensive fully stressed design (FSD) concept to treat the stress constraints, it can be expected that the zero order stress approximation feature of ACCESS 3 should be efficient for solving the 63-bar truss problem. Using this capability, each retained potentially critical stress constraint is replaced with its first order approximation only if the test stated in equation (2.59) is satisfied within a given tolerance, which must be supplied by the user [see Ref. 62]. The parameters permitting control over stress constraint approximations and deletion were chosen as follows:

EPS - initial	= 0.4	TRF - initial	= 0.01
EPS - min	= 0.1	TRF - max	= 0.8

[†]Compression stress in member 22 is not critical in the design of Ref. [5].

EPS - multiplier = 0.6

C - cutoff = 1.0

TRF - multiplier = 3.0

[see Ref. 62; Section 4.XVIII for EPS and Section 4.XIX for TRF]. The iteration history and runtime data obtained with these control parameter values are presented in Table 16 under the heading "DUAL 2 (with FSD)", as opposed to the results obtained with DUAL 2 when first order approximation is used for all the stress constraints ["DUAL 2 (without FSD)"]. It can be seen that the convergence characteristics of the overall optimization process remain attractive when zero order approximation is employed for representing part of the set of critical stress constraints. Also, the computational cost is reduced further. It is emphasized that only 13 out of 30 retain potentially active stress constraints are selected as requiring first order approximation. All the other stress constraints are replaced with side constraints, using a stress ratio formula (see Section 2.5.3). As a result, the dimensionality of the dual space, which is equal to the number of linearized behavior constraints, decreases and the cost related to the DUAL 2 optimizer is reduced substantially. Among the 14 linearized constraints (13 stress constraints and 1 slope constraint), 9 are found to be critical by DUAL 2, so the effective dimensionality of the dual problem never exceeds 10 during the optimization process (see Section 3.3).

6.5 Swept Wing Model (Problem 5)

The example problem treated in this section was set forth in Ref. [5]. The system considered represents an idealized swept wing structure shown in Fig. 21. The structure is taken to be symmetric with respect to the X-Y plane which corresponds to the wing middle surface. The upper half of the swept wing is modeled using sixty constant strain triangular (CST)

elements to represent the skin and seventy symmetric shear panel (SSP) elements for the vertical webs. Extensive but plausible design variable linking is employed and the total number of independent design variables after linking is eighteen, 7 for the skin thickness (see Fig. 22.A) and 11 for the vertical webs (see Fig. 22.B). The wing is subject to two distinct loading conditions and the material properties are representative of a typical aluminum alloy. Detailed input data for this problem including material properties, initial design, nodal coordinates, applied nodal loadings and constraint specification will be found in Tables 18 - 20. Element-node connectivity data and the linking scheme are depicted schematically in Fig. 21 and 22, respectively, and they can also be found in tabular form in Ref. [5], where this problem was designated as Problem 9.

The minimum mass optimum design of this idealized swept wing structure is sought, subject to the following constraints: (1) tip deflection is not to exceed 152.4 cm (60 in) at nodes 41 and 44 in Fig. 21; (2) Von Mises equivalent stress is not to exceed $172,375 \text{ kN/m}^2$ (25,000 psi) in any finite element; (3) minimum gage of skin and web material is not to be less than 0.0508 cm (0.020 in). Two cases will be considered, corresponding to pure continuous and pure discrete design variable problems. It should be noted that, unlike the other examples presented in this report, the swept wing problem was run using a double precision version of ACCESS 3 on the IBM 360/91 at CCN, UCLA.

6.5.1 Case A: Pure Continuous Problem

The pure continuous design variable case was run using both the NEWSUMT and the DUAL 2 optimizer options available in the ACCESS 3 program. Iteration history and runtime data are presented in Table 21. Iteration histories are also plotted in Fig. 23. Detailed material distribution data for the final design obtained are given in Table 22. Previously reported results from Refs. [5 and 28] are included in Tables 21 and 22, as well as in Fig. 23, to facilitate comparison. In Table 21, the unscaled DUAL 2 results correspond to a sequence of "exact" solutions obtained for each approximate primal problem and the mass at iteration 2 does not correspond to a feasible design. The scaled DUAL 2 results in Table 21 are all feasible and critical. They are obtained by scaling the "exact" solutions for each approximate problem so that a feasible design with at least one strictly critical constraint is produced. In Fig. 23, the convergence curve corresponding to DUAL 2 is plotted using the feasible scaled mass values of Table 21. It is emphasized that this procedure was employed for all examples previously discussed in this report (i.e., iteration history plots contain only feasible design points).

Examining Tables 21 and 22, it is seen that the final mass values and material distributions obtained by using the NEWSUMT and DUAL 2 options of ACCESS 3 are for practical purposes essentially the same. Those results are also seen to be in excellent agreement with those previously reported in Refs. [5 and 28]. Comparing the DUAL 2 results with the NEWSUMT results, both obtained with the ACCESS 3 program, it is seen that the advantages of using the dual approach are:

- (1) the number of structural analyses required for convergence drops from 10 (NEWSUMT) to 5 (DUAL 2);
- (2) the final mass obtained with DUAL 2 after 5 analyses is 0.5% lower than the final mass generated by the NEWSUMT option after 10 stages;
- (3) the total CPU time is reduced from 37.0 seconds for NEWSUMT to 19.4 seconds for DUAL 2;
- (4) the computer times expended in the optimizer part of the ACCESS 3 program are 4.5 seconds and 0.5 seconds for NEWSUMT and DUAL 2 respectively.

Note that the ACCESS 3, DUAL 2 total CPU time (Table 21) for the swept wing problem (19.4 seconds) is lower than the ACCESS 1 CPU time (21.5 seconds) in spite of the fact that ACCESS 1 is an all core program limited to relatively small problems. It should be recognized that ACCESS 3, by virtue of its greater generality and problem size capacity, carries a computational overhead burden (e.g., extensive use of auxiliary storage, etc.) when it is compared with programs like ACCESS 1 or that reported in Ref. [28]. Finally, it should be noted that the DUAL 2 final design has the following set of critical constraints: (1) minimum gage size for the skin elements 49-60 (see Fig. 21) in the outboard skin panel; (2) combined stress criteria in skin elements 8, 14 and 20 under load condition 1; combined stress criteria in web elements 20, 21, 30, 58 and 61 under load condition 1 as well as web elements 3, 5 and 42 under load condition 2. Several other stress constraints are nearly critical, but they are not identified as active constraints by the

DUAL 2 algorithm. This set of critical constraints at the DUAL 2 final design is essentially the same as that reported in Ref. [5] for the NEWSUMT final design (see Fig. 25 of Ref. 5).

6.5.2 Case B: Pure Discrete Problem

A pure discrete design variable problem was derived from the previously described swept wing example, by assuming that the skin and web thicknesses can only take on the discrete values given in Table 8 for problem 5. These discrete values are representative of available gage sizes of aluminum sheet metal (2024 Aluminum Alloy). The other input data are the same as in the pure continuous case (see Tables 18 - 20). The iteration history and runtime data obtained with the DUAL 1 optimizer are presented in Table 21. Only 6 reanalyses are needed to obtain a discrete optimum design. It should be noted that this solution is generated by DUAL 1 in less computer time than that required by NEWSUMT to yield a continuous optimum design.

The final discrete design produced by DUAL 1 is given in Table 22. For comparison, another discrete design is also presented, which is deduced from the continuous optimum design by rounding up all the thicknesses to the nearest available discrete value. It is seen that the DUAL 1 solution is 4% lighter than the intuitively derived design (both designs are feasible).

6.6 Delta Wing (Problem 6)

The last example treated here is a thin (3% thickness ratio) delta wing structure with graphite-epoxy skins and titanium webs. The problem

has been previously studied in Refs. [5, 6 and 7]. The structure is symmetric with respect to its middle surface which corresponds to the X-Y plane in Fig. 24. The skins are assumed to be made up of 0° , $\pm 45^\circ$ and 90° high strength graphite-epoxy laminates. It is understood that orientation angles are given with respect to the X reference coordinate in Fig. 24, that is material oriented at 0° has fibers running spanwise while material at 90° has fibers running chordwise. The laminates are required to be balanced and symmetric and they are represented by stacking four constant strain triangular orthotropic (CSTOR) elements in each triangular region shown in Fig. 24. Therefore, the upper half of the delta wing is modeled using $4 \times 63 = 252$ CSTOR elements to represent the skin and 70 symmetric shear panel (SSP) elements for the vertical webs. According to the linking scheme depicted in Fig. 25, it can be seen that the total number of independent design variables is equal to 60 made up as follows: 16 for 0° material; 16 for $\pm 45^\circ$ material; 16 for 90° material; and 12 for the web material.

The graphite epoxy and titanium material properties used in the delta wing example are listed in Table 23. The nodal coordinates defining the layout of the idealized structure shown in Fig. 24 are specified in Table 24. The wing is subjected to a single static load condition that is roughly equivalent to a uniformly distributed loading of 6.89 kN/m^2 (144 psf). The corresponding nodal force components are given in Table 23. It should be noted that, since some of the fiber composite allowable strains are different in tension and compression, the structural analysis of the symmetric delta wing must consider two loading conditions, the second load condition

being simply the negative of the first. Designing the upper half of the symmetric wing for both load conditions is then equivalent to designing the entire wing for one load condition while imposing midplane symmetry. Static deflection constraints of ± 256.0 cm (± 100.8 in) are imposed at the wing tip nodes (see Table 23). The strength requirements for the laminated skins are based on the maximum strain failure criterion [see Refs. 7, 61, and 62]. In addition, the fundamental natural frequency is required to be larger than 2 Hz, while fixed masses simulate fuel in the wing. The fuel mass distribution employed is taken to be roughly proportional to the wing depth distribution (see Table 25). Minimum gage requirements are also specified [0.0508 cm (0.02 in) for the titanium webs and 0.0127 cm (0.005 in) for the fiber composite lamina]. The thermal analysis capability of ACCESS 3 was also employed in this delta wing problem. It is assumed that the wing is subjected to the static loading conditions previously described while operating at a uniform soak temperature of -34.44°C (-30°F). The laminated skin and the webs are considered to be stress free at 76.7°C (170°F) and 21.1°C (70°F), respectively. Therefore, the mechanical load conditions are combined with the following temperature change inputs:

- (a) -129°C (-200°F) in the laminated fiber composite skins; and
- (b) -73.3°C (-100°F) in the titanium webs.

In this connection, it is important to point out that ACCESS 3 contains special features for handling midplane symmetric wing structures when temperature change effects are taken into account. The thermal analysis, with its midplane symmetric response, is treated separately from the midplane antisymmetric response due to the pressure loading and the results are then

superimposed [see Refs. 61 and 62].

The problem studied here has its genesis in an interesting scenario presented in Ref. 7. Using an all titanium structure it was possible to obtain a satisfactory wing weight even when a 2 Hz lower limit was placed on the fundamental frequency. However, when fixed fuel mass was added to the wing, it was necessary to introduce fiber composite skins in order to avoid an unacceptable increase in the minimum mass (approximately a factor of 4). Initially a high modulus graphite epoxy fiber-composite was employed, however subsequent consideration of temperature induced stresses made it necessary to switch to a high strength graphite-epoxy material. In this report the final version of the delta wing problem (Case 3B of Ref. 7) will be reconsidered using the dual method approach. It should be recalled that this problem involves:

- (1) the use of a laminated high strength graphite-epoxy skin;
- (2) temperature change effects;
- (3) consideration of fixed fuel mass;
- (4) a 2 Hz lower limit on the fundamental natural frequency
(which is a primary design driver).

6.6.1 Case A: Pure Continuous Problem

Initially the foregoing delta wing example will be studied as a pure continuous problem, with exactly the same data as in Ref. [7]. The aim is simply to compare the efficiency of the NEWSUMT and DUAL 2 optimizers of the ACCESS 3 program. Results for this case are presented in Table 26 (iteration histories) and Table 27 (final designs). Since the fundamental natural frequency constraint is the main design driver in this example, its

value as well as the mass for each design in the sequence is given in Table 26. Note that designs 3, 4 and 6 in the DUAL 2 sequence are slightly infeasible with respect to the frequency constraint. Tables 26 and 27 show that the advantages of the dual method approach are significant for the delta wing example:

- (1) the number of structural reanalyses required for convergence falls from 29 (NEWSUMT) to 15 (DUAL 2);
- (2) the final mass given by DUAL 2 after 15 analyses is 5% lower than the final mass generated by NEWSUMT in 29 analyses;
- (3) the total computer time is reduced from 719 sec^{*} for NEWSUMT to 261 sec^{*} for DUAL 2;
- (4) the computer times expended in the optimizer part of the program are 145 sec^{*} and 2 sec^{*} for NEWSUMT and DUAL 2, respectively.

Looking at the final designs generated by NEWSUMT and DUAL 2 (Table 27), it can be seen that the two designs are similar to each other. The smaller mass given by DUAL 2 appears to be due, at least in part, to the larger number of design variables that reach minimum gauge [0.0127 cm (0.005 in)]. In both cases, most of the fiber composite material in the laminated skin is oriented spanwise, with relatively small amounts placed at $\pm 45^\circ$. Over most of the skin, the 90° or chordwise material is minimum thickness critical [i.e., 0.0127 cm (0.005 in)]. The web material distribution is given in Table 28. For both the DUAL 2 and the NEWSUMT results, the contribution that the shear web structure makes to the total mass of

^{*}These times are for runs on the IBM 360/91 computer at CCN, UCLA.

the wing is small (11%). The final designs generated by both NEWSUMT and DUAL 2 are governed primarily by the critical frequency constraint. However, several skin strength constraints are critical in design variable regions 1 through 6 and 16 (see Table 27). These critical strength constraints are transverse tension strain limits in the bottom skin for material oriented at $\pm 45^\circ$ or 90° .

It should be emphasized that the DUAL 2 optimization algorithm effort accounts for less than 1% of the total computer time. This remarkably small computational cost suggest that algorithms like DUAL 2, which combine the generality of mathematical programming and the simplicity of optimality criteria, should find wide-spread acceptance in the next few years as a basis for major structural optimization codes.

6.6.2 Case B: Mixed Continuous-Discrete Problem

Attention is now directed towards the results obtained in the mixed continuous-discrete variable case, where the number of plies for the CSTOR elements are considered as discrete variables (more precisely, integer variables). The thicknesses of the shear panels representing the webs are still taken as continuous design variables. It should be recalled that the laminates are assumed to be balanced and symmetric. Therefore, the smallest change in lamina thickness is necessarily equal to two plies [or 0.0254 cm (0.010 in)]. Consequently, the set of available discrete values for the thicknesses of the skin lamina is given by {0.0254 cm, 0.0508 cm, 0.0762 cm,.....}{0.01 in., 0.02 in., 0.03 in.,.....} (see also Table 8). Results for the mixed continuous-discrete variable case

are presented in Table 26 (iteration history) and Table 27 (final design). Since discrete variables are involved, the DUAL 1 optimizer must be employed. In order to further illustrate how the DUAL 1 algorithm works Table 29 contains detailed iteration history data for each stage, namely: the number Q_R of potentially active constraints retained; the number $(Q_R - N)$ of non-zero dual variables (i.e., the number of strictly active behavior constraints found by DUAL 1 for the current approximate problem); the number P of discontinuity planes at the end of the stage; the number of restarts; the total number of ODM's required for convergence. For information the lower bound mass \underline{W} , the optimal dual objective function value ℓ^* , the final mass W^* and the upper bound mass \bar{W} at the end of each stage are also given. As expected, the inequality $\underline{W} \leq \ell^* \leq W^* \leq \bar{W}$ is satisfied at each stage (see Section 4.5.3). The DUAL 1 optimizer run time (12 sec) is higher than that for DUAL 2 (2 sec) but significantly lower than the NEWSUMT run time (145 sec) (see Table 26). The final mass generated by DUAL 1 is slightly heavier (4%) than that produced by DUAL 2, mainly because the minimum size for the CSTOR members has been increased from 0.0127 cm (0.005 in.) to 0.0254 cm (0.010 in.).

In Table 27, the final design for the mixed continuous-discrete variable case is given as follows: the first value represents the thickness and the integer number in parentheses is the number of plies. Again most of the fiber composite material is oriented in the 0° direction (spanwise). The design is still governed primarily by the frequency constraint but some skin strength constraints are critical in design variable regions

1 through 6 and 15 (see Table 27). The web thicknesses are presented in Table 28. It can be seen that the web mass remains small compared to the skin mass.

To conclude the description of the delta wing example attention is focused on a comparison of the NEWSUMT and DUAL 1 results given in Tables 26 and 27 and illustrated in Fig. 26 (convergence curves):

- (1) the pure continuous variable problem solved by NEWSUMT requires 29 structural reanalyses while the mixed continuous-discrete variable problem is solved by DUAL 1 in 13 reanalyses;
- (2) despite the more realistic formulation of the problem (discrete variables and balanced laminate requirements) DUAL 1 is capable of producing a lighter design than NEWSUMT [6026.5 kg (13,286 lbm) versus 6111.8 kg (13,474 lbm)];
- (3) the total computer time is reduced from 719 sec[†] employing NEWSUMT to 253 sec[†] using DUAL 1;
- (4) the computer times associated with the optimization effort alone are respectively 145 sec[†] (NEWSUMT) and 12 sec[†] (DUAL 1).

Note that the DUAL 1 iteration history presented in Fig. 26 does not correspond to a sequence of all feasible designs (see Table 26), since scaling cannot be employed in this example (because it contains discrete variables).

[†]CPU time on the IBM 360/91 computer at CCN, UCLA.

7. CONCLUSIONS

Considering first the case where all the design variables are continuous, the fundamental reasons underlying the efficiency achieved by combining approximation concepts and dual methods are seen to reside in the following points:

- (1) dual methods exploit the special algebraic structure of the approximate problem generated at each stage;
- (2) since the approximate primal problem at each stage is convex, separable and algebraically simple, it is possible to construct an explicit dual function;
- (3) most of the computational effort in the optimization part of the program is expended on finding the maximum of the dual function subject only to simple nonnegativity constraints on the dual variables;
- (4) the dimensionality of each dual space, namely the number of critical and potentially critical behavior constraints retained during that stage, is relatively small for many problems of practical interest;
- (5) The DUAL 2 optimizer has been especially devised so that it seeks the maximum of the dual function by operating in a sequence of dual subspaces with gradually increasing dimension, such that the dimensionality of the maximization problem never exceeds the number of strictly critical constraints by more than one;

- (6) finally, by seeking the "exact" solution of each approximate problem using the DUAL 2 option, rather than a partial solution of each approximate problem using the NEWSUMT option, the number of stages needed to converge the overall iterative design process is usually reduced.

The joining together of approximation concepts and dual methods provides further insight into the relationship between mathematical programming methods and optimality criteria techniques. It is well known that the essential difficulties involved in applying conventional optimality criteria methods are those associated with identifying the correct critical constraint set and the proper corresponding subdivision of passive and active design variables. Special purpose maximization algorithms such as DUAL 2, which also operate on the Lagrangian multipliers associated with the behavior constraints, intrinsically deal with and resolve these two crucial difficulties. The subdivision of passive and active design variables is dealt with by the closed form relations expressing the primal design variables as functions of the Lagrangian multipliers (i.e., dual variables). Identification of the critical constraint set is automatically handled by taking the nonnegativity constraints on the dual variables into account when seeking the maximum of the dual function. Thus, the combining of approximation concepts and dual methods leads to a perspective where optimality criteria techniques are seen to reside within the general framework of a mathematical programming approach to structural optimization.

Another important achievement reported in this work is the treatment of discrete problems using the dual method approach. The description of fiber composite laminates, which are fabricated from individual plies, naturally

involves discrete (integer) design variables. It is also well known that conventional metal alloy sheet material is frequently only available in standard gauge thicknesses, which again leads to discrete variables. It is therefore interesting and significant that the dual method has been extended to deal with structural synthesis problems involving either pure discrete or mixed continuous-discrete design variables. This extension of the dual methods provides a remarkably efficient minimum mass design optimization capability for structural sizing problems involving discrete variables. This efficiency is due primarily to the following characteristics:

- (1) the dual method implemented herein treats discrete or mixed design variable problems by operating on a continuous dual function;
- (2) as in the pure continuous case, the dimensionality of the dual problem is considerably lower than that of the primal problems and it is independent of the number of design variables;
- (3) the DUAL 1 algorithm incorporates special features for handling dual function gradient discontinuities that arise from the primal discrete variables;

It should be recognized that when discrete variables are introduced, the approximate primal problem is no longer convex and, therefore, the dual formulation does not necessarily yield the true optimum design. Nevertheless, the computational experience reported in this work shows that, although the extension of dual methods to discrete variable problems lacks rigor, it frequently gives useful and plausible results [see Refs. 57 and 60].

It is concluded, based on the results reported in this work, that combining approximation concepts with dual methods provides a firm foundation

for the development of rather general and highly efficient structural synthesis capabilities. Although ACCESS 3 is a research type program of limited scope, a substantial body of computational experience supports the conclusion that the dual method approach leads to a powerful capability for minimum mass optimum sizing of structural systems subject to stress, deflection, slope, minimum gauge and natural frequency constraints. Using this approach, the computational effort expended in the optimization portion of the program has been reduced to a small fraction (e.g., less than 1% in the delta wing example with the DUAL 2 option) of the modest total run time required to obtain a minimum mass design.

It is important to point out that the method presented is not restricted to the specific type of application that has been made in ACCESS 3 (i.e., sizing optimization with bar and membrane finite element models), but it could form the basis of a powerful optimizer embedded in a more general structural synthesis program, such as the PROSSS program of Ref. [66] or the PARS program of Ref. [67]. In this connection, it should be recognized that, when using dual optimizers such as DUAL 1 or DUAL 2, the only essential requirement is that all the functions describing the primal problem must be of separable form.

REFERENCES

1. Schmit, L.A., "Structural Synthesis by Systematic Synthesis," Proc. 2nd Conf. on Electronic Computation ASCE, New York, 1960, pp. 105-122.
2. Haftka, R.T., "Automated Procedure for Design of Wing Structures to Satisfy Strength and Flutter Requirements," NASA TN D-7264, 1973.
3. Haftka, R.T. and Starnes, J.H., "Applications of a Quadratic Extended Interior Penalty Function for Structural Optimization," AIAA Journal, Vol. 14, No. 6, June 1976, pp. 718-724.
4. Starnes, J.H. and Haftka, R.T., "Preliminary Design of Composite Wings for Buckling, Strength and Displacement Constraints," Proc. AIAA/ASME 19th Structures, Structural Dynamics and Materials Conference, Bethesda, Maryland, April 1978, pp. 1-13.
5. Schmit, L.A. and Miura, H., "Approximation Concepts for Efficient Structural Synthesis," NASA CR-2552, March 1976.
6. Schmit, L.A. and Miura, H., "A New Structural Analysis/Synthesis Capability - ACCESS 1," AIAA Journal, Vol. 14, No. 5, May 1976, pp. 661-671.
7. Schmit, L.A. and Miura, H., "An Advanced Structural Analysis/Synthesis Capability - ACCESS 2," Int. J. Num. Meth. Engng, Vol. 12, No. 2, February 1978, pp. 353-377.
8. Venkayya, V.B., Khot, N.S. and Reddy, V.S., "Optimization of Structures based on the Study of Energy Distribution," Proc. 2nd Conf. on Matrix Methods in Structural Mech., WPAFB, AFFDL-TR-68-150, U.S. Air Force, Dec. 1969, pp. 111-153.
9. Dwyer, W., Rosenbaum, J., Shulman, M. and Pardo, H., "Fully-Stressed Design of Airframe Redundant Structures," Proc. 2nd Conf. on Matrix Methods in Structural Mech., AFFDL-TR-68-150, 1968, pp. 155-181.
10. Lansing, W., Dwyer, W., Emerton, R. and Ranalli, E., "Application of Fully-Stressed Design Procedures to Wing and Empennage Structures," J. of Aircraft, Vol. 8, No. 9, 1971, pp. 683-688.
11. Venkayya, V.B., "Design of Optimum Structures," J. of Computers and Structures, Vol. 1, No. 1-2, 1971, pp. 265-309.
12. Dwyer, W.J., Emerton, R.K. and Ojalvo, I.U., "An Automated Procedure for the Optimization of Practical Aerospace Structures, Vol. I - Theoretical Development and User's Information," AFFDL-TR-70-118, U.S. Air Force, Apr. 1971.

13. Gellatly, R.A. and Berke, L., "Optimal Structural Design," AFFDL-TR-70-165, 1971.
14. Prager, W. and Marcal, P.V., "Optimality Criteria in Structural Design," AFFDL-TR-70-166, 1971.
15. Taig, I.C. and Kerr, R.I., "Optimization of Aircraft Structures with Multiple Stiffness Requirements," AGARD Conf. Proc. No. 123, 2nd Symposium on Structural Optimization, Milan, Italy, April 1973.
16. Venkayya, V.B., Khot, N.S. and Berke, L., "Application of Optimality Criteria Approaches to Automated Design of Large Practical Structures," AGARD Conf. Proc. No. 123, 2nd Symposium on Structural Optimization, Milan, Italy, April 1973.
17. Berke, L. and Khot, N.S., "Use of Optimality Criteria Methods for Large Scale Systems," AGARD Lecture Series No. 70, Structural Optimization, October 1974, pp. 1-29.
18. Dwyer, W.J., "An Improved Automated Structural Optimization Program," AFFDL-TR-74-96, September 1974.
19. Isakson, G. and Pardo, H., "ASOP-3: A Program for the Minimum Weight Design of Structures Subjected to Strength and Deflection Gradients AFFDL-TR-76-157, December 1976.
20. Isakson, G., Pardo, H., Lerner, E. and Venkayya, V., "ASOP-3: A Program for the Optimum Design of Metallic and Composite Structures Subjected to Strength and Deflection Constraints," Proc. AIAA/ASME/SAE 18th Structures, Structural Dynamics and Materials Conference, San Diego, California, March 1977, pp. 93-100.
21. Austin, F., "A Rapid Optimization Procedure for Structures Subjected to Multiple Constraints," Proc. AIAA/ASME/SAE 18th Structures, Structural Dynamics and Materials Conference, San Diego, California, March 1977, pp. 71-79.
22. Wilkinson, K., et al., "An Automated Procedure for Flutter and Strength Analysis and Optimization of Aerospace Vehicles, Vol. I - Theory and Application," AFFDL-TR-75-137, U.S. Air Force, Dec. 1975.
23. Wilkinson, K., Markowitz, J., Lerner, E. and George, D., "Application of the Flutter and Strength Optimization Program (FASTOP) to the Sizing of Metallic and Composite Lifting - Surface Structures," Proc. AIAA/ASME/SAE 17th Structures, Structural Dynamics and Materials Conference, King of Prussia, Pennsylvania, May 1976, pp. 463-472.
24. Lerner, E. and Markowitz, J., "An Efficient Structural Resizing Procedure for Meeting Static Aeroelastic Design Objectives," Proc. AIAA/ASME 19th Structures, Structural Dynamics and Materials Conference, Bethesda, Maryland, April 1978, pp. 59-66.

25. Schmit, L.A. and Farshi, B., "Some Approximation Concepts for Structural Synthesis," AIAA Journal, Vol. 12, No. 5, 1974, pp. 692-699.
26. Kiusalaas, J., "Minimum Weight Design of Structures via Optimality Criteria," NASA TN D-7115, December 1972.
27. Dobbs, M.W. and Nelson, R.B., "Application of Optimality Criteria to Automated Structural Design," AIAA Journal, Vol. 14, No. 10, October 1976, pp. 1436-1443.
28. Rizzi, D., "Optimization of Multi-Constrained Structures Based on Optimality Criteria," Proc. AIAA/ASME/SAE 17th Structures, Structural Dynamics and Materials Conference, King of Prussia, Pennsylvania, May 1976, pp. 448-462.
29. Segenreich, S.A., Zouain, N.A. and Herskovits, J., "An Optimality Criteria Method Based on Slack Variables Concept for Large Scale Structural Optimization," Proc. Symposium on Applications of Computer Methods in Engineering, University of Southern California, Los Angeles, California, August 1977, pp. 563-572.
30. Fleury, C. and Sander, G., "Structural Optimization by Finite Element," LTAS Report SA-58, University of Liege, Belgium, January 1978.
31. Fleury, C., "Structural Weight Optimization by Dual Methods of Convex Programming," Int. J. Num. Meth. Engng, Vol. 14, No. 12, 1979, pp. 1761-1783.
32. Fleury, C., "An Efficient Optimality Criteria Approach to the Minimum Weight Design of Elastic Structures," J. of Computers and Structures, Vol. 11, 1980, pp. 163-173.
33. Fleury, C. and Sander, G., "Relations between Optimality Criteria and Mathematical Programming in Structural Optimization," Proc. Symposium on Applications of Computer Methods in Engineering, University of Southern California, Los Angeles, California, August 1977, pp. 507-520.
34. Fleury, C., "A Unified Approach to Structural Weight Minimization," Computer Methods in Applied Mechanics and Engineering, 1979, Vol. 20, No. 1, pp. 17-38.
35. Fiacco, A.V. and McCormick, G.P., Nonlinear Programming: Sequential Unconstrained Minimization Techniques, John Wiley, New York, 1968.
36. Gellatly, R.A., "Development of Procedures for Large Scale Automated Minimum Weight Structural Design," AFFDL-TR-66-180, 1966.

37. Tocher, J.L. and Karnes, R.N., "The Impact of Automated Structural Optimization on Actual Design," AIAA Paper No. 73-361, April 1971.
38. Brown, D.M. and Ang, A.H.S., "Structural Optimization by Nonlinear Programming," J. of the Structural Div., ASCE, Vol. 92, No. ST6, 1966, pp. 319-340.
39. Vanderplaats, G.N. and Moses, F., "Structural Optimization by Methods of Feasible Directions," J. of Computers and Structures, Vol. 3, No. 4, 1973, pp. 739-755.
40. Luenberger, D.G., Introduction to Linear and Nonlinear Programming, Addison-Wesley, Reading, 1973.
41. Schmit, L.A. and Fox, R.L., "An Integrated Approach to Structural Synthesis and Analysis," AIAA Journal, Vol. 3, No. 6, 1965, pp. 1104-1112.
42. Marcal, P.V. and Gellatly, R.A., "Application of the Created Response Surface Technique to Structural Optimization," Proc. 2nd Conf. on Matrix Methods in Structural Mech., WPAFB, AFFDL-TR-68-150, 1968.
43. Kavlie, D. and Moe, J., "Automated Design of Frame Structures," J. of the Structural Division, ASCE, Vol. 97, No. ST1, 1971, pp. 33-62.
44. Moe, J., "Penalty Function Methods," in Optimum Structural Design - Theory and Applications, Gallagher, R.H. and Zienkiewicz, O.C. (ed.), John Wiley, London, 1973, pp. 143-177.
45. Gellatly, R.A., Berke, L. and Gibson, W., "The Use of Optimality Criteria in Automated Structural Design," Paper presented at the 3rd Conf. on Matrix Methods in Structural Mech., WPAFB, Ohio, October 1971.
46. Moses, F., "Optimum Structural Design using Linear Programming," J. of the Structural Division, ASCE, Vol. 90, No. ST6, 1964, pp. 89-104.
47. Pope, G.G., "The Application of Linear Programming Techniques in the Design of Optimum Structures," AGARD Conf. Proc. No. 36-70, 1st Symposium on Structural Optimization, Istanbul, Turkey, 1970.
48. Reinschmidt, K.F., Cornell, A.C. and Brothie, J.F., "Iterative Design and Structural Optimization," J. of the Structural Division, ASCE, Vol. 92, No. ST6, 1966, pp. 281-318.
49. Pope, G.G., "Optimum Design of Stressed Skin Structures," AIAA J., Vol. 11, No. 11, 1973, pp. 1545-1552.

50. Imai, K., "Configuration Optimization of Trusses by the Multiplier Method," Report UCLA-ENG-7842, August 1978.
51. Vanderplaats, G.N., "CONMIN - A Fortran Program for Constrained Function Minimization. User's Manual, "NASA TM X-62,282, 1973.
52. Cassis, J.H. and Schmit, L.A., "On Implementation of the Extended Interior Penalty Function," Int. J. Num. Meth. Engng., Vol. 10, 1976, pp. 3-23.
53. Fleury, C. and Fraeijs de Veubeke, B., "Structural Optimization," Proc. 6th IFIP Conf. on Optimization Techniques, Novosibirsk, USSR, 1974; in Lecture Notes in Computer Science, No. 27, Springer Verlag, 1975, pp. 314-326.
54. Fleury, C. and Geradin, M., "Optimality Criteria and Mathematical Programming in Structural Weight Optimization," J. of Computers and Structures, Vol. 8, No. 1, 1978, pp. 7-17.
55. Sander, G. and Fleury, C., "A Mixed Method in Structural Optimization," Int. J. Num. Meth. Engng., Vol. 13, No. 2, 1978, pp. 385-404.
56. Fleury, C., "Le Dimensionnement Automatique des Structures Elastiques," Doctoral dissertation, LTAS, Universite de Liege, 1978.
57. Lasdon, L.S., Optimization Theory for Large Systems, Macmillan, New York, 1970.
58. Fox, R.L., Optimization Methods for Engineering Design, Addison-Wesley, Reading, 1971.
59. Cella, A. and Soosaar, K., "Discrete Variables in Structural Optimization," in Optimum Structural Design - Theory and Applications, Gallagher, R.H. and Zienkiewicz, O.C. (ed.), John Wiley, London, 1973, pp. 201-222.
60. Fisher, M.L., Northup, W.D. and Shapiro, J.F., "Using Duality to Solve Discrete Optimization Problems: Theory and Computational Experience," Mathematical Programming Study 3, North Holland Publishing Company, 1975, pp. 56-94.
61. Miura, H. and Schmit, L.A., "ACCESS 2 - Approximation Concepts Code for Efficient Structural Synthesis - User's Guide, NASA CR-158949, September 1978.
62. Fleury, C. and Schmit, L.A., "ACCESS 3 - Approximation Concepts Code for Efficient Structural Synthesis - User's Guide," NASA CR - 159260, 1980.

63. Miura, H. and Schmit, L.A., "Second Order Approximation of Natural Frequency Constraints in Structural Synthesis," Int. J. Num. Meth. Engng., Vol. 13, No. 2, 1978, pp. 337-351.
64. Khot, N.S., Berke, L. and Venkayya, V.B., "Comparison of Optimality Criteria Algorithms for Minimum Weight Design of Structures," Proc. AIAA/ASME 19th Structures, Structural Dynamics and Materials Conference, Bethesda, Maryland, April 1978, pp. 37-46.
65. Gellatly, R.A. and Marcal, P.V., "Investigation of Advanced Spacecraft Structural Design Technology," Bell Aerosystems Report No. 2356-960001, July 1967.
66. Sobieszczanski-Sobieski, J. and Bhat, R.B., "Adaptable Structural Synthesis using Advanced Analysis and Optimization Coupled by a Computer Operating System," Proc. AIAA/ASME/ASCE/AHS 20th Structures, Structural Dynamics and Materials Conference, St. Louis, Missouri, April 1979, pp. 60-71.
67. Haftka, R.T. and Prasad, B., "Programs for Analysis and Resizing of Complex Structures," J. of Computers and Structures, Vol. 10, 1979, pp. 323-330.

Table 1. Alternate Paths After Solving ODM (Dual 1)

	Block	Path 1	Path 2	Path 3	Path 4	Path 5	Path 6
Solve ODM Update $\vec{\lambda}_t$	[6]	X	X	X	X	X	X
On New Discontinuity Plane?	[7]	F	F	F	F	T	T
On New Base Plane?	[8]	F	F	T	T		
No Discontinuity Planes?	[9]+ [10]	F	[9] — T — [10]	T	F		
First Discontinuity Plane?	[11]					T	F
Initialize [P] Matrix	[12]					X	
Update [P] Matrix Eqs. (4.51, 4.52)	[13]						X
Update [P] Matrix Eqs. (4.47, 4.48)	[14]				X		
Calculate \vec{S}_t	[15]	X			X	X	X
Calculate \vec{S}_t	[2]		X	X			

Table 2. Available Options for Frequency Constraints

$\lambda = \omega^2$ Algorithm \ Approx.	1st Order Reciprocal DV's	1st Order Direct DV's	2nd Order Direct DV's
NEWSUMT	*	*	*
PRIMAL2	*	—	—
DUAL1	*	—	—
DUAL2	*	—	—

* available combination in ACCESS-3 Program

Table 3. Algorithm Options for Various Kinds of Problems

$\lambda = \omega^2$ Algorithm \ Approx.	Pure Continuous	Pure Discrete	Mixed- Continuous Discrete
NEWSUMT	*	—	—
PRIMAL2	*	—	—
DUAL1	*	*	*
DUAL2	*	—	—

* available for application in ACCESS-3 Program

Table 4A. Definition of Problem 1
Planar 10-Bar Cantilever Truss
(SI Units)

Material : Aluminum

Young's modulus : $E = 68.95 \times 10^6 \text{ kN/m}^2$

Specific weight : $\rho = 2768 \text{ kg/m}^3$

Allowable stress : $\sigma_a = \pm 172,375 \text{ kN/m}^2$

Minimum area : $D^{(L)} = 0.6452 \text{ cm}^2$

Uniform initial area : $D^{(0)} = 129.0 \text{ cm}^2$

Nodal Loading (1 load case)

Node	Load components (N)		
	X	Y	Z
2	0	-444,800	0
4	0	-444,800	0

Displacement Constraints

Problem Name	Node	Direction	Displacement limits (cm)	
			Lower	Upper
Case A	1	Y	-5.08	-5.08
	3	Y	-2.54	-2.54
Cases B-F	1-4	Y	-5.08	+5.08

Table 4B. Definition of Problem 1
Planar 10-Bar Cantilever Truss
(U.S. Customary Units)

Material : Aluminum

Young's modulus : $E = 10^7$ psi

Specific weight : $\rho = 0.1$ lbm/in³

Allowable stress : $\sigma_a = \pm 25,000$ psi

Minimum area : $D^{(L)} = 0.1$ in²

Uniform initial area : $D^{(0)} = 20.0$ in²

Nodal Loading (1 load case)

Node	Load components (lbf)		
	X	Y	Z
2	0	-100,000	0
4	0	-100,000	0

Displacement Constraints

Problem Name	Node	Direction	Displacement limits (in)	
			Lower	Upper
Case A	1	Y	-2.0	-2.0
	3	Y	-1.0	-1.0
Cases B-F	1-4	Y	-2.0	+2.0

Table 5A. Iteration History Data for Problem 1 (Case A)
Planar 10-Bar Cantiliever Truss
(SI Units)

Analysis No.	Mass (kg)	Y-Displacements (cm)		Stress (kN/m ²) Member 6
		Node 1	Node 3	
1	3807.03	-4.8197	-2.1264	13831
2	2149.32	-5.4315	-2.6965	105666
3	1991.37	-5.1920	-2.8763	146050
4	1916.27	-5.1808	-2.4022	146615
5	1832.77	-5.2944	-2.4834	144719
6	1834.82	-5.0937	-2.5397	171286
7	1836.64	-5.0797	-2.5400	172389
8	1836.54	-5.0803	-2.5400	172382
9	1836.61	-5.0800	-2.5400	172375
CPU	Total	4.46		
Time	Anal.	2.73		
(Sec)	Optim.	0.28		

Table 5B. Iteration History Data for Problem 1 (Case A)
Planar 10-Bar Cantilever Truss
(U.S. Customary Units)

Analysis No.		Mass (lbm)	y-Displacements (in)		Stress (psi) Member 6
			Node 1	Node 3	
1		8392.92	-1.8975	-0.83717	2006
2		4738.37	-2.1384	-1.0616	15325
3		4390.14	-2.0441	-1.1324	21182
4		4224.58	-2.0397	-0.94574	21264
5		4040.49	-2.0844	-0.97773	20989
6		4045.01	-2.0054	-0.99987	24842
7		4049.03	-1.9999	-1.0000	25002
8		4048.81	-2.0001	-1.0000	25001
9		4048.96	-2.0000	-1.0000	25000
CPU	Total	4.46			
Time	Anal.	2.73			
(Sec)	Optim.	0.28			

Table 6A. Final Designs for Problem 1
Planar 10-Bar Cantilever Truss
(SI Units)

Member No.	Cross-Sectional Area (cm ²)				†
	Case A DUAL 2	Case B		Case F DUAL 1	
		NEWSUMT	DUAL 2		
1	146.2	199.7	196.9	196.786	(61)
2	9.039	0.6452	0.6452	0.6452	
3	139.2	168.3	149.7	148.396*	(46)
4	54.42	97.04	98.20	100.006	(31)
5	0.6452	0.6452	0.6452	0.6452	
6	0.6452	1.265	3.555	3.226	(1)
7	81.88	52.79	48.11	48.390	(15)
8	93.81	130.5	135.8	135.492	(42)
9	76.97	130.5	138.9	138.718	(43)
10	12.79	0.6452	0.6452	0.6452	
Mass (kg)	1836.61	2308.73	2295.60	2295.16	
No. of Analyses	9	13	13	13	

* This design is slightly infeasible. The feasible design at iteration 11 with mass 2303 kg (See Table 7A) is the same except that the area of member 3 is 151.622 cm².

† Except for the minimum size members [2, 5, 10] the cross sectional areas in Case F are integer multiples of 3.226 cm² as noted in parentheses ().

Table 6B. Final Designs for Problem 1
Planar 10-Bar Cantilever Truss
(U.S. Customary Units)

Member No.	Cross-sectional Area (in ²)			
	Case A DUAL2	Case B		Case F DUAL1
		NEWSUMT	DUAL2	
1	22.66	30.95	30.52	30.5
2	1.401	0.1	0.1	0.1
3	21.58	26.08	23.20	23.0(*)
4	8.434	15.04	15.22	15.5
5	0.1	0.1	0.1	0.1
6	0.1	0.1960	0.5510	0.5
7	12.69	8.182	7.457	7.5
8	14.54	20.22	21.04	21.0
9	11.93	20.22	21.53	21.5
10	1.982	0.1	0.1	0.1
Mass (lbm)	4048.96	5089.80	5060.85	5059.88
No. of Analyses	9	13	13	13

(*) This design is slightly infeasible. The feasible design at iteration 11 with mass 5078 lbm (see Table 7B) is the same except that the area of member 3 is 23.5 in².

Table 7A. Iteration History Data for Problem 1 (Cases B-F)
Planar 10-Bar Cantilever Truss
(SI Units)

Analysis No.		Mass (kg)						
		Case B (Pure Continuous)			Case C (Pure Discrete)	Case D (Mixed Continuous Discrete)+	Case E (Mixed Continuous Discrete)*	Case F (Pure Discrete)
		NEWSUMT (0.3x2)	DUAL 2					
			Unscaled	Scaled				
1		3807	3807	3749	3807	3807	3807	3807
2		3190	2720	2719	2751	2723	2749	2727
3		2687	2547	2628	2537	2555	2522	2659
4		2627	2602	2578	2601	2597	2588	2585
5		2561	2551	2525	2562	2541	2566	2557
6		2499	2495	2467	2538	2488	2515	2501
7		2442	2433	2401	2466	2417	2459	2445
8		2394	2358	2359	2418	2336	2396	2370
9		2345	2259	2319	2338	2277	2323	2272
10		2324	2295	2302	2288	2295	2285	2312
11		2309	2298	2297	2301	2281	2295	2303
12		2309	2296	2296	2296	2292	2300	2295
13		<u>2309</u>	<u>2296</u>	<u>2296</u>	<u>2296</u>	<u>2296</u>	2299	<u>2295</u>
14							2296	
15							<u>2296</u>	
CPU	Total	5.88	4.39		7.71	6.32	6.19	6.58
Time	Anal.	3.12	3.12		3.79	3.18	3.17	3.59
(Sec)	Optim.	1.62	0.14		0.47	0.38	0.26	0.52

+ design variables 1,3,6,8,10 are discrete

* design variables 2,4,5,7,9 are discrete

Table 7B. Iteration History Data for Problem 1 (Cases B-F)
Planar 10-Bar Cantilever Truss
(U.S. Customary Units)

Analysis No.		Mass (lbm)						
		Case B (Pure Continuous)			Case C (Pure Discrete)	Case D (Mixed Continuous Discrete)+	Case E (Mixed Continuous Discrete)*	Case F (Pure Discrete)
		NEWSUMT (0.3x2)	DUAL2					
			Unscaled	Scaled				
1		8393	8393	8266	8393	8393	8393	8393
2		7032	5996	5994	6064	6002	6060	6013
3		5924	5614	5793	5592	5632	5560	5861
4		5792	5737	5683	5735	5725	5706	5699
5		5647	5623	5566	5648	5602	5658	5637
6		5510	5500	5438	5595	5486	5544	5514
7		5383	5363	5294	5436	5328	5422	5391
8		5278	5198	5200	5330	5149	5282	5225
9		5169	4980	5112	5155	5019	5121	5009
10		5124	5059	5075	5044	5060	5038	5096
11		5090	5067	5065	5073	5029	5059	5078
12		5090	5061	5061	5061	5053	5071	5060
13		<u>5090</u>	<u>5061</u>	<u>5061</u>	<u>5061</u>	<u>5061</u>	5069	<u>5060</u>
14							5061	
15							<u>5061</u>	
CPU	Total	5.88	4.39		7.71	6.32	6.19	6.58
Time	Anal.	3.12	3.12		3.79	3.18	3.17	3.59
(Sec)	Optim.	1.62	0.14		0.47	0.38	0.26	0.52

+ design variables 1,3,6,8,10 are discrete

* design variables 2,4,5,7,9 are discrete

Table 8. Available Discrete Values for All Example Problems

Problem Name	Normalized discrete areas (A/A_r) or thicknesses (t/t_r)
Problem 1 10-Bar Truss Cases C through E (A/A_r)	0.1 , 0.551 , 1.0 , 2.0 , 3.0 , 4.0 , 5.0 , 6.0 , 7.0 , 7.457 , 8.0 , 9.0 , 10.0 , 11.0 , 12.0 , 13.0 , 14.0 , 15.0 , 15.22 , 16.0 , 17.0 , 18.0 , 19.0 , 20.0 , 21.0 , 21.04 , 21.53 , 22.0 , 23.0 , 23.20 , 24.0 , 15.0 , 26.0 , 27.0 , 28.0 , 29.0 , 30.0 , 30.52 , 31.0 , 32.0 , 33.0 , 34.0 , 35.0 , 36.0 , 37.0 , 38.0 , 39.0 , 40.0
Problem 1 10-Bar Truss Case F (A/A_r)	0.1 , 0.5 , 1.0 , 1.5 , 2.0 , 2.5 , 3.0 , 3.5 , 4.0 , 4.5 , , 38.0 , 39.5 , 40.0
Problem 2 25-Bar Truss Case B (A/A_r)	0.01, 0.1 , 0.2 , 0.3 , 0.4 , 0.5 , 0.6 , 0.7 , 0.8 , 0.9 , , 5.4 , 5.5 , 5.6
Problem 2 25-Bar Truss Case C (A/A_r)	0.01, 0.4 , 0.8 , 1.2 , 1.6 , 2.0 , 2.4 , 2.8 , 3.2 , 3.6 , 4.0 , 4.4 , 4.8 , 5.2 , 5.6
Problem 2 25-Bar Truss Case D (A/A_r)	0.01, 0.8 , 1.6 , 2.4 , 3.2 , 4.0 , 4.8 , 5.6
Problem 5 Swept Wing Case B (t/t_r)	0.020, 0.025 , 0.032 , 0.040, 0.050, 0.063, 0.071, 0.080, 0.090, 0.100 , 0.125 , 0.160, 0.190, 0.250, 0.313, 0.375, 0.500, 0.625 , 0.750 , 1.000
Problem 6 Delta-Wing Case B (t/t_r)	0.01 , 0.02 , 0.03 , 0.04 , 0.05 , 0.06 , 0.07 , 0.08 , 0.09, 0.10, , 1.98 , 1.99 , 2.00

$$A_r = 6.452 \text{ cm}^2 (1.00 \text{ in}^2) ; t_r = 2.54 \text{ cm (1.00 in)}$$

Table 9A. Definition of Problem 2
25-Bar Space Truss
(SI Units)

Material	:	Aluminum
Young's modulus	:	$E = 68.95 \times 10^6 \text{ kN/m}^2$
Specific mass	:	$\rho = 2768 \text{ kg/m}^3$
Minimum area	:	$D^{(L)} = 0.06452 \text{ cm}^2$
Uniform initial area	:	$D^{(o)} = 19.356 \text{ cm}^2$

Allowable Stresses

Members	Stress limits (kN/m ²)		Members	Stress limits (kN/m ²)	
	tension	compression		tension	compression
1	275,800	-241,959	12, 13	275,800	-241,959
2 - 5	275,800	- 79,913	14 - 17	275,800	- 46,603
6 - 9	275,800	-119,318	18 - 21	275,800	- 47,982
10, 11	275,800	-241,959	22 - 25	275,800	- 76,410

Nodal Loading (2 load cases)

Load Case	Node	Load components (N)		
		X	Y	Z
1	1	4,448	44,480	-22,240
	2	0	44,480	-22,240
	3	2,224	0	0
	6	2,224	0	0
2	5	0	88,960	-22,240
	6	0	-88,960	-22,240

Displacement constraints

Node	Displacement limits (cm)		
	X	Y	Z
1	± 0.889	± 0.889	± 0.889
2	± 0.889	± 0.889	± 0.889

Table 9B. Definition of Problem 2
25-Bar Space Truss
(U.S. Customary Units)

Material : Aluminum

Young's modulus : $E = 10^7$ psi

Specific mass : $\rho = 0.1$ lbm/in³

Minimum area : $D^{(L)} = 0.01$ in²

Uniform initial area : $D^{(o)} = 3.0$ in²

Allowable Stresses

Members	Stress limits (psi)		Members	Stress limits (psi)	
	tension	compression		tension	compression
1	40,000	-35,092	12,13	40,000	-35,092
2 - 5	40,000	-11,590	14 - 17	40,000	- 6,759
6 - 9	40,000	-17,305	18 - 21	40,000	- 6,959
10, 11	40,000	-35,092	22 - 25	40,000	-11,082

Nodal Loading (2 load cases)

Load Case	Node	Load components (lbf)		
		X	Y	Z
1	1	1,000	10,000	-5,000
	2	0	10,000	-5,000
	3	500	0	0
	6	500	0	0
2	5	0	20,000	-5,000
	6	0	-20,000	-5,000

Displacement constraints

Node	Displacement limits (in)		
	X	Y	Z
1	±0.35	±0.35	±0.35
2	±0.35	±0.35	±0.35

Table 10A. Iteration History Data for Problem 2
25-Bar Space Truss
(SI Units)

Analysis No.		Mass (kg)							
		Pure Continuous Case (Case A)				Pure Discrete Cases			
		NEWSUMT (0.3x2)	DUAL 2		Ref. [30] Fleury- Sander	Ref. [13] Gellatly- Berke	Case B $\frac{A}{A_r}=0.1$	Case C $\frac{A}{A_r}=0.4$	Case D $\frac{A}{A_r}=0.8$
unscaled	scaled								
1		450.1	450.1	333.1	333.1	333.1	360.0	360.0	360.0
2		318.6	256.6	256.4	256.4	252.1	258.6	268.3	294.3
3		265.8	248.0	248.0	248.0	249.1	250.8	263.0	283.5
4		252.6	247.6	247.6	247.6	247.9	<u>250.8</u>	261.0	<u>283.5</u>
5		248.9	247.4	247.4	247.4	247.6		<u>261.0</u>	
6		247.8	<u>247.3</u>	<u>247.3</u>	<u>247.3</u>	247.4			
7		<u>247.4</u>				<u>247.4</u>			
CPU	Total	5.20	2.75				2.85	2.85	2.21
Time	Analys.	3.35	1.93				1.85	1.92	1.56
(sec)	Optim.	1.02	0.05				0.15	0.13	0.10

Table 10B. Iteration History Data for Problem 2
25-Bar Space Truss
(U.S. Customary Units)

Analysis No.		Mass (lbm)							
		Pure Continuous Case (Case A)				Pure Discrete Cases			
		NEWSUMT (0.3x2)	DUAL2		Ref.[30] Fleury- Sander	Ref.[13] Gellatly- Berke	Case B $\frac{A}{A_r}=0.1$	Case C $\frac{A}{A_r}=0.4$	Case D $\frac{A}{A_r}=0.8$
			unscaled	scaled					
1		992.2	992.2	734.4	734.4	734.4	793.7	793.7	793.7
2		702.3	565.6	565.3	565.3	555.7	570.1	591.4	648.7
3		585.9	546.8	546.8	546.8	549.1	553.0	579.7	624.9
4		556.9	545.8	545.8	545.8	546.5	<u>553.0</u>	575.4	<u>624.9</u>
5		548.7	545.4	545.4	545.4	545.9		<u>575.4</u>	
6		546.2	<u>545.2</u>	<u>545.2</u>	<u>545.2</u>	545.5			
7		<u>545.5</u>				<u>545.4</u>			
CPU	Total	5.20	2.75		/	/	2.85	2.85	2.21
Time	Analys.	3.35	1.93				1.89	1.92	1.56
(sec.)	Optim	1.02	0.05				0.15	0.13	0.10

Table 11A. Final Designs for Problem 2
25-Bar Space Truss
(SI Units)

Design Variable Group No. (members)	Cross-Sectional Area (cm) ²					
	Case A (continuous) DUAL 2	Case B $A/A_r=0.1$ DUAL 1	Case C $A/A_r=0.4$		Case D $A/A_r=0.8$	
			DUAL 1	Ref. [65]	DUAL 1	Ref. [65]
1 (1)	0.0645	0.6452	2.581	12.962	5.162	10.065
2 (2-5)	12.820	12.904	12.904	15.485	15.485	15.485
3 (6-9)	19.298	19.356	20.646	15.485	20.646	15.485
4 (10,11)	0.0645	0.0645	0.0645	0.071	0.0645	0.071
5 (12,13)	0.0774	0.6452	0.0645	0.071	5.162	0.071
6 (14-17)	4.407	4.516	5.162	5.162	5.162	5.162
7 (18-21)	10.833	10.968	12.904	12.904	10.323	15.485
8 (22-25)	17.188	17.420	15.485	18.066	20.646	20.646
Mass (kg)	247.31	250.84	261.01	270.07	283.44	291.39
No. of Analyses	6	4	5	-	4	-

Table 11B. Final Designs for Problem 2
25-Bar Space Truss
(U.S. Customary Units)

Design Variable Group No. (members)	Cross-sectional Area (in ²)					
	Case A	Case B	Case C		Case D	
	(continuous) DUAL2	$A/A_r=0.1$ DUAL1	DUAL1	$A/A_r=0.4$ Ref [65]	DUAL1	$A/A_r=0.8$ Ref. [65]
1 (1)	0.010	0.1	0.4	2.009	0.8	1.560
2 (2-5)	1.987	2.0	2.0	2.400	2.4	2.400
3 (6-9)	2.991	3.0	3.2	2.400	3.2	2.400
4 (10,11)	0.010	0.01	0.01	0.011	0.01	0.011
5 (12,13)	0.012	0.1	0.01	0.011	0.8	0.011
6 (14-17)	0.683	0.7	0.8	0.800	0.8	0.800
7 (18-21)	1.679	1.7	2.0	2.000	1.6	2.400
8 (22-25)	2.664	2.7	2.4	2.800	3.2	3.200
Mass (lbm)	545.22	553.00	575.41	595.4	624.87	642.4
No. of Analyses	6	4	5	-	4	-

Table 12A. Definition of Problem 3
72-Bar Space Truss
(SI Units)

Material : Aluminum

Young's modulus : $E = 68.95 \times 10^6 \text{ kN/m}^2$

Specific mass : $\rho = 2768 \text{ kg/m}^3$

Allowable stress : $\sigma_a = \pm 172,375 \text{ kN/m}^2$

Minimum area : $D(L) = 0.6452 \text{ cm}^2$

Uniform initial area : $D(o) = 6.452 \text{ cm}^2$

Nodal loading (2 load cases)

Load Case	Node	Load components (N)		
		X	Y	Z
1	1	22,240	22,240	-22,240
2	1	0	0	-22,240
	2	0	0	-22,240
	3	0	0	-22,240
	4	0	0	

Displacement constraints

Node	Displacement limits (cm)		
	X	Y	Z
1	± 0.635	± 0.635	-
2	± 0.635	± 0.635	-
3	± 0.635	± 0.635	-
4	± 0.635	± 0.635	-

Table 12B. Definition of Problem 3
72-Bar Space Truss
(U.S. Customary Units)

Material : Aluminum

Young's modulus : $E = 10^7$ psi

Specific mass : $\rho = 0.1$ lbm/in³

Allowable stress : $\sigma_a = \pm 25,000$ psi

Minimum area : $D^{(L)} = 0.1$ in²

Uniform initial area : $D^{(o)} = 1.0$ in²

Nodal loading (2 load cases)

Load Case	Node	Load components (lbf)		
		X	Y	Z
1	1	5,000	5,000	-5,000
2	1	0	0	-5,000
	2	0	0	-5,000
	3	0	0	-5,000
	4	0	0	-5,000

Displacement constraints

Node	Displacement limits (in)		
	X	Y	Z
1	± 0.25	± 0.25	-
2	± 0.25	± 0.25	-
3	± 0.25	± 0.25	-
4	± 0.25	± 0.25	-

Table 13A. Iteration History Data for Problem 3
72-Bar Space Truss
(SI Units)

Analysis No.		Mass (kg)						
		NEWSUMT (0.5x1)	NEWSUMT (0.3x2)	NEWSUMT (0.1x3)	DUAL 2		Ref. [15] Taig-Kerr Ref. [30] Fleury- Sander	Ref. [17] Berke- Khot
					unscaled	scaled		
1		387.0	387.0	387.0	387.0	297.9	297.9	297.9
2		258.9	224.2	189.4	183.2	175.7	175.7	175.5
3		231.6	185.7	172.7	172.3	172.3	172.3	172.2
4		214.9	176.3	172.2	172.2	172.2	172.2	<u>172.3</u>
5		202.3	173.4	<u>172.2</u>	<u>172.2</u>	<u>172.2</u>	<u>172.2</u>	
6		193.1	172.6					
7		186.7	<u>172.3</u>					
8		182.4						
9		179.4						
10		177.3						
CPU	Total	12.20	9.71	8.41	6.52		/	/
Time	Anal	9.38	7.10	5.78	5.54			
(sec)	Optim	1.35	1.46	1.89	0.02			

Table 13B. Iteration History Data for Problem 3
72-Bar Space Truss
(U.S. Customary Units)



Analysis No.		Mass (lbm)						
		NEWSUMT (0.5x1)	NEWSUMT (0.3x2)	NEWSUMT (0.1x3)	DUAL2		Ref. [15] Taig-Kerr Ref. [30] Fleury- Sander	Ref. [17] Berke- khot
					unscaled	scaled		
1		853.1	853.1	853.1	853.1	656.8	656.8	656.8
2		570.7	494.3	417.6	403.9	387.3	387.3	387.0
3		510.6	409.3	380.8	379.9	379.8	379.8	379.7
4		473.8	388.6	379.7	379.7	379.7	379.7	<u>379.9</u>
5		445.9	382.3	<u>379.7</u>	<u>379.7</u>	<u>379.7</u>	<u>379.7</u>	
6		425.7	380.5					
7		411.7	<u>379.9</u>					
8		402.1						
9		395.4						
10		390.8						
CPU	Total	12.20	9.71	8.41	6.52			
Time	Anal.	9.38	7.10	5.78	5.54			
(sec)	Optim.	1.35	1.46	1.89	0.02			

Table 14A. Final Designs for Problem 3
72-Bar Space Truss
(SI Units)

Design Variable Group No.	Members	Cross-sectional area (cm ²)		
		ACCESS 3 (DUAL 2)	Ref. [15] Taig-Kerr Ref. [30] Fleury-Sander	Ref. [17] Berke-Khot
1	1-4	1.014	1.014	1.014
2	5-12	3.456	3.456	3.474
3	13-16	2.648	2.645	2.681
4	17,18	3.667	3.671	3.555
5	19-22	3.270	3.269	3.279
6	23-30	3.355	3.355	3.352
7	31-34	0.6452	0.6452	0.6452
8	35,36	0.6452	0.6452	0.6452
9	37-40	8.259	8.259	8.252
10	41-48	3.321	3.321	3.332
11	49-52	0.6452	0.6452	0.6452
12	53,54	0.6452	0.6452	0.6452
13	55-58	12.239	12.239	12.214
14	59-66	3.328	3.328	3.336
15	67-70	0.6452	0.6452	0.6452
16	71,72	0.6452	0.6452	0.6452
Mass (kg)		172.22	172.21	172.22
No. of Analyses		5	5	4

Table 14B. Final Designs for Problem 3
72-Bar Space Truss
(U.S. Customary Units)

Design Variable Group No.	Members	Cross-sectional area (in ²)		
		ACCESS3 (DUAL2)	Ref.[15] Taig-Kerr Ref.[30] Fleury-Sander	Ref.[17] Berke-Khot
1	1-4	0.1572	0.1571	0.1571
2	5-12	0.5356	0.5356	0.5385
3	13-16	0.4104	0.4099	0.4156
4	17,18	0.5683	0.5690	0.5510
5	19-22	0.5068	0.5067	0.5082
6	23-30	0.5200	0.5200	0.5196
7	31-34	0.1	0.1	0.1
8	35,36	0.1	0.1	0.1
9	37-40	1.280	1.280	1.279
10	41-48	0.5148	0.5148	0.5149
11	49-52	0.1	0.1	0.1
12	53,54	0.1	0.1	0.1
13	55-58	1.897	1.897	1.893
14	59-66	0.5158	0.5158	0.5171
15	67-70	0.1	0.1	0.1
16	71,72	0.1	0.1	0.1
Mass (lbm)		379.67	379.66	379.67
No. of Analyses		5	5	4

Table 15A. Definition of Problem 4
63-Bar Space Truss
(SI Units)

Material	:	Titanium alloy
Young's modulus	:	$E = 110.32 \times 10^2 \text{ kN/m}^2$
Specific mass	:	$\rho = 4428.8 \text{ kg/m}^3$
Allowable stress	:	$\sigma_a = 689,500 \text{ kN/m}^2$
Minimum area	:	$D(L) = 0.06452 \text{ cm}^2$
Uniform initial area	:	$D(o) = 774.24 \text{ cm}^2$

Nodal Coordinates

Node	Coordinates (cm)			Node	Coordinates (cm)		
	X	Y	Z		X	Y	Z
1	0.0	355.6	50.8	10	76.2	203.2	-7.62
2	0.0	355.6	0.0	11	-76.2	101.6	139.7
3	-76.2	304.8	53.34	12	-76.2	101.6	-12.7
4	-76.2	304.8	-2.54	13	76.2	101.6	139.7
5	76.2	304.8	53.34	14	76.2	101.6	-12.7
6	76.2	304.8	-2.54	15	-76.2	0.0	152.4
7	-76.2	203.2	76.2	16	-76.2	0.0	-17.78
8	-76.2	203.2	-7.62	17	76.2	0.0	152.4
9	76.2	203.2	76.2	18	76.2	0.0	-17.78

Nodal Loading (2 load cases)

Load Case	Node	Load components (MN)		
		X	Y	Z
1	1	11.12	-22.24	1.112
	2	-11.12	22.24	1.112
2	1	22.24	-11.12	1.112
	2	-22.24	11.12	1.112

Displacement constraint: $\pm 2.54 \text{ cm}$ limits on the relative displacement at nodes 1 and 2 in the x-direction.

Table 15B. Definition of Problem 4
63-Bar Space Truss
(U.S. Customary Units)

Material : Titanium alloy
 Young's modulus : $E = 1.6 \times 10^7$ psi
 Specific mass : $\rho = 0.16$ lbm/in³
 Allowable stress : $\sigma_a = 100,000$ psi
 Minimum area : $D^{(L)} = 0.01$ in²
 Uniform initial area : $D^{(o)} = 120$ in²

Nodal coordinates

Node	Coordinates (in)			Node	Coordinates (in)		
	X	Y	Z		X	Y	Z
1	0.0	140.0	20.0	10	30.0	80.0	-3.0
2	0.0	140.0	0.0	11	-30.0	40.0	55.0
3	-30.0	120.0	21.0	12	-30.0	40.0	-5.0
4	-30.0	120.0	-1.0	13	30.0	40.0	55.0
5	30.0	120.0	21.0	14	30.0	40.0	-5.0
6	30.0	120.0	-1.0	15	-30.0	0.0	60.0
7	-30.0	80.0	30.0	16	-30.0	0.0	-7.0
8	-30.0	80.0	-3.0	17	30.0	0.0	60.0
9	30.0	80.0	30.0	18	30.0	0.0	-7.0

Nodal Loading (2 load cases)

Load Case	Node	Load components (lbf)		
		X	Y	Z
1	1	2.5×10^6	-5.0×10^6	2.5×10^5
	2	-2.5×10^6	5.0×10^6	2.5×10^5
2	1	5.0×10^6	-2.5×10^6	2.5×10^5
	2	-5.0×10^6	2.5×10^6	2.5×10^5

Displacement constraint: ± 1.0 in limits on the relative displacement at nodes 1 and 2 in the x-direction.

Table 16A. Iteration History Data for Problem 4
63-Bar Space Truss
(SI Units)

Analysis No.		Mass (kg)								
		NEWSUMT (0.5x1)	NEWSUMT (0.5x2)	DUAL 2 (w/o FSD)		DUAL 2 (w/FSD)		Ref. [30] Fleury- Sander	Ref. [17] Berke- Khot	Ref. [5] Schmit- Miura
				unscaled	scaled	unscaled	scaled			
1		30222	30222	30222	13705	30222	13705	13705	13705	30222
2		7672	5690	3042	3435	3060	3459	3484	3437	5907
3		5052	3931	2865	3969	2861	3192	2990	3123	4332
4		4236	3308	2810	3054	2815	3121	2902	3143	3422
5		3767	3038	2793	2854	2802	2953	2844	3085	3088
6		3456	2904	2784	2832	2782	2898	2833	2998	2929
7		3245	2839	2780	2813	2778	2851	2812	2936	2851
8		3101	2807	2778	2795	2776	2820	2794	2898	2813
9		3003	2791	2776	2781	2776	2801	2779	2873	2794
10		2933	2784	2776	2777	2776	2789	2777	2855	2794
11		2886	2780	2776	2776	2775	2784	2776	2841	2786
12		2853	2777	2775	2776	<u>2775</u>	<u>2781</u>	2776	2831	2778
13		2830	2776	<u>2775</u>	<u>2776</u>			2776	2826	<u>2776</u>
14		2814	2776					2775	2820	
15		2802	<u>2776</u>					<u>2775</u>	2821	
...		
50									<u>2794</u>	
CPU	Total	108	163	60.1		33.7				87.5
Time	Anal	44	46	41.2		27.9				19.8
(Sec)	Optim	59	113	13.9		2.8		-	-	66.7

Table 16B. Iteration History Data for Problem 4
63-Bar Space Truss
(U.S. Customary Units)

Analysis No.		Mass (lbm)								
		NEWSUMT (0.5x1)	NEWSUMT (0.5x2)	DUAL2 (w/o FSD)		DUAL2 (w/FSD)		Ref. [30] Fleury- Sander	Ref. [17] Berke- Khot	Ref. [5] Schmit- Miura
				unscaled	scaled	unscaled	scaled			
1		66628	66628	66628	30214	66628	30214	30214	30214	66628
2		16914	12543	6706	7573	6746	7625	7680	7577	13023
3		11137	8667	6316	6546	6307	7037	6591	6884	9551
4		9338	7293	6195	6733	6207	6880	6398	6928	7544
5		8305	6697	6157	6292	6177	6510	6270	6801	6807
6		7620	6402	6138	6243	6134	6388	6246	6609	6457
7		7154	6259	6129	6201	6125	6286	6199	6473	6285
8		6836	6189	6124	6161	6121	6216	6159	6388	6202
9		6620	6154	6121	6132	6120	6175	6126	6333	6160
10		6467	6137	6120	6123	6119	6149	6123	6293	6160
11		6362	6128	6119	6121	6118	6137	6121	6263	6141
12		6289	6123	6118	6120	<u>6118</u>	<u>6130</u>	6120	6241	6124
13		6238	6121	<u>6118</u>	<u>6119</u>			6119	6231	<u>6121</u>
14		6203	6120					6118	6216	
15		6178	<u>6119</u>					<u>6118</u>	6220	
...		
50									<u>6159</u>	
CPU	Total	108	163	60.1		33.7				87.5
Time	Anal.	44	46	41.2		27.9				19.8
(Sec)	Optim.	59	113	13.9		2.8		-	-	66.7

Table 17A. Final Designs for Problem 4
63-Bar Space Truss
(SI Units)

Member No.	Connecting Nodes		Cross-sectional Area (cm ²)			
			DUAL 2 (w/o FSD)	Ref. [30] Fleury- Sander	Ref. [17] Berke- Khot	Ref. [5] Schmit- Miura
	1	2				
1	1	3	242.5	242.8	237.8	242.3
2	2	4	235.0	234.8	238.1	235.4
3	1	5	339.2	339.0	344.1	339.8
4	2	6	346.9	347.1	344.0	346.9
5	3	7	153.0	152.7	155.7	153.5
6	4	8	186.7	186.9	179.5	186.8
7	5	9	111.3	111.4	111.9	111.4
8	6	10	137.7	137.3	141.9	138.1
9	7	11	168.1	168.4	151.1	168.1
10	8	12	161.9	162.1	167.4	162.3
11	9	13	56.76	56.74	60.91	56.67
12	10	14	58.04	58.11	63.36	57.85
13	11	15	150.8	151.1	144.3	151.2
14	12	16	126.1	126.4	119.9	126.3
15	13	17	33.40	33.37	37.36	33.32
16	14	18	19.02	19.02	28.84	19.07
17	3	5	239.4	239.5	238.0	239.2
18	4	6	240.7	241.0	242.1	240.7
19	7	9	0.065	0.065	0.065	0.065
20	8	10	0.065	0.065	0.065	0.065
21	11	13	1.038	0.639	0.968	1.407
22	12	14	0.895	0.394	0.065	1.097
23	1	2	0.065	0.065	0.065	0.065
24	3	4	0.065	0.065	0.161	0.065
25	5	6	0.065	0.065	0.065	0.065
26	7	8	26.63	26.08	39.42	27.04
27	9	10	6.568	5.878	0.065	6.355
28	11	12	20.94	20.98	28.58	21.19
29	13	14	0.065	0.065	7.420	0.065
30	3	9	52.72	53.31	44.78	50.72
31	4	10	51.54	52.03	62.97	50.32
32	5	7	58.17	57.38	71.17	60.00
33	6	8	58.51	57.95	52.20	59.55
34	7	13	61.10	60.27	74.78	63.03
35	8	14	58.51	57.96	52.20	59.55
36	9	11	55.38	56.00	47.10	53.27
37	10	12	51.55	52.04	63.04	50.33
38	11	17	52.75	52.80	45.03	50.86

Table 17A., contd.

Member	Connecting Nodes		Cross-sectional Area (cm ²)			
			DUAL 2 (w/o FSD)	Ref. [30] Fleury- Sander	Ref. [17] Berke- Khot	Ref. [5] Schmit- Miura
	1	2				
39	12	18	51.82	52.16	63.04	50.66
40	13	15	57.55	57.64	70.46	59.26
41	14	16	58.26	57.86	52.20	59.24
42	1	6	163.1	164.4	158.8	162.8
43	1	4	175.0	176.3	158.3	174.7
44	2	5	124.2	122.9	127.6	124.8
45	2	3	136.0	129.6	139.6	136.7
46	5	10	108.0	107.1	110.9	108.5
47	3	8	81.30	80.39	83.75	81.62
48	6	9	119.9	120.8	116.7	119.7
49	4	7	128.7	129.6	126.9	128.5
50	9	14	42.97	43.01	43.42	42.91
51	7	12	36.72	36.69	48.33	37.15
52	10	13	51.83	52.27	61.29	52.44
53	8	11	24.52	24.75	0.065	23.50
54	13	18	38.20	38.36	43.81	38.62
55	11	16	76.84	77.23	57.42	76.97
56	14	17	37.87	37.92	24.52	37.73
57	12	15	10.79	10.28	21.81	10.91
58	4	5	0.065	0.065	0.065	0.065
59	3	6	0.065	0.065	0.065	0.065
60	8	9	0.065	0.065	0.065	0.065
61	7	10	0.065	0.065	0.065	0.065
62	12	13	0.065	0.065	0.065	0.065
63	11	14	0.065	0.065	0.065	0.065
Mass (kg)			2775.11	2774.90	2793.86	2776.44
No. of Analyses			13	17	50	13

Table 17B. Final Designs for Problem 4
63-Bar Space Truss
(U.S. Customary Units)

Member No.	Connecting Nodes		Cross-sectional Area (in ²)			
			DUAL2 (w/o FSD)	Ref. [30] Fleury-Sander	Ref. [17] Berke-Khot	Ref. [5] Schmit-Miura
	1	2				
1	1	3	37.58	37.63	36.86	37.55
2	2	4	36.43	36.39	36.90	36.49
3	1	5	52.58	52.54	53.33	52.66
4	2	6	53.76	53.80	53.31	53.76
5	3	7	23.71	23.67	24.13	23.79
6	4	8	28.94	28.97	27.82	28.95
7	5	9	17.25	17.26	17.35	17.26
8	6	10	21.34	21.28	22.00	21.40
9	7	11	26.06	26.10	23.42	26.06
10	8	12	25.10	25.13	25.95	25.15
11	9	13	8.798	8.794	9.44	8.784
12	10	14	8.996	9.007	9.82	8.966
13	11	15	23.38	23.42	22.37	23.43
14	12	16	19.55	19.59	18.59	19.57
15	13	17	5.176	5.172	5.79	5.165
16	14	18	2.948	2.948	4.47	2.956
17	3	5	37.10	37.12	36.89	37.07
18	4	6	37.31	37.35	37.52	37.30
19	7	9	0.01	0.01	0.01	0.01
20	8	10	0.01	0.01	0.01	0.01
21	11	13	0.1609	0.099	0.15	0.218
22	12	14	0.1387	0.061	0.01	0.170
23	1	2	0.01	0.01	0.01	0.01
24	3	4	0.01	0.01	0.18	0.01
25	5	6	0.01	0.01	0.01	0.01
26	7	8	4.127	4.042	6.11	4.191
27	9	10	1.018	0.911	0.01	0.985
28	11	12	3.245	3.251	4.43	3.285
29	13	14	0.01	0.01	1.15	0.01
30	3	9	8.171	8.263	6.94	7.861
31	4	10	7.988	8.064	9.76	7.799
32	5	7	9.016	8.894	11.03	9.300
33	6	8	9.068	8.982	8.09	9.229
34	7	13	9.470	9.342	11.59	9.769
35	8	14	9.069	8.983	8.09	9.230
36	9	11	8.583	8.679	7.30	8.257
37	10	12	7.990	8.066	9.77	7.801
38	11	17	8.176	8.183	6.98	7.883

Table 17B., contd.

Member No.	Connecting Nodas		Cross-sectional Area(in ²)			
	1	2	DUAL2 (w/o FSD)	Ref. [30] Fleury-Sander	Ref. [17] Berke-Khot	Ref. [5] Schmit-Miura
39	12	18	8.032	8.084	9.77	7.852
40	13	15	8.919	8.934	10.92	9.184
41	14	16	9.030	8.968	8.09	9.181
42	1	6	25.28	25.48	24.61	25.23
43	1	4	27.12	27.32	24.54	27.07
44	2	5	19.25	19.05	19.78	19.35
45	2	3	21.08	20.09	21.63	21.18
46	5	10	16.74	16.60	17.19	16.81
47	3	8	12.60	12.46	12.98	12.65
48	6	9	18.59	18.73	18.09	18.55
49	4	7	19.95	20.09	19.67	19.91
50	9	14	6.660	6.666	6.73	6.650
51	7	12	5.692	5.686	7.49	5.758
52	10	13	8.033	8.102	9.50	8.128
53	8	11	3.801	3.836	0.01	3.642
54	13	18	5.921	5.946	6.79	5.986
55	11	16	11.91	11.97	8.90	11.93
56	14	17	5.870	5.877	3.80	5.848
57	12	15	1.672	1.593	3.38	1.691
58	4	5	0.01	0.01	0.01	0.01
59	3	6	0.01	0.01	0.01	0.01
60	8	9	0.01	0.01	0.01	0.01
61	7	10	0.01	0.01	0.01	0.01
62	12	13	0.01	0.01	0.01	0.01
63	11	14	0.01	0.01	0.01	0.01
Mass (lbm)			6117.97	6117.5	6159.3	6120.9
No. of Analyses			13	17	50	13

Table 18A. Definition of Problem 5
Swept Wing Model
(SI Units)

Material	:	Aluminum
Young's modulus	:	$E = 73.09 \times 10^6 \text{ kN/m}^2$
Poisson's ratio	:	$\nu = 0.3$
Specific mass	:	$\rho = 2657 \text{ kg/m}^3$
Allowable stress	:	$\sigma_a = \pm 172,375 \text{ kN/m}^2$
Minimum thickness	:	$D^{(L)} = 0.0508 \text{ cm}$
Initial thickness		
skin (CST)	:	$D^{(o)} = 0.762 \text{ cm}$
webs (SSP)	:	$D^{(o)} = 0.381 \text{ cm}$

Displacement constraints

Node	Displacement limits (cm)		
	X	Y	Z
41	-	-	± 152.4
44	-	-	± 152.4

Table 18B. Definition of Problem 5
Swept Wing Model
(U.S. Customary Units)

Material : Aluminum

Young's modulus : $E = 1.06 \times 10^7$ psi

Poisson's ratio : $\nu = 0.3$

Specific mass : $\rho = 0.096$ lbm/in³

Allowable stress : $\sigma_a = \pm 25,000$ psi

Minimum thickness : $D^{(L)} = 0.02$ in

Initial thickness

skin (CST) : $D^{(o)} = 0.30$ in

webs (SSP) : $D^{(o)} = 0.15$ in

Displacement constraints

Node	Displacement limits (in)		
	X	Y	Z
41	-	-	± 60.0
44	-	-	± 60.0

Table 19A. Nodal Coordinates for Swept Wing Model (Problem 5)
(SI Units)

Node No.	X (cm)	Y (cm)	Z (cm)
1	0.0	762.0	25.4
2	0.0	635.0	38.1
3	0.0	469.9	33.02
4	0.0	254.0	12.70
5	254.0	656.1	21.80
6	254.0	544.1	32.59
7	254.0	399.3	28.14
8	254.0	211.7	11.01
9	482.6	560.8	18.56
10	482.6	462.0	27.64
11	482.6	335.5	23.77
12	482.6	173.6	9.482
13	660.4	486.9	16.045
14	660.4	398.3	23.79
15	660.4	286.0	20.36
16	660.4	143.9	8.298
17	825.5	418.1	13.706
18	825.5	339.1	20.21
19	825.5	240.1	17.20
20	825.5	116.4	7.196
21	977.9	354.6	11.547
22	977.9	284.5	16.91
23	977.9	197.7	14.28
24	977.9	91.01	6.180
25	1117.6	296.4	9.568
26	1117.6	234.5	13.89
27	1117.6	158.8	11.62
28	1117.6	67.74	5.250
29	1244.6	243.4	7.767
30	1244.6	189.0	11.13
31	1244.6	123.5	9.164
32	1244.6	46.56	4.402
33	1358.9	195.8	6.149
34	1358.9	148.1	8.656
35	1358.9	91.67	6.975
36	1358.9	27.51	3.640
37	1447.8	158.8	4.890
38	1447.8	116.2	6.731
39	1447.8	66.93	5.271
40	1447.8	12.70	3.048
41	1524.0	127.0	3.810
42	1524.0	88.90	5.080
43	1524.0	45.72	3.810
44	1524.0	0.0	2.540

Table 19B. Nodal Coordinates for Swept Wing Model (Problem 5)
(U.S. Customary Units)

Node No.	X (in)	Y (in)	Z (in)
1	0.0	300.0	10.00
2	0.0	250.0	15.00
3	0.0	185.0	13.00
4	0.0	100.0	5.000
5	100.0	258.3	8.583
6	100.0	214.2	12.83
7	100.0	157.2	11.08
8	100.0	83.33	4.333
9	190.0	220.8	7.308
10	190.0	181.9	10.88
11	190.0	132.1	9.358
12	190.0	68.33	3.733
13	260.0	191.7	6.317
14	260.0	156.8	9.366
15	260.0	112.6	8.017
16	260.0	56.67	3.267
17	325.0	164.6	5.396
18	325.0	133.5	7.958
19	325.0	94.54	6.771
20	325.0	45.83	2.833
21	385.0	139.6	4.546
22	385.0	112.0	6.658
23	385.0	77.84	5.621
24	385.0	35.83	2.433
25	440.0	116.7	3.767
26	440.0	92.33	5.467
27	440.0	62.53	4.567
28	440.0	26.67	2.067
29	490.0	95.83	3.058
30	490.0	74.42	4.383
31	490.0	48.62	3.608
32	490.0	18.33	1.733
33	535.0	77.08	2.421
34	535.0	58.29	3.408
35	535.0	36.09	2.746
36	535.0	10.83	1.433
37	570.0	62.50	1.925
38	570.0	45.75	2.650
39	570.0	26.35	2.075
40	570.0	5.00	1.200
41	600.0	50.00	1.500
42	600.0	35.00	2.000
43	600.0	18.00	1.500
44	600.0	0.00	1.000

Table 20A. Applied Nodal Loading for Swept Wing Model (Problem 5)
(SI Units)

For all nodes, $P_x = 0.0$ and $P_y = 0.0$

Node No.	P_z (N)	Node No.	P_z (N)	Node No.	P_z (N)
Load Condition 1					
5	5702.3	19	6462.9	33	916.3
6	11480.3	20	4701.5	34	1917.1
7	15114.3	21	2041.6	35	2504.2
8	10586.2	22	4261.2	36	1703.6
9	4350.1	23	5564.4	37	640.5
10	8953.8	24	3789.7	38	1343.3
11	11533.7	25	1610.2	39	1757.0
12	7846.3	26	3362.7	40	1196.5
13	3233.7	27	4385.7	41	275.8
14	6164.9	28	2984.6	42	573.8
15	8477.9	29	1254.3	43	751.7
16	5769.1	30	2619.9	44	516.0
17	2535.4	31	3416.1		
18	5293.1	32	2321.9		
Load Condition 2					
5	10501.7	19	4559.2	33	1788.1
6	17240.4	20	1579.0	34	2873.4
7	10266.0	21	3749.7	35	17701.3
8	3527.3	22	6111.6	36	685.0
9	7881.9	23	3669.6	37	1383.3
10	12877.0	24	1263.2	38	2143.9
11	7583.8	25	2957.9	39	1361.1
12	2588.7	26	4857.2	40	600.5
13	5826.9	27	2895.6	41	591.6
14	9496.5	28	996.4	42	916.3
15	5595.6	29	2304.1	43	582.7
16	1926.0	30	3785.2	44	258.0
17	4657.1	31	2259.6		
18	7646.1	32	778.4		

Table 20B. Applied Nodal Loading for Swept Wing Model (Problem 5)
(U.S. Customary Units)

For all nodes, $P_x = 0.0$ and $P_y = 0.0$

Node No.	P_z (lbf)	Node No.	P_z (lbf)	Node No.	P_z (lbf)
Load Condition 1					
5	1282.0	19	1453.0	33	206.0
6	2581.0	20	1057.0	34	431.0
7	3398.0	21	459.0	35	563.0
8	2380.0	22	958.0	36	383.0
9	978.0	23	1251.0	37	144.0
10	2013.0	24	852.0	38	302.0
11	2593.0	25	362.0	39	395.0
12	1764.0	26	756.0	40	269.0
13	727.0	27	986.0	41	62.0
14	1386.0	28	671.0	42	129.0
15	1906.0	29	282.0	43	169.0
16	1297.0	30	589.0	44	116.0
17	570.0	31	768.0		
18	1190.0	32	522.0		
Load Condition 2					
5	2361.0	19	1025.0	33	402.0
6	3876.0	20	355.0	34	646.0
7	2308.0	21	843.0	35	398.0
8	793.0	22	1374.0	36	154.0
9	1772.0	23	825.0	37	311.0
10	2895.0	24	284.0	38	482.0
11	1705.0	25	665.0	39	306.0
12	582.0	26	1092.0	40	135.0
13	1310.0	27	651.0	41	133.0
14	2135.0	28	224.0	42	206.0
15	1258.0	29	518.0	43	131.0
16	433.0	30	851.0	44	58.0
17	1047.0	31	508.0		
18	1719.0	32	175.0		

Table 21A. Iteration History Data for Problem 5
Swept Wing Model
(SI Units)

Analysis No.		Mass (kg)					
		NEWSUMT (0.5x2)	DUAL 2		Ref. [5] Schmit- Miura	Ref. [28] Rizzi	DUAL 1 Discrete Case
			Unscaled	Scaled			
1		2249	2249	1751	2249	2249	2249
2		1609	1114	1313	1534	1303	1235
3		1365	1121	1121	1226	1216	1245
4		1235	1119	1119	1147	1163	1238
5		1174	<u>1118</u>	<u>1118</u>	1125	1128	1230
6		1146			1120	1116	<u>1230</u>
7		1133			1117	1118	
8		1127			<u>1117</u>	1118	
9		1125				1118	
10		<u>1123</u>				1117	
...						...	
17						<u>1117</u>	
CPU	Total	37.0	19.4		21.5	-	25.6
Time	Anal.	30.8	17.7		17.0	-	21.1
(Sec)	Opt.	4.5 f	0.5 f		3.1 f	0.44 ff	3.0 f

f IBM 360/91

ff CDC 7600 (for comparison, time should be multiplied by 5)

Table 21B. Iteration History Data for Problem 5
Swept Wing Model
(U.S. Customary Units)

Analysis No.		Mass (lbm)					
		NEWSUMT (0.5x2)	DUAL2		Ref. [5] Schmit- Miura	Ref. [28] Rizzi	DUAL1 discrete case
			unscaled	scaled			
1		4959	4959	3861	4959	4959	4959
2		3548	2455	2894	3381	2873	2722
3		3009	2471	2471	2702	2681	2744
4		2723	2466	2466	2528	2563	2730
5		2588	<u>2464</u>	<u>2464</u>	2480	2486	2712
6		2526			2469	2460	<u>2712</u>
7		2498			2463	2464	
8		2484			<u>2463</u>	2464	
9		2480				2464	
10		<u>2475</u>				2463	
...						...	
17						<u>2462</u>	
CPU	Total	37.0	19.4		21.5	-	25.6
Time	Anal.	30.8	17.7		17.0	-	21.1
(Sec)	Opt.	4.5 /	0.5 /		3.1 /	0.44 //	3.0 /

/ IBM 360/91

// CDC 7600 (for comparison, time should be multiplied by 5)

Table 22A. Final Designs for Problem 5
Swept Wing Model
(SI Units)

Linked Design Variable Region	Thickness (cm)					
	NEWSUMT (0.5x2)	DUAL 2	Ref. [5] Schmit- Miura	Ref. [28] Rizzi	Discrete case	
					DUAL 1	Rounding up
CST 1	0.5210	0.5187	0.5179	0.5166	0.6350	0.6350
2	0.4539	0.4516	0.4514	0.4503	0.4826	0.4826
3	0.4013	0.3988	0.3985	0.3970	0.4064	0.4064
4	0.3327	0.3287	0.3292	0.3284	0.4064	0.4064
5	0.2969	0.2944	0.2929	0.2819	0.3175	0.3175
6	0.2629	0.2621	0.2609	0.2423	0.2286	0.3175
7	0.0510	0.0508	0.0508	0.0508	0.0508	0.0508
SSP 1	0.0758	0.0682	0.0745	0.0819	0.0635	0.0813
2	0.0563	0.0562	0.0553	0.0508	0.0635	0.0635
3	0.1097	0.1426	0.1128	0.0878	0.1600	0.1600
4	0.0924	0.0907	0.0897	0.1159	0.0813	0.1016
5	0.5288	0.5014	0.5306	0.5573	0.4826	0.6350
6	0.0717	0.0773	0.0948	0.2421	0.0635	0.0813
7	0.2389	0.2371	0.2296	0.2261	0.2540	0.2540
8	0.2058	0.1999	0.2032	0.1514	0.1803	0.2032
9	0.0834	0.0763	0.0827	0.0887	0.0635	0.0813
10	0.1123	0.1282	0.1247	0.1533	0.1016	0.1600
11	0.1470	0.1694	0.1634	0.2576	0.1600	0.1803
Skin Mass (kg)	995.67	989.75	988.22	--	1106.13	1128.79
Webs Mass (kg)	127.14	128.12	128.91	--	124.09	151.48
Total Mass (kg)	1122.81	1117.87	1117.14	1116.65	1230.23	1280.27
No. of Analyses	10	5	8	17	6	--

Table 22B. Final Designs for Problem 5
Swept Wing Model
(U.S. Customary Units)

Linked Design Variable Region	Thickness (in)					
	NEWSUMT (0.5x2)	DUAL2	Ref[5] Schmit-Miura	Ref. [28] Rizzi	Discrete case	
					DUAL1	Rounding up
CST 1	0.2051	0.2042	0.2039	0.2034	0.250	0.250
2	0.1787	0.1778	0.1777	0.1773	0.190	0.190
3	0.1580	0.1570	0.1569	0.1563	0.160	0.160
4	0.1310	0.1294	0.1296	0.1293	0.160	0.160
5	0.1169	0.1159	0.1153	0.1110	0.125	0.125
6	0.1035	0.1032	0.1027	0.09541	0.090	0.125
7	0.02008	0.02	0.02	0.02	0.020	0.020
SSP 1	0.02983	0.02686	0.02932	0.03223	0.025	0.032
2	0.02216	0.02213	0.02177	0.02	0.025	0.025
3	0.04320	0.05613	0.04439	0.03455	0.063	0.063
4	0.03636	0.03570	0.03531	0.04563	0.032	0.040
5	0.2082	0.1974	0.2089	0.2194	0.190	0.250
6	0.02821	0.03045	0.03732	0.09530	0.025	0.032
7	0.09405	0.09335	0.09038	0.08901	0.100	0.100
8	0.08104	0.07869	0.07999	0.05959	0.071	0.080
9	0.03283	0.03005	0.03255	0.03494	0.025	0.032
10	0.04422	0.05047	0.04911	0.06036	0.040	0.063
11	0.05788	0.06669	0.06435	0.1014	0.063	0.071
Skin Mass (lbm)	2195.04	2181.98	2178.62	-	2438.56	2488.52
Webs Mass (lbm)	280.30	282.46	284.20	-	273.56	333.94
Total Mass (lbm)	2475.34	2464.44	2462.82	2461.76	2712.14	2822.46
No. of Analyses	10	5	8	17	6	-

Table 23A. Definition of Problem 6
Delta Wing Model
(SI Units)

	<u>Skin</u>	<u>Webs</u>
Material	: graphite-epoxy	Titanium
Young's moduli	: $E_L = 144.8 \times 10^6 \text{ kN/m}^2$ $E_T = 11.72 \times 10^6 \text{ kN/m}^2$	$E = 113.1 \times 10^6 \text{ kN/m}^2$
Shear modulus	: $G_{LT} = 4.482 \times 10^6 \text{ kN/m}^2$	
Poisson's ratio	: $\nu_{LT} = 0.21$	$\nu = 0.3$
Specific mass	: $\rho = 1550 \text{ kg/m}^3$	$\rho = 4429 \text{ kg/m}^3$
Thermal expansion coefficients	: $\alpha = -0.378 \text{ } \mu\text{m/m}^\circ\text{C}$ $\alpha = 28.8 \text{ m/m}^\circ\text{C}$	$\alpha = 10.08 \text{ } \mu\text{m/m}^\circ\text{C}$
Allowable stress	:	
Allowable strain	: $\epsilon_L^t = 0.008571 \text{ m/m}$ $\epsilon_L^c = -0.008571 \text{ m/m}$ $\epsilon_T^t = 0.004706 \text{ m/m}$ $\epsilon_T^c = -0.017647 \text{ m/m}$ $\gamma_{LT} = 0.018462$	$\sigma_a = 861,875 \text{ kN/m}^2$
Minimum thickness	: $D^{(L)} = 0.0127 \text{ cm}$	$D^{(L)} = 0.0508 \text{ cm}$
Initial thickness	See Table 27A.	$D^{(o)} = 0.381 \text{ cm}$

Nodal Loading (2 load cases)

Load Case	Node	Load Components (N)		
		X	Y	Z
1	10-44	0	0	35,918
2	10-44	0	0	-35,918

Displacement Constraints

Node	Displacement Limits (cm)		
	X	Y	Z
43	-	-	± 256.0
44	-	-	± 256.0

Table 23B. Definition of Problem 6
Delta Wing Model
(U.S. Customary Units)

	<u>Skin</u>	<u>Webs</u>
Material :	graphite-epoxy	titanium
Young's moduli :	$E_L = 21 \times 10^6$ psi $E_T = 1.7 \times 10^6$ psi	$E = 1.64 \times 10^7$ psi
Shear modulus :	$G_{LT} = 0.65 \times 10^6$ psi	
Poisson's ratio :	$\nu_{LT} = 0.21$	$\nu = 0.3$
Specific mass :	$\rho = 0.056$ lbm/in ³	$\rho = 0.16$ lbm/in ³
Thermal expansion coefficients :	$\alpha_L = -0.21 \times 10^{-6}$ in/in°F $\alpha_T = 16 \times 10^{-6}$ in/in°F	$\alpha = 5.6 \times 10^{-6}$ in/in°F
Allowable stress :		
Allowable strain :	$\epsilon_L^t = 0.008571$ in/in. $\epsilon_L^c = -0.008571$ in/in. $\epsilon_T^t = 0.004706$ in/in. $\epsilon_T^c = -0.017647$ in/in. $\gamma_{LT} = 0.018462$	$\sigma_a = 125,000$ psi
Minimum thickness :	$D^{(L)} = 0.005$ in.	$D^{(L)} = 0.02$ in.
Initial thickness	See Table 27.A	$D^{(o)} = 0.15$ in.

Nodal Loading (2 load cases)

Load Case	Node	Load components (lbf)		
		X	Y	Z
1	10-44	0	0	8075
2	10-44	0	0	-8075

Displacement constraints

Node	Displacement limits (in)		
	X	Y	Z
43	-	-	± 100.8
44	-	-	± 100.8

Table 24A. Nodal Coordinates for Delta Wing Model (Problem 6)
(SI Units)

Node No.	X (cm)	Y (cm)	Z (cm)
1	0.0	2438.4	16.43
2	0.0	2133.6	29.13
3	0.0	1828.8	38.13
4	0.0	1524.0	43.38
5	0.0	1219.2	44.93
6	0.0	914.4	42.77
7	0.0	609.6	36.88
8	0.0	304.8	27.28
9	0.0	0.0	13.95
10	254.0	2133.6	16.22
11	254.0	1828.8	28.30
12	254.0	1524.0	36.22
13	254.0	1219.2	40.03
14	254.0	914.4	39.67
15	254.0	609.6	35.20
16	254.0	304.8	26.57
17	254.0	0.0	13.80
18	508.0	1828.8	15.95
19	508.0	1524.0	27.23
20	508.0	1219.2	33.86
21	508.0	914.4	35.79
22	508.0	609.6	33.07
23	508.0	304.8	25.68
24	508.0	0.0	13.62
25	762.0	1524.0	15.61
26	762.0	1219.2	25.88
27	762.0	914.4	30.78
28	762.0	609.6	30.33
29	762.0	304.8	24.54
30	762.0	0.0	13.38
31	1016.0	1219.2	15.15
32	1016.0	914.4	24.04
33	1016.0	609.6	26.64
34	1016.0	304.8	22.99
35	1016.0	0.0	13.06
36	1270.0	914.4	14.50
37	1270.0	609.6	21.44
38	1270.0	304.8	20.81
39	1270.0	0.0	12.61
40	1524.0	609.6	13.52
41	1524.0	304.8	17.49
42	1524.0	0.0	11.93
43	1854.2	213.4	11.07
44	1854.2	0.0	10.06

Table 24B. Nodal Coordinates for Delta Wing Model (Problem 6)
(U.S. Customary Units)

Node No.	X (in)	Y (in)	Z (in)
1	0.0	960.0	6.468
2	0.0	840.0	11.47
3	0.0	720.0	15.01
4	0.0	600.0	17.08
5	0.0	480.0	17.69
6	0.0	360.0	16.84
7	0.0	240.0	14.52
8	0.0	120.0	10.74
9	0.0	0.0	5.492
10	100.0	840.0	6.385
11	100.0	720.0	11.14
12	100.0	600.0	14.26
13	100.0	480.0	15.76
14	100.0	360.0	15.62
15	100.0	240.0	13.86
16	100.0	120.0	10.46
17	100.0	0.0	5.434
18	200.0	720.0	6.281
19	200.0	600.0	10.72
20	200.0	480.0	13.33
21	200.0	360.0	14.09
22	200.0	240.0	13.02
23	200.0	120.0	10.11
24	200.0	0.0	5.362
25	300.0	600.0	6.146
26	300.0	480.0	10.19
27	300.0	360.0	12.12
28	300.0	240.0	11.94
29	300.0	120.0	9.660
30	300.0	0.0	5.268
31	400.0	480.0	5.966
32	400.0	360.0	9.463
33	400.0	240.0	10.49
34	400.0	120.0	9.051
35	400.0	0.0	5.143
36	500.0	360.0	5.710
37	500.0	240.0	8.441
38	500.0	120.0	8.193
39	500.0	0.0	4.966
40	600.0	240.0	5.322
41	600.0	120.0	6.887
42	600.0	0.0	4.696
43	730.0	84.0	4.360
44	730.0	0.0	3.959

Table 25A. Fuel Mass Distribution for Delta Wing Model
(Problem 6)
(SI Units)

Node No.	Fuel Mass (kg)	Node No.	Fuel Mass (kg)	Node No.	Fuel Mass (kg)
10	866.4	22	1765	34	1225
11	1510	23	1370	35	694.9
12	1932	24	725.8	36	772.0
13	2132	25	831.0	37	1143
14	2118	26	1377	38	1107
15	1878	27	1642	39	671.3
16	1415	28	1619	40	721.2
17	734.8	29	1293	41	934.4
18	849.1	30	714.0	42	635.0
19	1452	31	808.3	43	589.7
20	1810	32	1279	44	535.2
21	1910	33	1420		

Total fuel mass = 42,480 kg

Table 25B. Fuel Weight Distribution for Delta Wing Model
(Problem 6)
(U.S. Customary Units)

Node No.	Fuel Mass (lbm)	Node No.	Fuel Mass (lbm)	Node No.	Fuel Mass (lbm)
10	1910	22	3890	34	2700
11	3330	23	3020	35	1532
12	4260	24	1600	36	1702
13	4700	25	1832	37	2520
14	4670	26	3036	38	2440
15	4140	27	3620	39	1480
16	3120	28	3570	40	1590
17	1620	29	2850	41	2060
18	1872	30	1574	42	1400
19	3200	31	1782	43	1300
20	3990	32	2820	44	1180
21	4210	33	3130		

Total fuel mass = 93,650 lbm.

Table 26A. Iteration History Data for Problem 6
Delta Wing Model
(SI Units)

Analysis No.	NEWSUMT (continuous)		DUAL 2 (continuous)		DUAL 1 (mixed)	
	Mass (Mg)	Frequency (Hz)	Mass (Mg)	Frequency (Hz)	Mass (Mg)	Frequency (Hz)
1	39.38	2.829	39.38	2.829	39.38	2.829
2	31.87	2.650	9.703	2.016	9.448	2.009
3	26.36	2.516	7.598	1.961	7.788	2.000
4	22.30	2.396	6.505	1.937	6.985	1.974
5	19.34	2.293	6.736	2.007	6.799	2.000
6	17.25	2.209	6.341	1.987	6.532	1.994
7	15.39	2.127	6.264	2.003	6.387	1.996
8	13.54	2.042	6.178	2.007	6.314	2.003
9	12.15	2.010	6.083	2.005	6.133	1.998
10	11.14	2.009	6.006	2.004	6.083	2.003
11	10.27	2.010	5.942	2.002	6.065	2.009
12	9.503	2.010	5.892	2.001	6.028	2.003
13	8.836	2.010	5.856	2.001	<u>6.028</u>	2.000
14	8.260	2.010	5.829	2.000		
15	7.766	2.009	<u>5.811</u>	2.000		
..				
20	6.378	2.003				
25	6.151	2.002				
29	<u>6.110</u>	2.002				
CPU Total	719		261		253	
Time Analy	564		252		234	
(sec) Opt	145		2		12	

Table 26B. Iteration History Data for Problem 6
Delta Wing Model
(U.S. Customary Units)

Analysis No.		NEWSUMT(continuous)		DUAL2 (continuous)		DUAL1 (mixed)	
		Mass (x10 ³ lbm)	Frequency (Hz)	Mass (x10 ³ lbm)	Frequency (Hz)	Mass (x10 ³ lbm)	Frequency (Hz)
1		86.82	2.829	86.82	2.829	86.82	2.829
2		70.26	2.650	21.39	2.016	20.83	2.009
3		58.11	2.516	16.75	1.961	17.17	2.000
4		49.16	2.396	14.34	1.937	15.40	1.974
5		42.64	2.293	14.85	2.007	14.99	2.000
6		38.04	2.209	13.98	1.987	14.40	1.994
7		33.93	2.127	13.81	2.003	14.08	1.996
8		29.86	2.042	13.62	2.007	13.92	2.003
9		26.78	2.010	13.41	2.005	13.52	1.998
10		24.56	2.009	13.24	2.004	13.41	2.003
11		22.64	2.010	13.10	2.002	13.37	2.009
12		20.95	2.010	12.99	2.001	13.29	2.003
13		19.48	2.010	12.91	2.001	<u>13.29</u>	2.000
14		18.21	2.010	12.85	2.000		
15		17.12	2.009	<u>12.81</u>	2.000		
..					
20		14.06	2.003				
25		13.56	2.002				
29		<u>13.47</u>	2.002				
CPU	Total	719		261		253	
Time	Analy	564		252		234	
(sec)	opt.	145		2		12	

Table 27A. Initial and Final Design for Problem 6
Delta Wing Model
(SI Units)

Linked Design Variable Region	Fiber Orientation	Initial Design (cm)	NEWSUMT continuous case (cm)	DUAL 2 continuous case (cm)	DUAL 1 mixed case (cm)
1	0°	0.3810	0.0244	0.0198	0.0254 (2)
	±45°	0.3810	0.0193	0.0127*	0.0254 (2)
	90°	0.3810	0.0213*	0.0127*	0.0254*(2)
2	0°	1.5240	0.0714	0.1191	0.1016 (8)
	±45°	1.2700	0.0414*	0.0127*	0.0254*(2)
	90°	0.2540	0.0160*	0.0127*	0.0254*(2)
3	0°	3.8100	0.3787	0.2306	0.2540 (20)
	±45°	2.5400	0.0594*	0.0325*	0.0508*(4)
	90°	0.7620	0.0127*	0.0127*	0.0254*(2)
4	0°	3.8100	2.3731	2.9464	2.7940 (220)
	±45°	2.5400	0.0899*	0.0607*	0.0762*(6)
	90°	0.7620	0.0348	0.0203	0.0254 (2)
5	0°	1.5240	0.0343	0.0531	0.0508 (4)
	±45°	1.2700	0.0249	0.0127	0.0254 (2)
	90°	0.2540	0.0127	0.0127	0.0254*(2)
6	0°	3.8100	0.2891	0.1412	0.1778 (14)
	±45°	2.5400	0.0803	0.0277	0.0254 (2)
	90°	0.7620	0.0127	0.0127*	0.0254*(2)
7	0°	3.8100	1.9205	2.1064	2.1082 (166)
	±45°	2.5400	0.0859	0.0328	0.0508 (4)
	90°	0.7620	0.0404	0.0300	0.0254 (2)
8	0°	0.5080	0.0175	0.0127	0.0254 (2)
	±45°	0.5080	0.0127	0.0127	0.0254 (2)
	90°	0.2540	0.0127	0.0127	0.0254 (2)
9	0°	2.5400	0.2055	0.0775	0.1016 (8)
	±45°	1.2700	0.1031	0.0450	0.0508 (4)
	90°	0.5080	0.0127	0.0127	0.0254 (2)
10	0°	2.5400	1.4732	1.5890	1.5494 (122)
	±45°	1.2700	0.1029	0.0638	0.0762 (6)
	90°	0.5080	0.0127	0.0127	0.0254 (2)
11	0°	2.5400	0.1044	0.0338	0.0508 (4)
	±45°	1.2700	0.1130	0.0569	0.0762 (6)
	90°	0.5080	0.0127	0.0127	0.0254 (2)
12	0°	2.5400	0.9517	1.0132	0.9906 (78)
	±45°	1.2700	0.1417	0.0980	0.1016 (8)
	90°	0.5080	0.0127	0.0127	0.0254 (2)
13	0°	0.5080	0.0267	0.0127	0.0254 (2)
	±45°	0.5080	0.0757	0.0389	0.0508 (4)
	90°	0.2540	0.0127	0.0127	0.0254 (2)
14	0°	0.7620	0.5151	0.5415	0.5334 (42)
	±45°	0.2540	0.1486	0.1184	0.1270 (10)
	90°	0.2540	0.0127	0.0127	0.0254 (2)
15	0°	0.7620	0.2169	0.2273	0.2286 (18)
	±45°	0.2540	0.1143	0.1128	0.1270 (10)
	90°	0.2540	0.0127	0.0127	0.0254*(2)
16	0°	0.2540	0.0724	0.0668	0.0762 (6)
	±45°	0.2540	0.0262*	0.0315*	0.0254 (2)
	90°	0.2540	0.0127*	0.0127*	0.0254 (2)
Skin Mass (kg)		37757.1	5475.74	5253.96	5456.33
Web Mass (kg)		1624.6	635.84	557.81	570.22
Total Structural Mass (kg)		39381.7	6111.58	5811.77	6026.55
No. of Analyses		---	29	15	13

* Transverse tension strain limit is attained in material of the bottom skin (within 5%).

Table 27B. Initial and Final Designs for Problem 6
Delta Wing Model
(U.S. Customary Units)

Linked Design Variable Region	Fiber Orientation	Initial Design (in)	NEWSUMT continuous case (in)	DUAL 2 continuous case (in)	DUAL 1 mixed case (in)
1	0°	0.15	0.0096	0.0078	0.01 (2)
	+45°	0.15	0.0076	0.0050*	0.01 (2)
	90°	0.15	0.0084*	0.0059*	0.01* (2)
2	0°	0.60	0.0281	0.0469	0.04 (8)
	+45°	0.50	0.0163*	0.0050*	0.01* (2)
	90°	0.10	0.0063*	0.0050*	0.01* (2)
3	0°	1.5	0.1491	0.0908	0.10 (20)
	+45°	1.0	0.0234*	0.0128*	0.02* (4)
	90°	0.3	0.0050*	0.0050*	0.01* (2)
4	0°	1.5	0.9343	1.160	1.10 (220)
	+45°	1.0	0.0354*	0.0239*	0.03* (6)
	90°	0.3	0.0137	0.0080	0.01 (2)
5	0°	0.60	0.0135	0.0209	0.02 (4)
	+45°	0.50	0.0098	0.0050	0.01 (2)
	90°	0.10	0.0050	0.0050*	0.01* (2)
6	0°	1.5	0.1138	0.0556	0.07 (14)
	+45°	1.0	0.0316	0.0109	0.01 (2)
	90°	0.3	0.0050	0.0050*	0.01* (2)
7	0°	1.5	0.7561	0.8293	0.83 (166)
	+45°	1.0	0.0338	0.0129	0.02 (4)
	90°	0.3	0.0159	0.0118	0.01 (2)
8	0°	0.2	0.0069	0.0050	0.01 (2)
	+45°	0.2	0.0050	0.0050	0.01 (2)
	90°	0.1	0.0050	0.0050	0.01 (2)
9	0°	1.0	0.0809	0.0305	0.04 (8)
	+45°	0.5	0.0406	0.0177	0.02 (4)
	90°	0.2	0.0050	0.0050	0.01 (2)
10	0°	1.0	0.5800	0.6256	0.61 (122)
	+45°	0.5	0.0405	0.0251	0.03 (6)
	90°	0.2	0.0050	0.0050	0.01 (2)
11	0°	1.0	0.0411	0.0133	0.02 (4)
	+45°	0.5	0.0445	0.0224	0.03 (6)
	90°	0.2	0.0050	0.0050	0.01 (2)
12	0°	1.0	0.3747	0.3989	0.39 (78)
	+45°	0.5	0.0558	0.0386	0.04 (8)
	90°	0.2	0.0050	0.0050	0.01 (2)
13	0°	0.2	0.0105	0.0050	0.01 (2)
	+45°	0.2	0.0298	0.0153	0.02 (4)
	90°	0.1	0.0050	0.0050	0.01 (2)
14	0°	0.3	0.2028	0.2132	0.21 (42)
	+45°	0.1	0.0585	0.0466	0.05 (10)
	90°	0.1	0.0050	0.0050	0.01 (2)
15	0°	0.3	0.0854	0.0895	0.09 (18)
	+45°	0.1	0.0450	0.0444	0.05 (10)
	90°	0.1	0.0050	0.0050	0.01* (2)
16	0°	0.1	0.0285	0.0263	0.03 (6)
	+45°	0.1	0.0103*	0.0124*	0.01 (2)
	90°	0.1	0.0050*	0.0050*	0.01 (2)
Skin Mass (lbm)		83238.8	12071.74	11582.80	12028.94
Web Mass (lbm)		3581.5	1401.76	1229.74	1257.10
Total Structural Mass (lbm)		86820.4	13473.50	12812.54	13286.04
No. of Analyses		---	29	15	13

* Transverse tension strain limit is attained in material of the bottom skin (within 5%).

Table 28A. Final Webs Thicknesses for Problem 6
Delta Wing Model
(SI Units)

Linked Design Variable Region	NEWSUMT (continuous case) (cm)	DUAL 2 (continuous case) (cm)	DUAL 1 (mixed case) (cm)
1	0.0508	0.0508	0.0508
2	0.0508	0.0508	0.0508
3	0.0873	0.0741	0.0763
4	0.05083	0.0508	0.0508
5	0.05083	0.0508	0.0508
6	0.05113	0.0508	0.0508
7	0.0508	0.0508	0.0569
8	0.05999	0.0508	0.0508
9	0.3363	0.2199	0.2576
10	0.6830	0.6782	0.6480
11	0.3612	0.2447	0.2764
12	0.0508	0.0508	0.0508
Mass (kg)	635.84	557.81	570.22

Table 28B. Final Webs Thicknesses for Problem 6
Delta Wing Model
(U.S. Customary Units)

Linked Design Variable Region	NEWSUMT (continuous case) (in)	DUAL2 (continuous case) (in)	DUAL1 (mixed case) (in)
1	0.02	0.02	0.02
2	0.02	0.02	0.02
3	0.03437	0.02917	0.03004
4	0.02001	0.02	0.02
5	0.02001	0.02	0.02
6	0.02013	0.02	0.02
7	0.02	0.02	0.02240
8	0.02362	0.02	0.02
9	0.1324	0.08657	0.1014
10	0.2689	0.2670	0.2551
11	0.1422	0.09635	0.1088
12	0.02	0.02	0.02
Mass (lbm)	1401.76	1229.74	1257.10

Table 29. Detailed Iteration History Data for Problem 6
Delta Wing Model-Mixed Case (DUAL1)

Stage No.	No. of Retained Constraints Q_R	No. of Active Constraints $Q_R - N$	No. of Discon. Planes P	No. of Restarts	No. of O.D.M's	Lower Bound Weight \underline{W}	Dual Function ℓ^*	Final Weight	Upper Bound Weight W
1	127	3	3	4	138	10376	10412	10417	10444
2	136	3	3	4	44	8519	8545	8583	8583
3	119	6	6	3	19	7623	7650	7699	7739
4	119	4	3	4	20	7454	7481	7493	7493
5	94	6	6	2	15	7110	7175	7200	7227
6	38	4	4	4	20	6976	7006	7041	7041
7	34	5	4	2	10	6885	6915	6962	6962
8	33	5	5	2	12	6683	6730	6762	6776
9	35	6	6	2	19	6640	6706	6706	6760
10	35	5	5	2	16	6608	6658	6687	6700
11	36	8	7	2	17	6552	6613	6645	6672
12	35	7	6	2	17	6551	6611	6643	6656
13	35	7	6	4	33	6539	6586	6643	6657

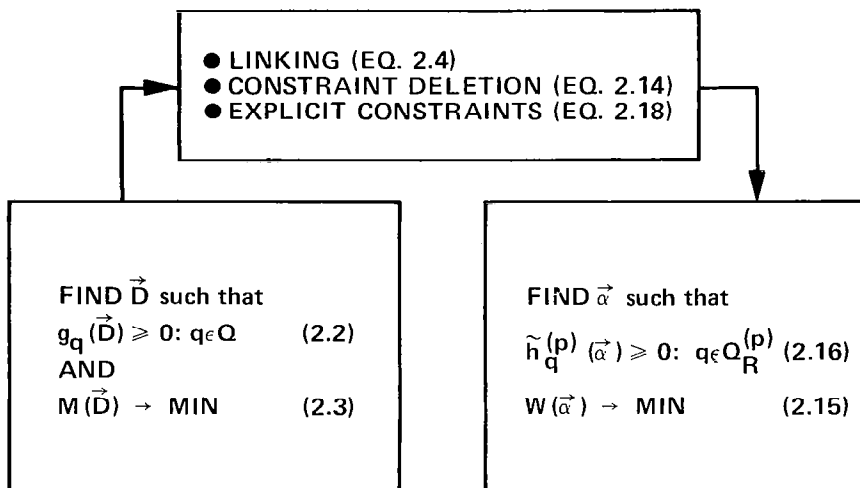


Figure 1. Key to a Tractable Formulation

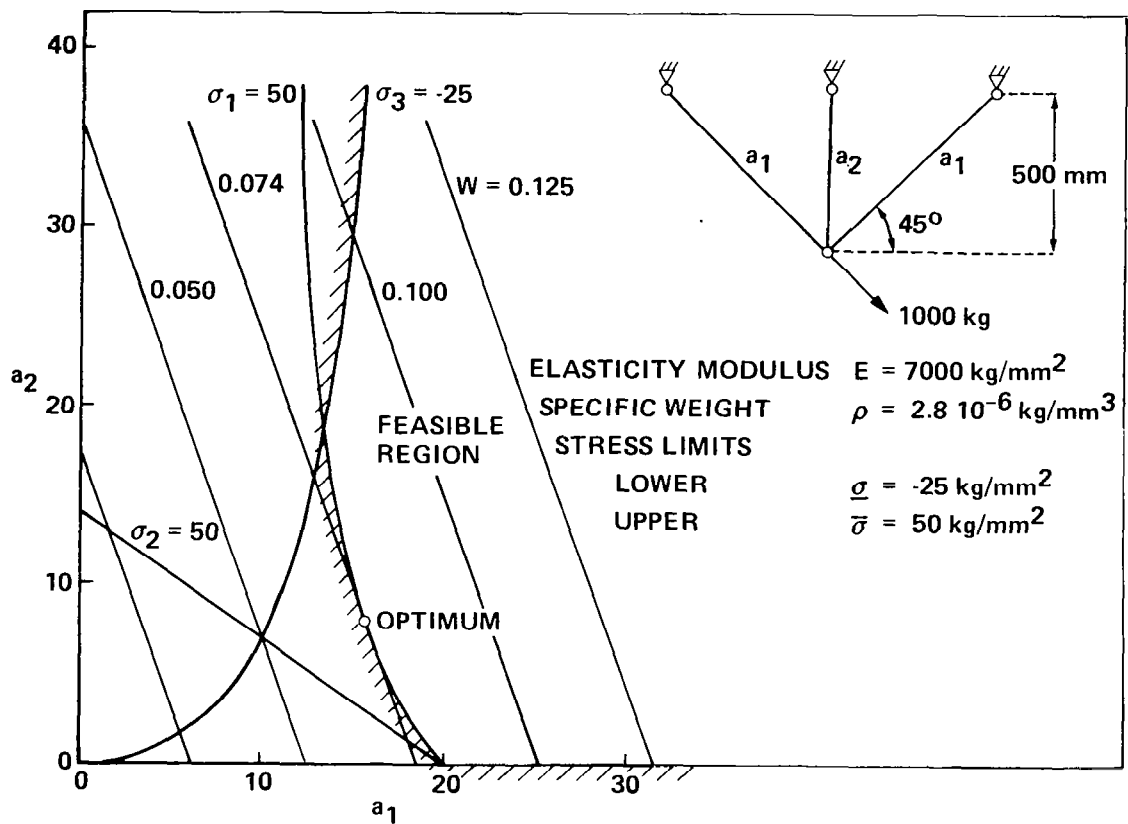


Figure 2. Design Space For 3-Bar Truss

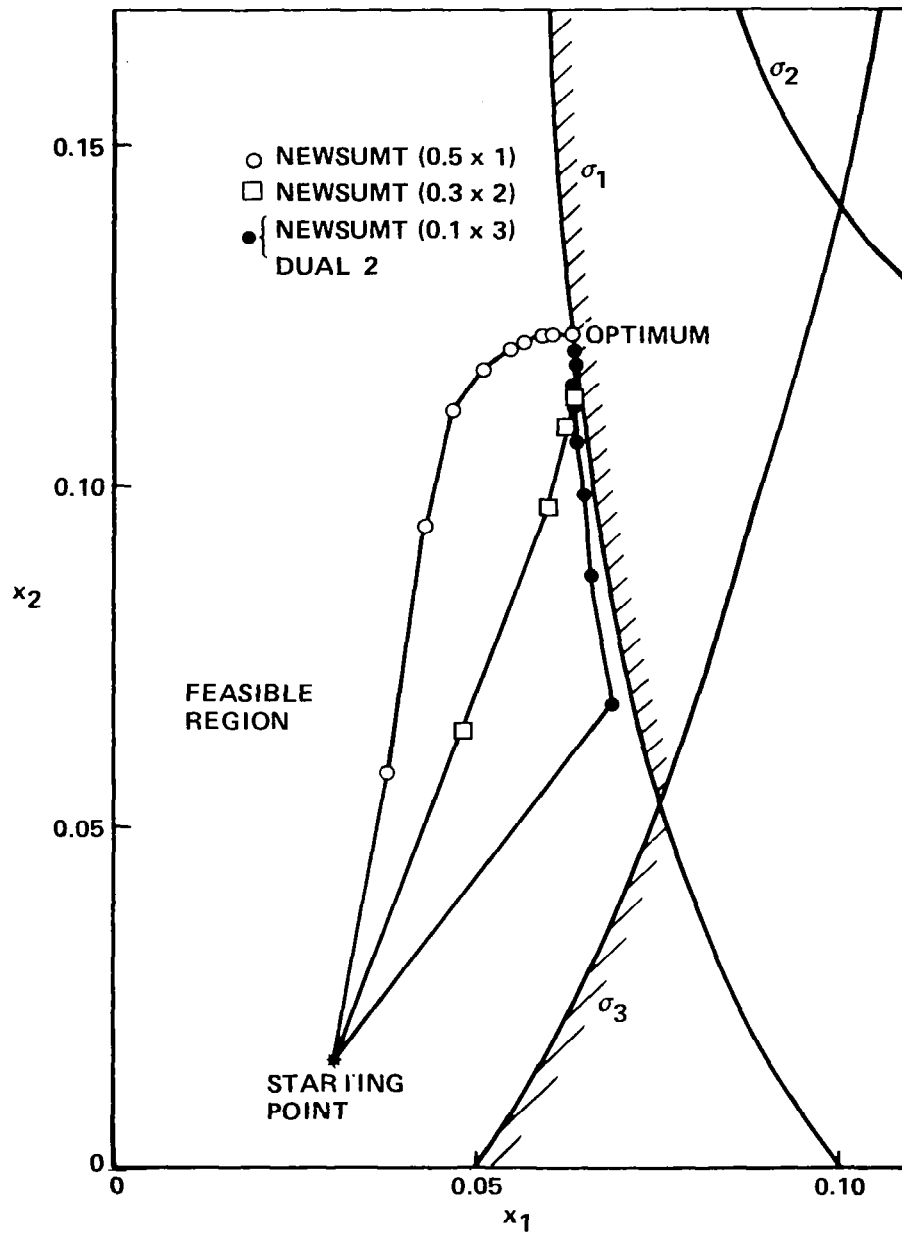


Figure 3. 3-Bar Truss - Trajectories in Reciprocal Space

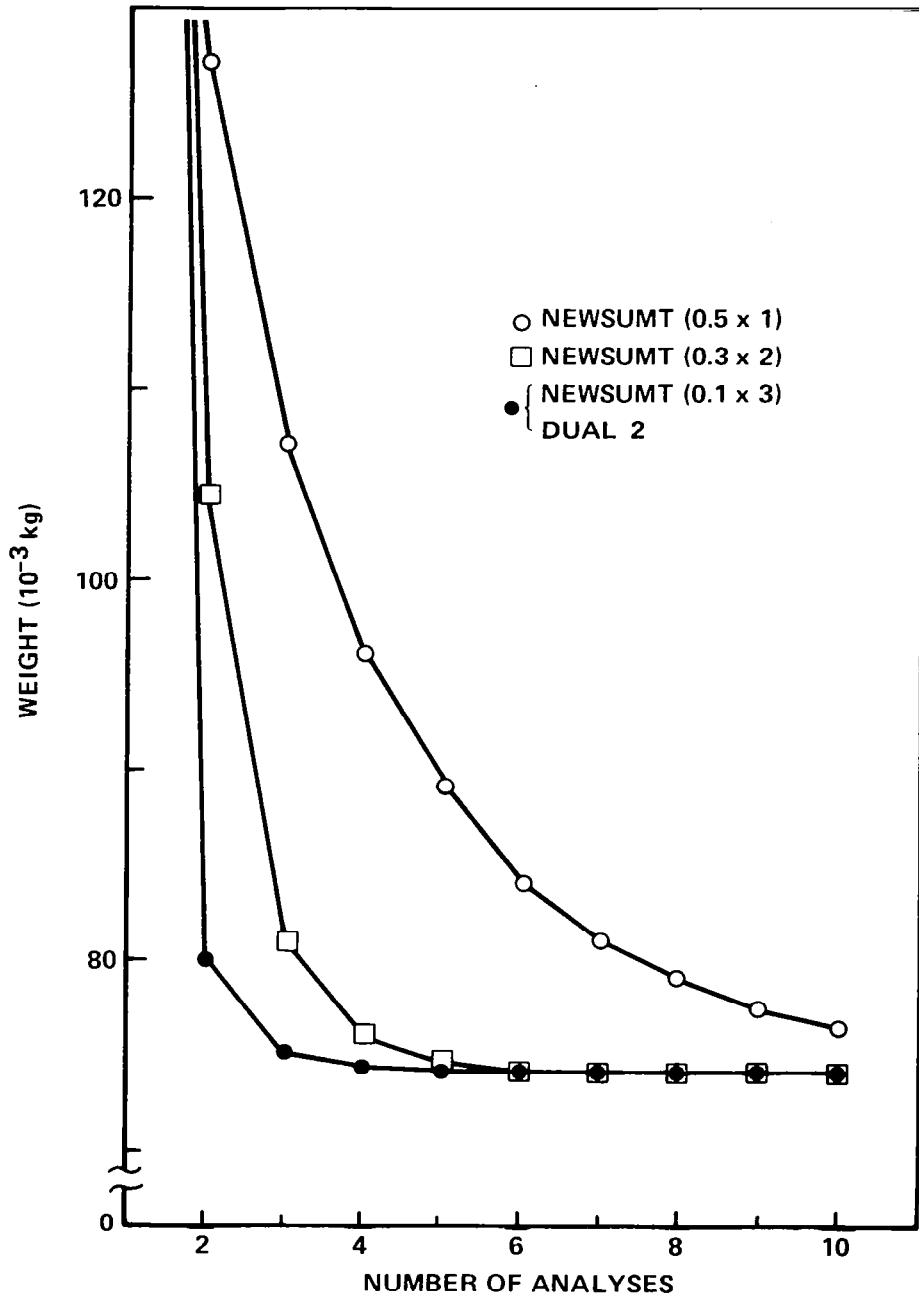


Figure 4. 3-Bar Truss - Convergence of Weight

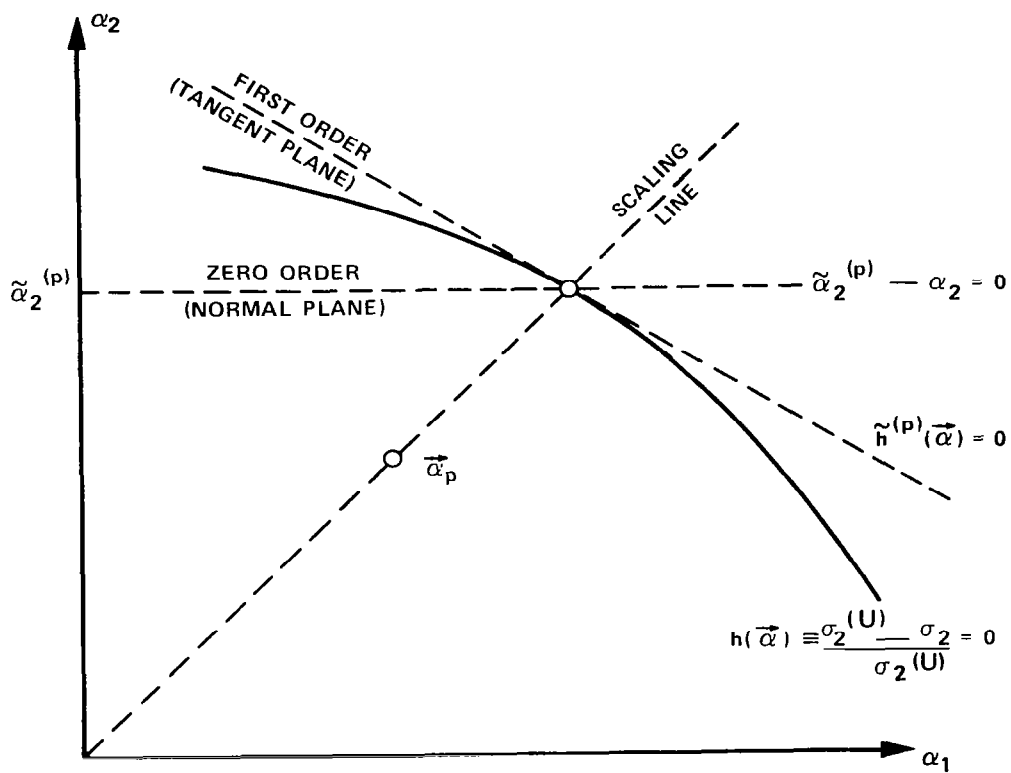


Figure 5. Zero and First Order Approximations

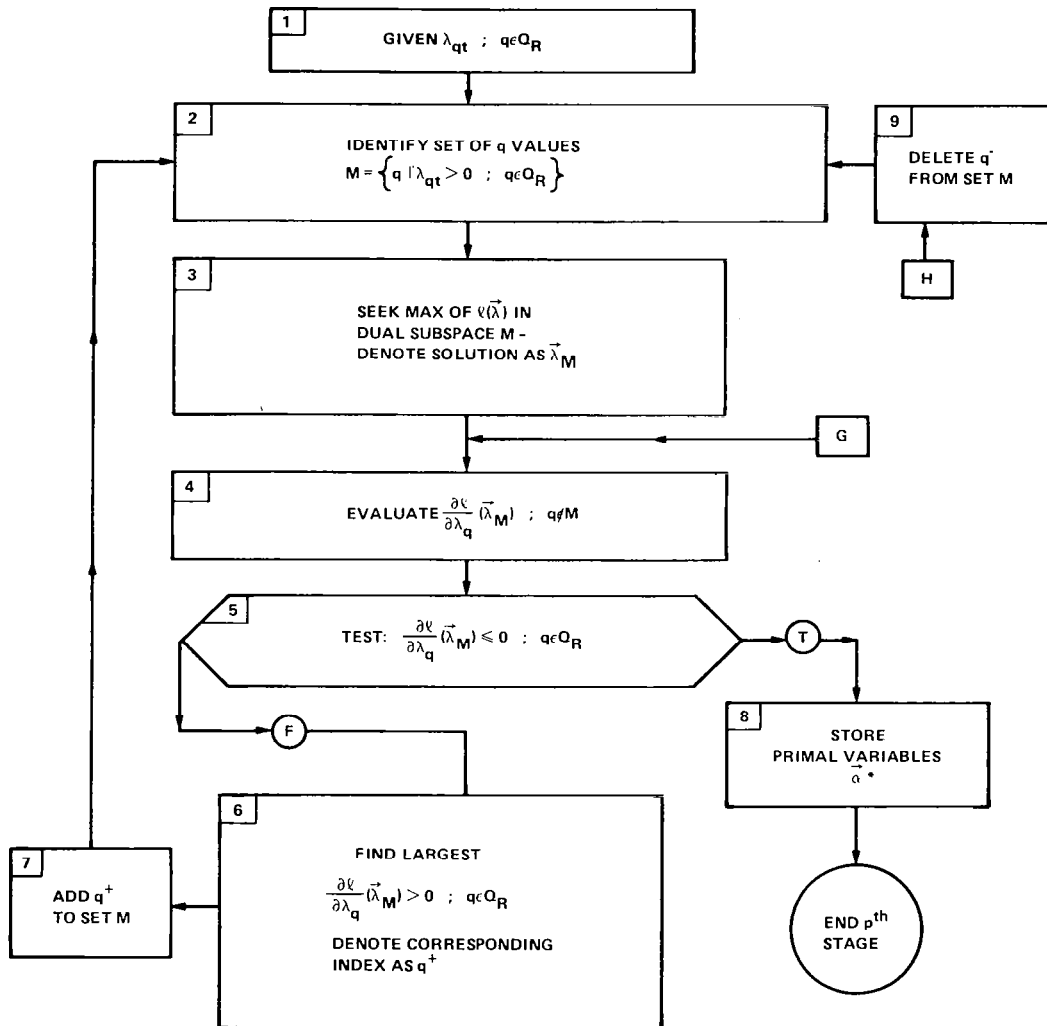


Figure 6. Dual 2 Algorithm – Block Diagram.

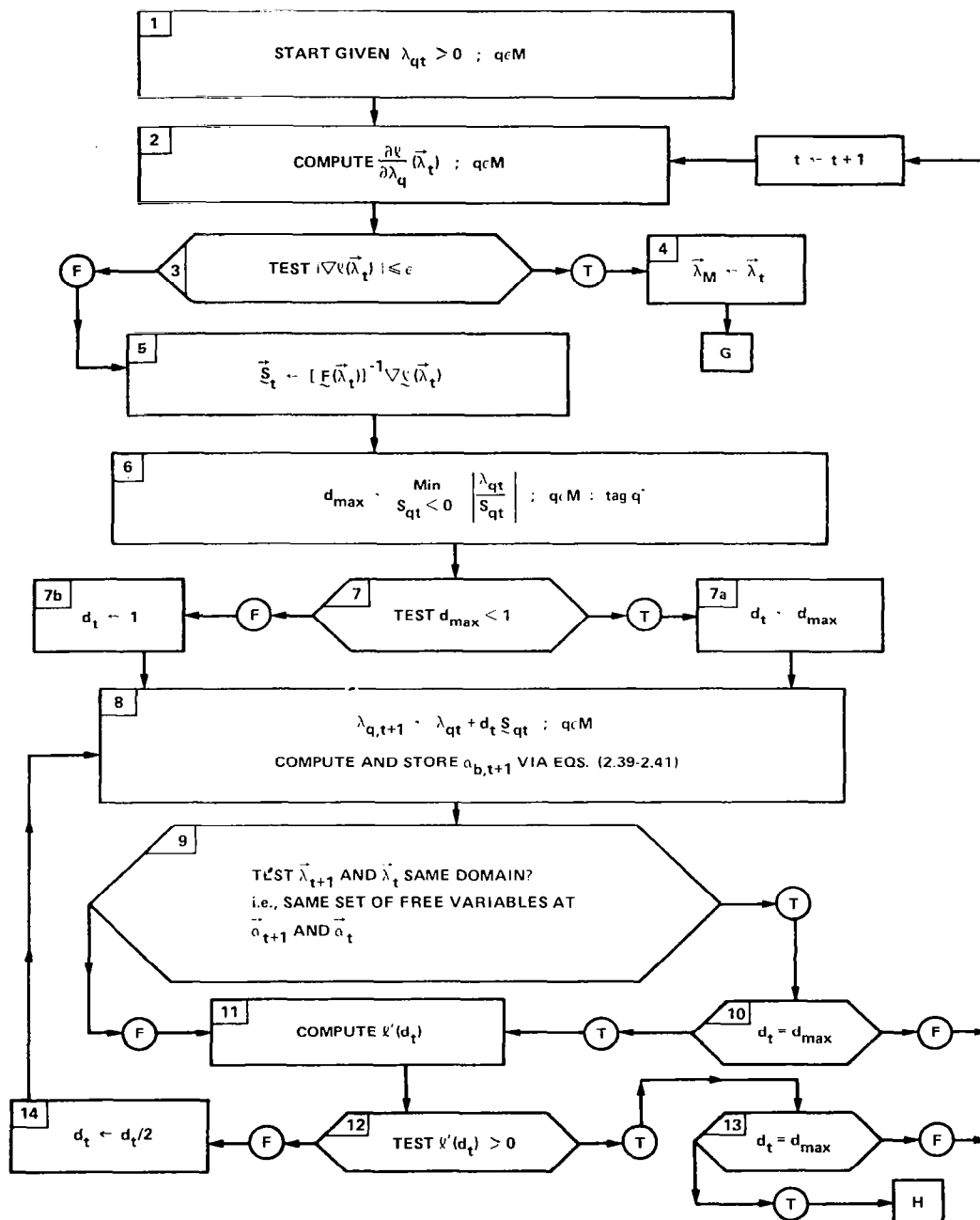
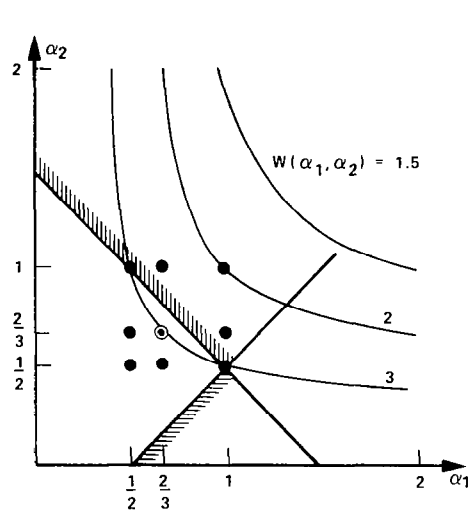
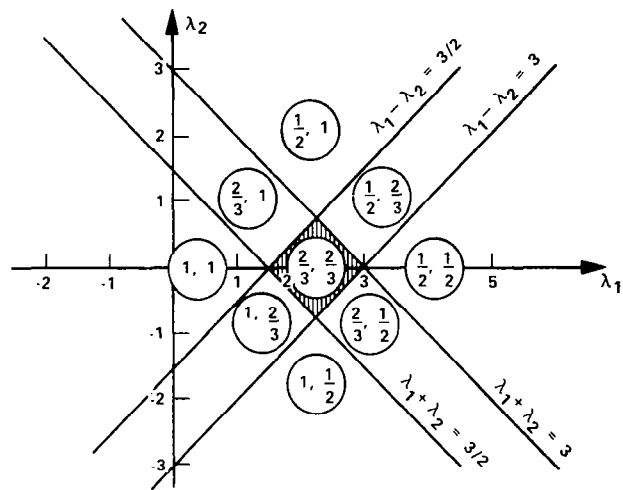


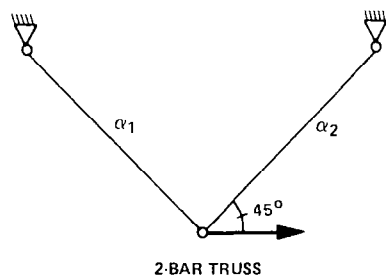
Figure 7. Seek Max of $l(\vec{\lambda})$ in Subspace M



A. Discrete Points in Primal Space



B. Regions in Dual Space



C. Contours of Dual Function

Figure 8. Simple 2 D Example - Pure Discrete Problem

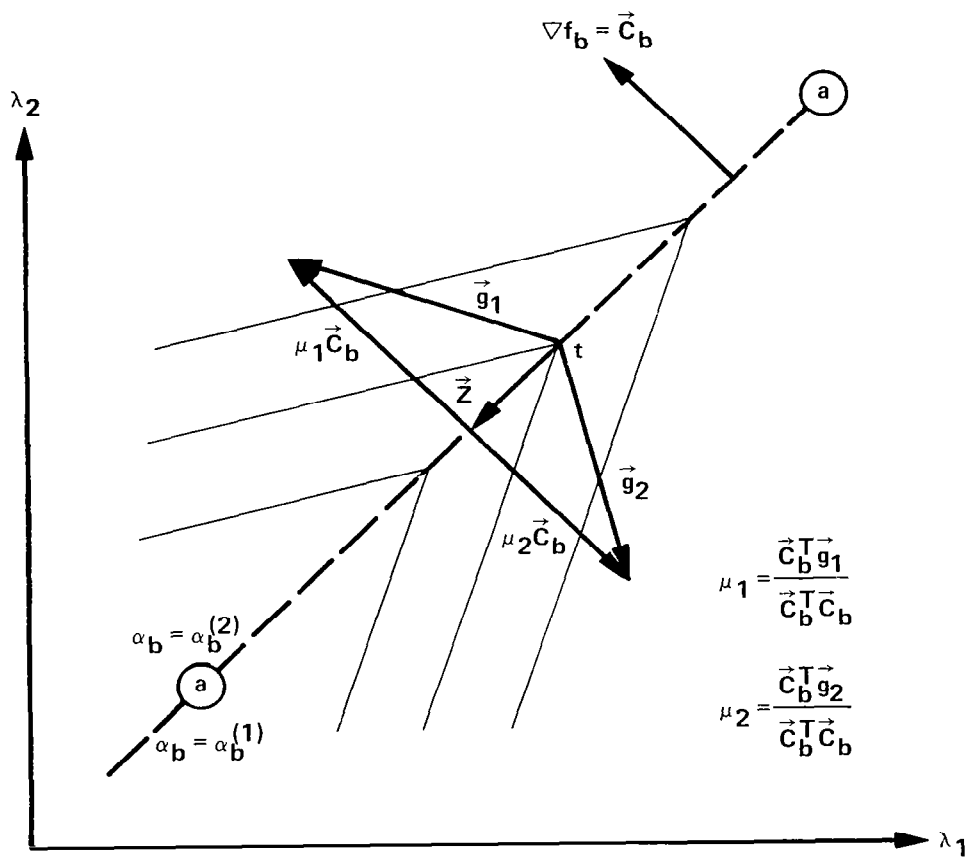


Figure 9. Projecting Multiple Gradients Into Discontinuity Plane

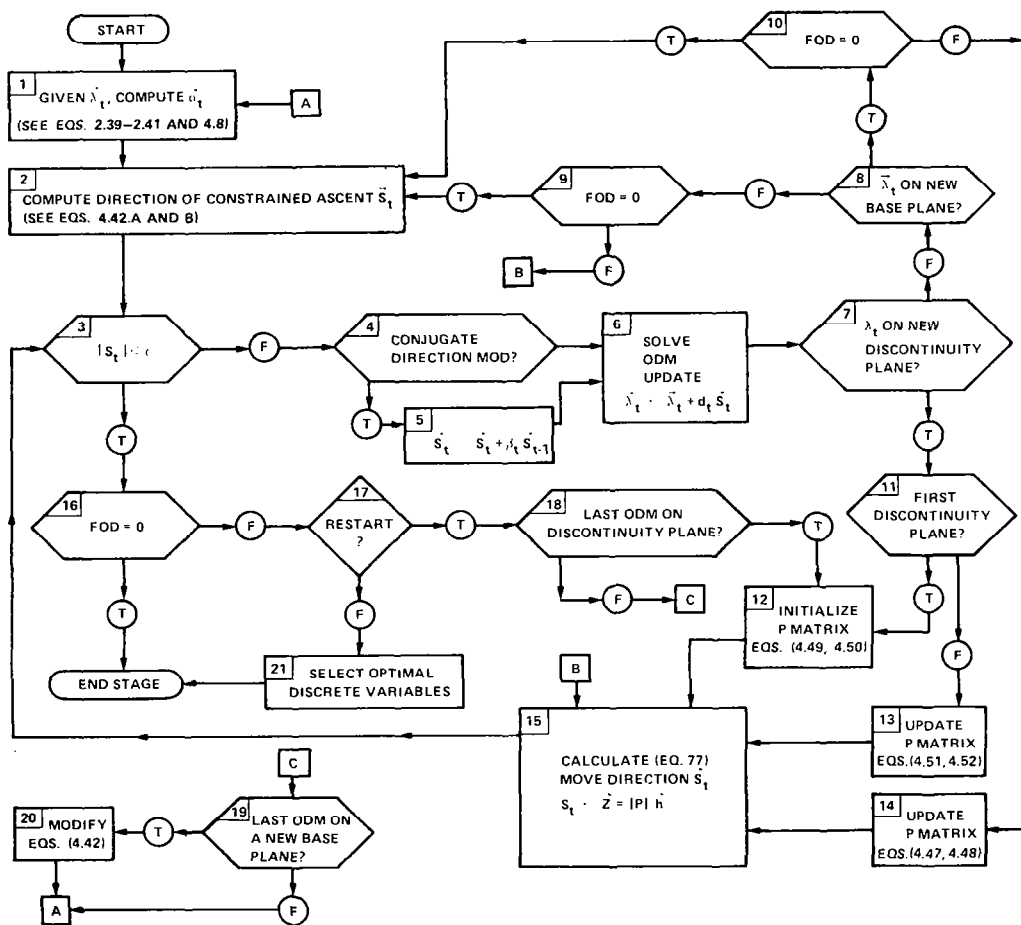


Figure 10. Dual 1 Algorithm – Block Diagram.

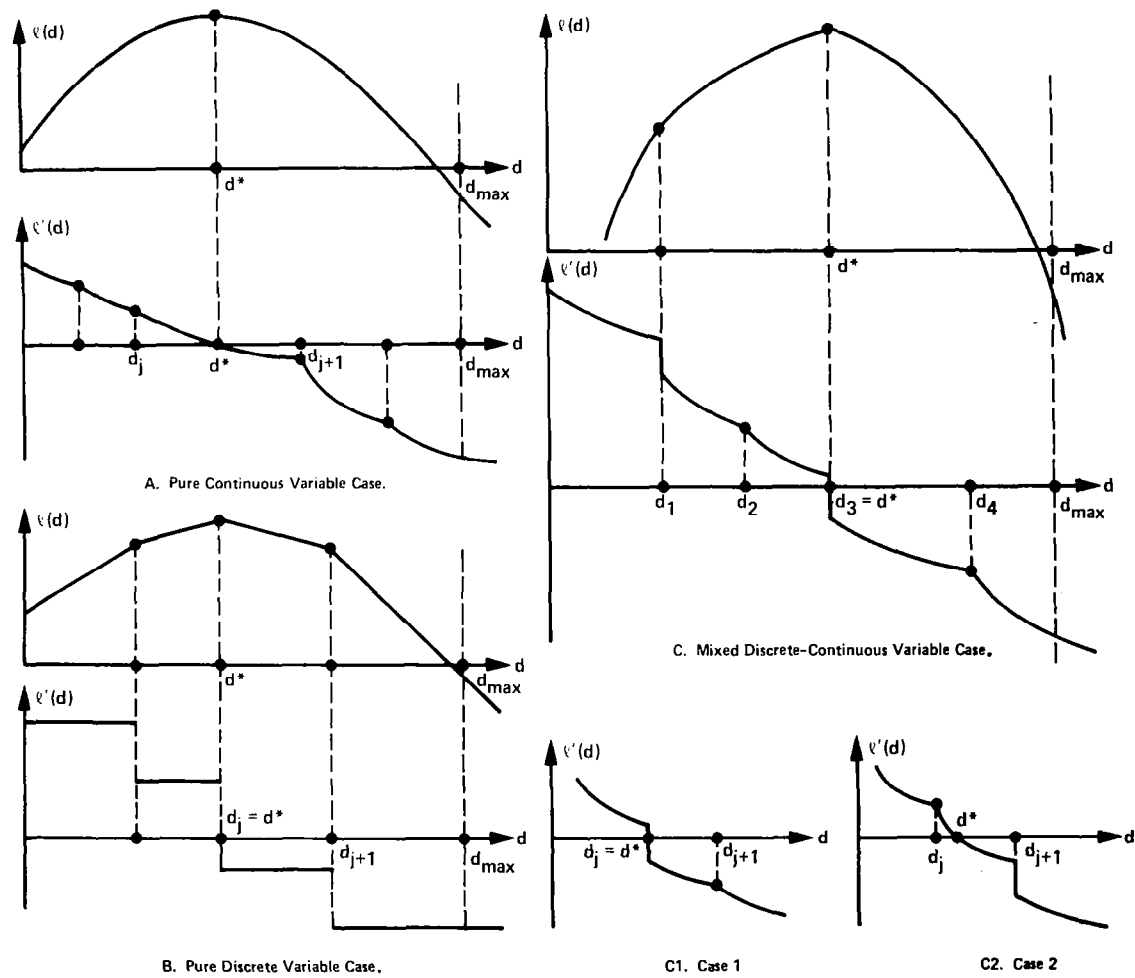


Figure 11. One Dimensional Maximization Scheme (Dual 1).

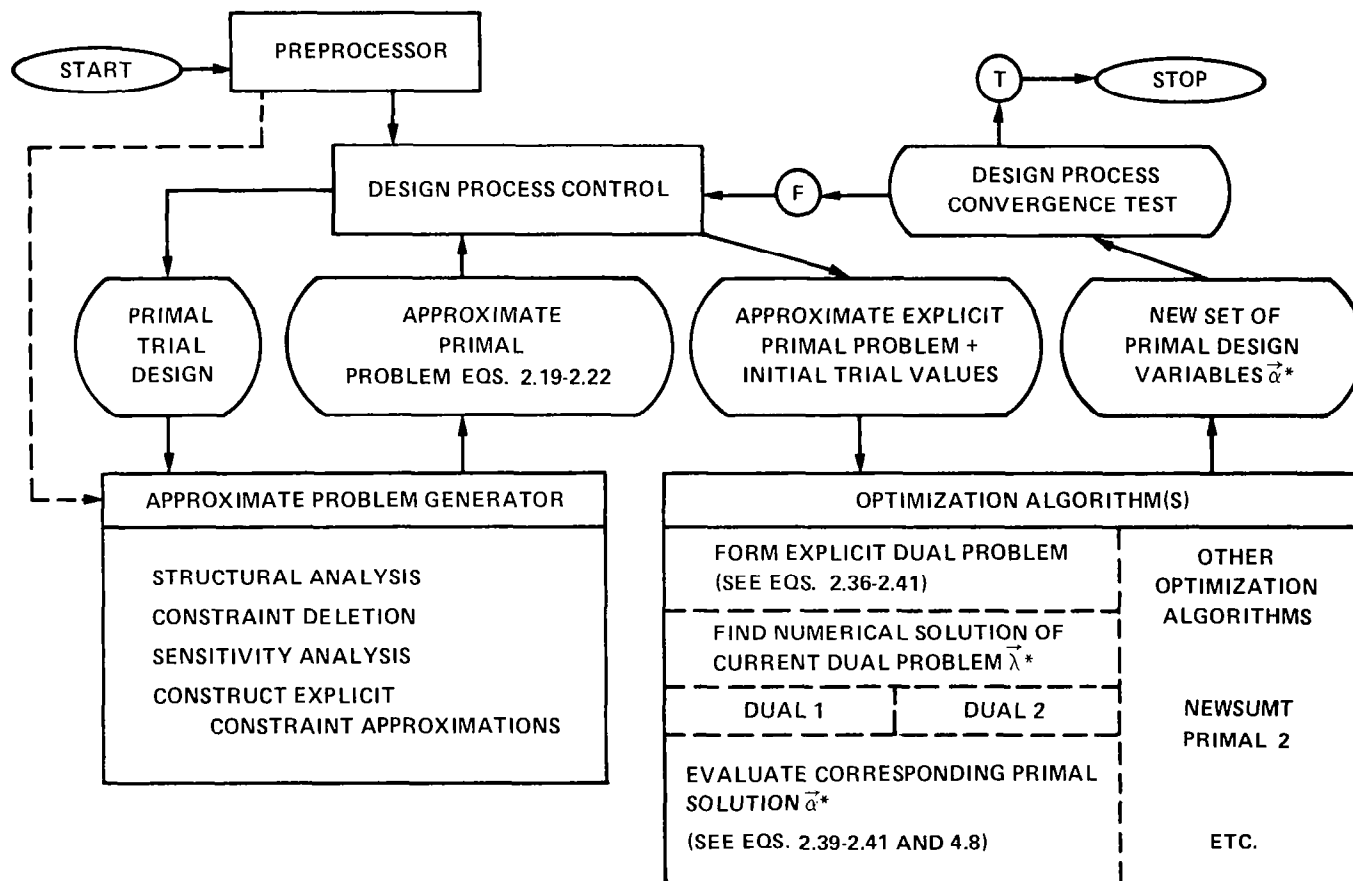


Figure 12. Basic Organization of ACCESS 3.

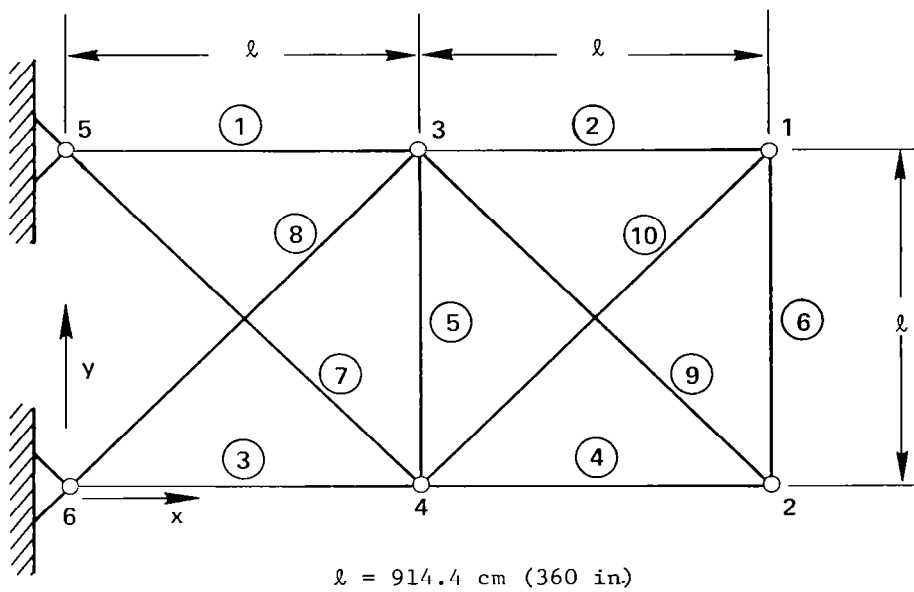


Figure 13. Planar Ten-Bar Cantilever Truss (Problem 1).

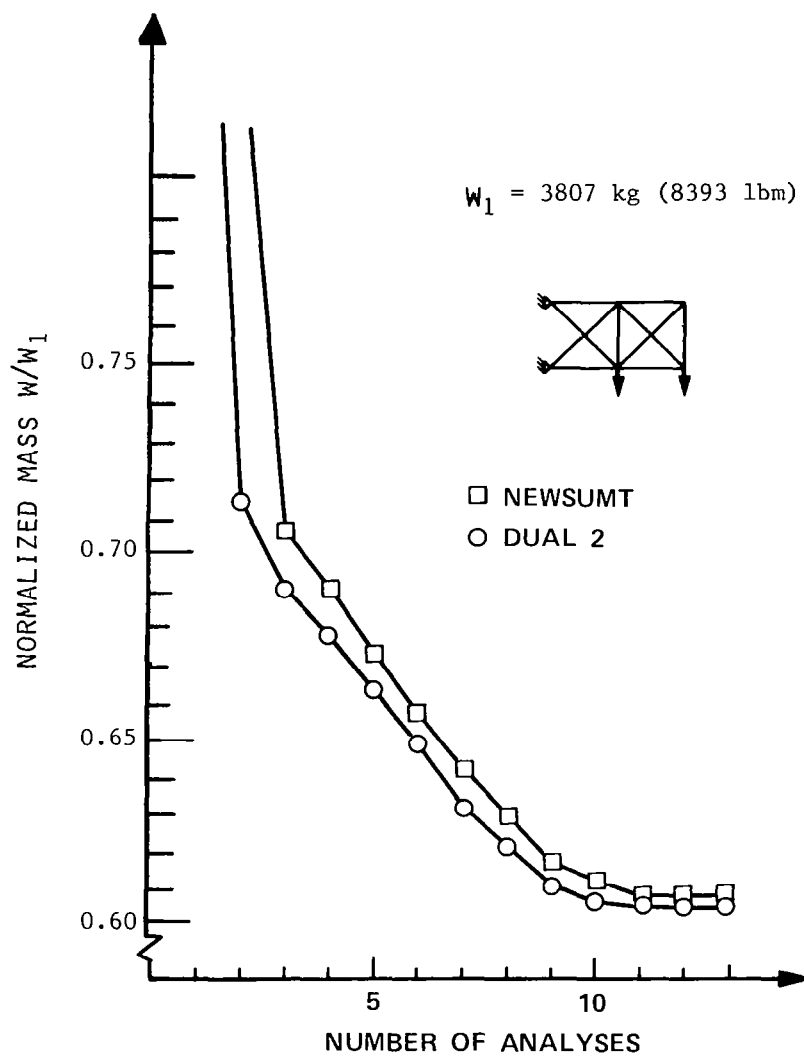


Figure 14. Iteration History for Problem 1 (Case B)
 Ten-Bar Cantilever Truss.

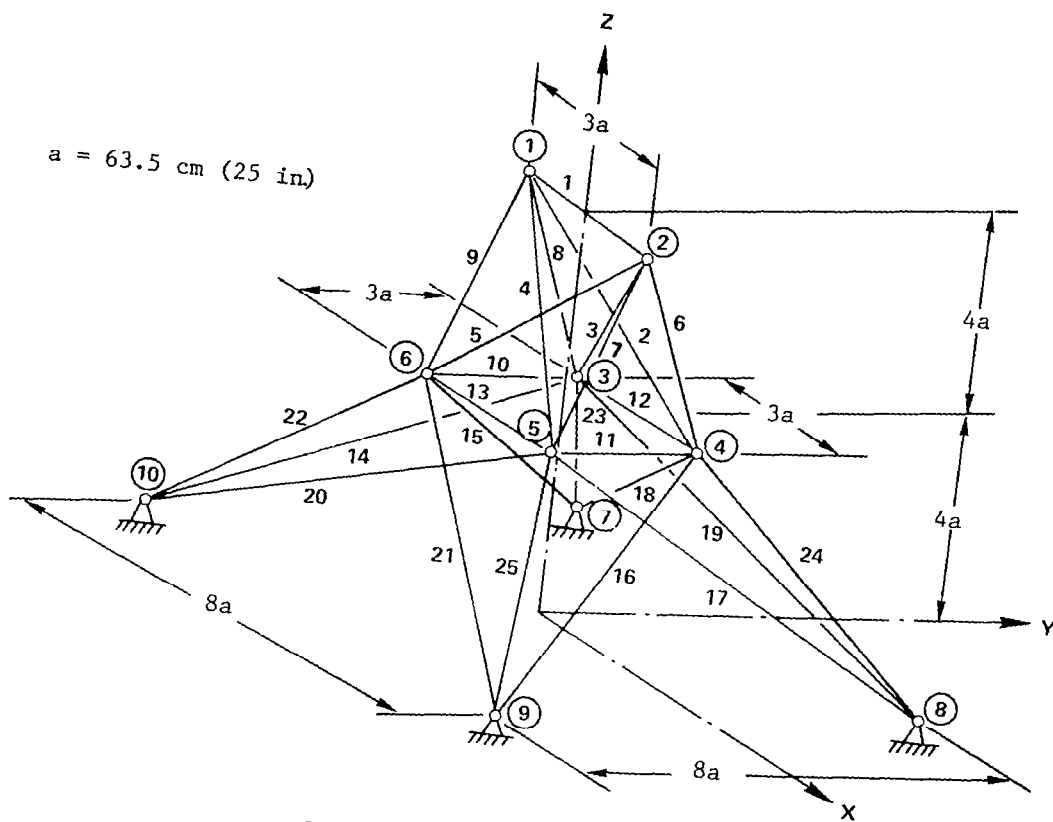


Figure 15. 25-Bar Space Truss (Problem 2).

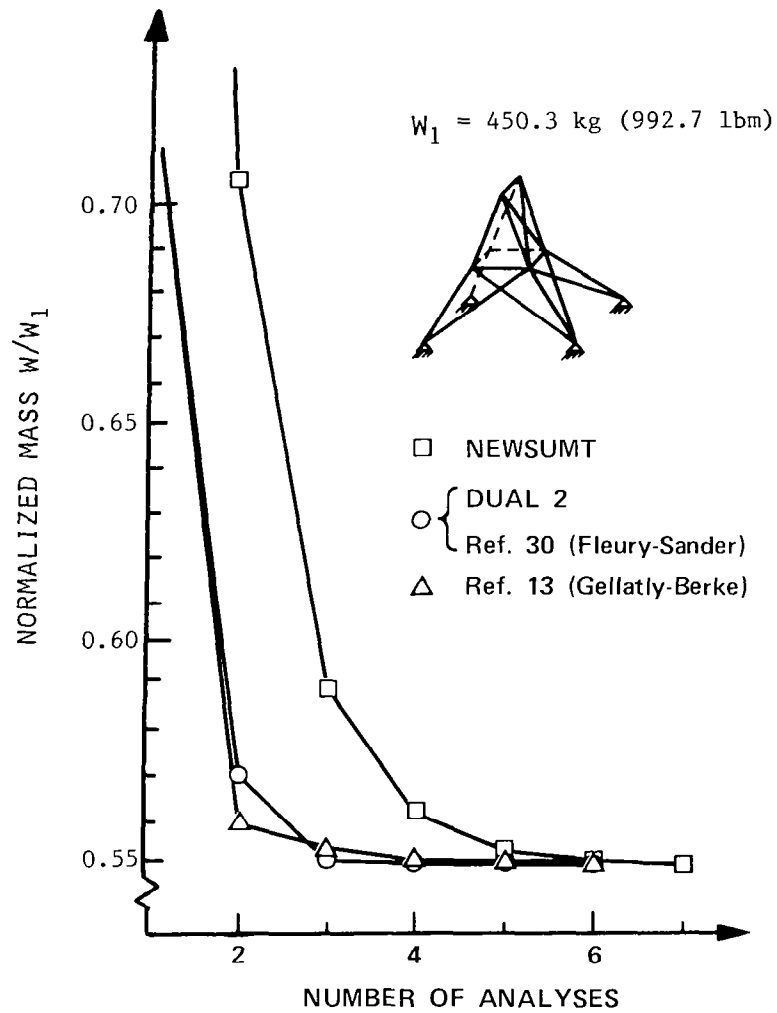
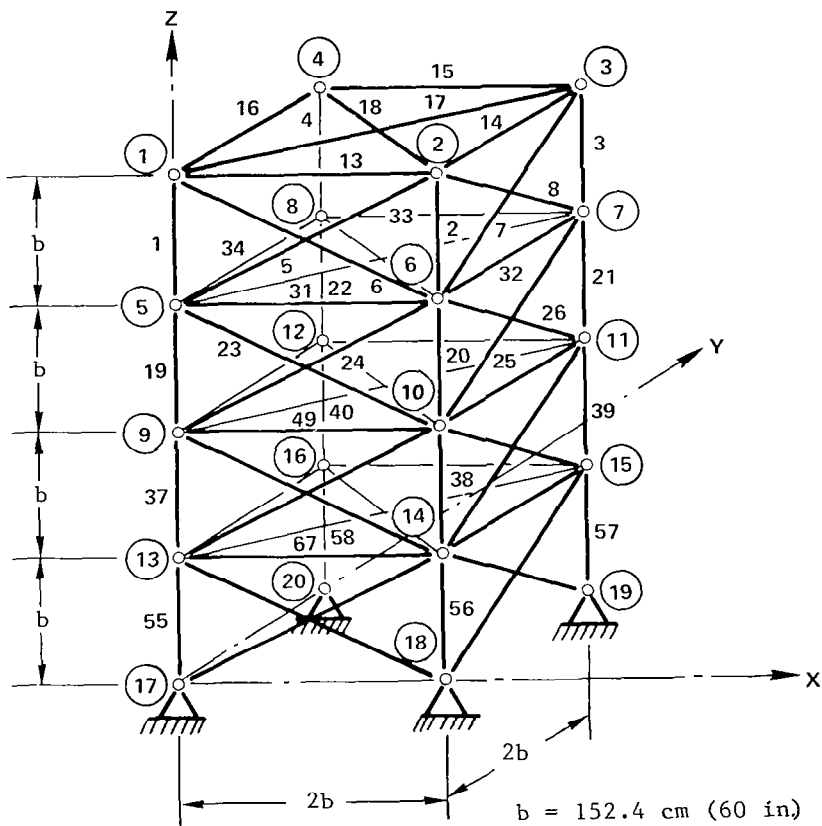


Figure 16. Iteration History for Problem 2 (Case A)
25-Bar Space Truss.



Note: For the sake of clarity, not all elements are drawn in this figure.

Figure 17. 72-Bar Space Truss (Problem 3).

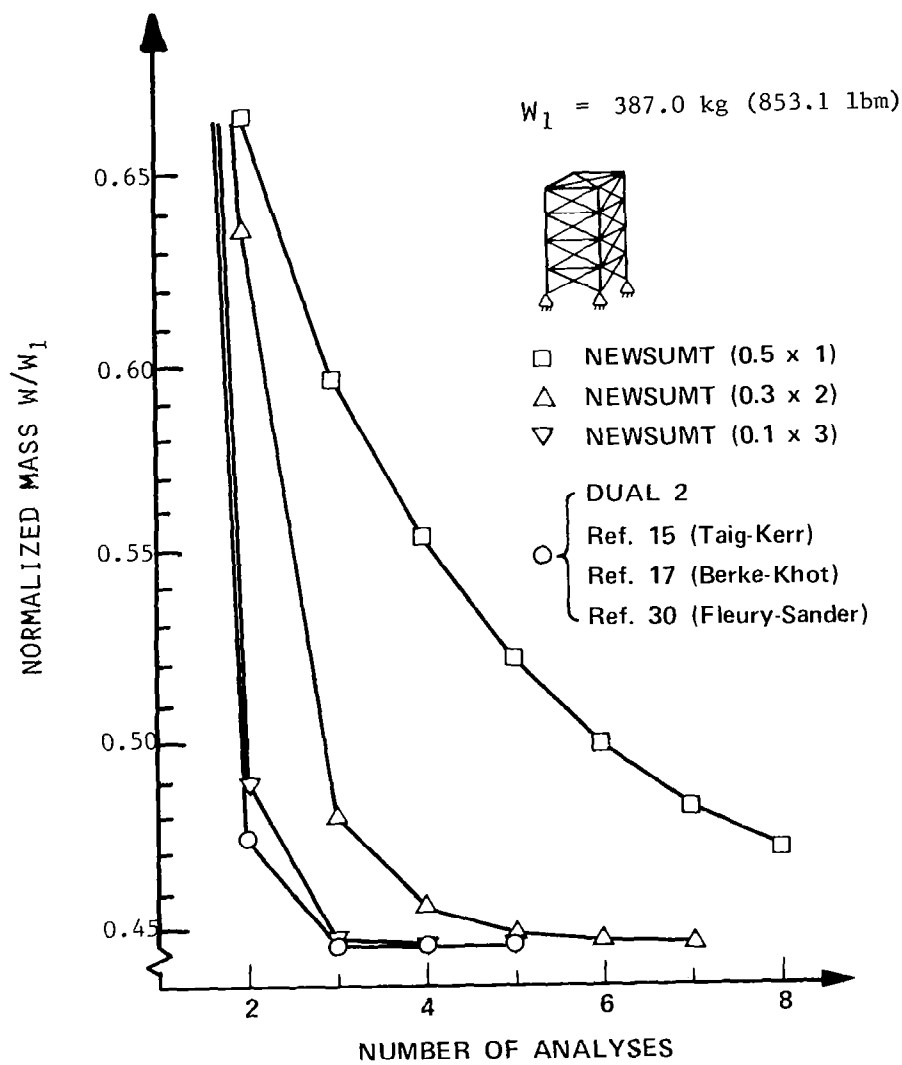
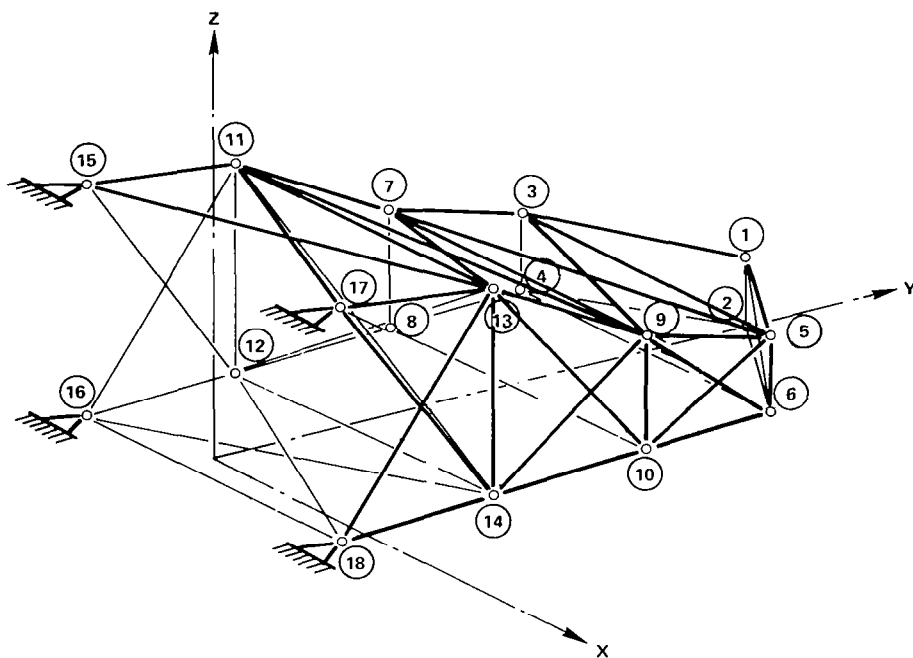


Figure 18. Iteration History for Problem 3
72-Bar Space Truss.



Note: For the sake of clarity, not all elements are drawn in the figure.
[See Table 15 for nodal coordinate data]

Figure 19. 63-Bar Space Truss (Problem 4).

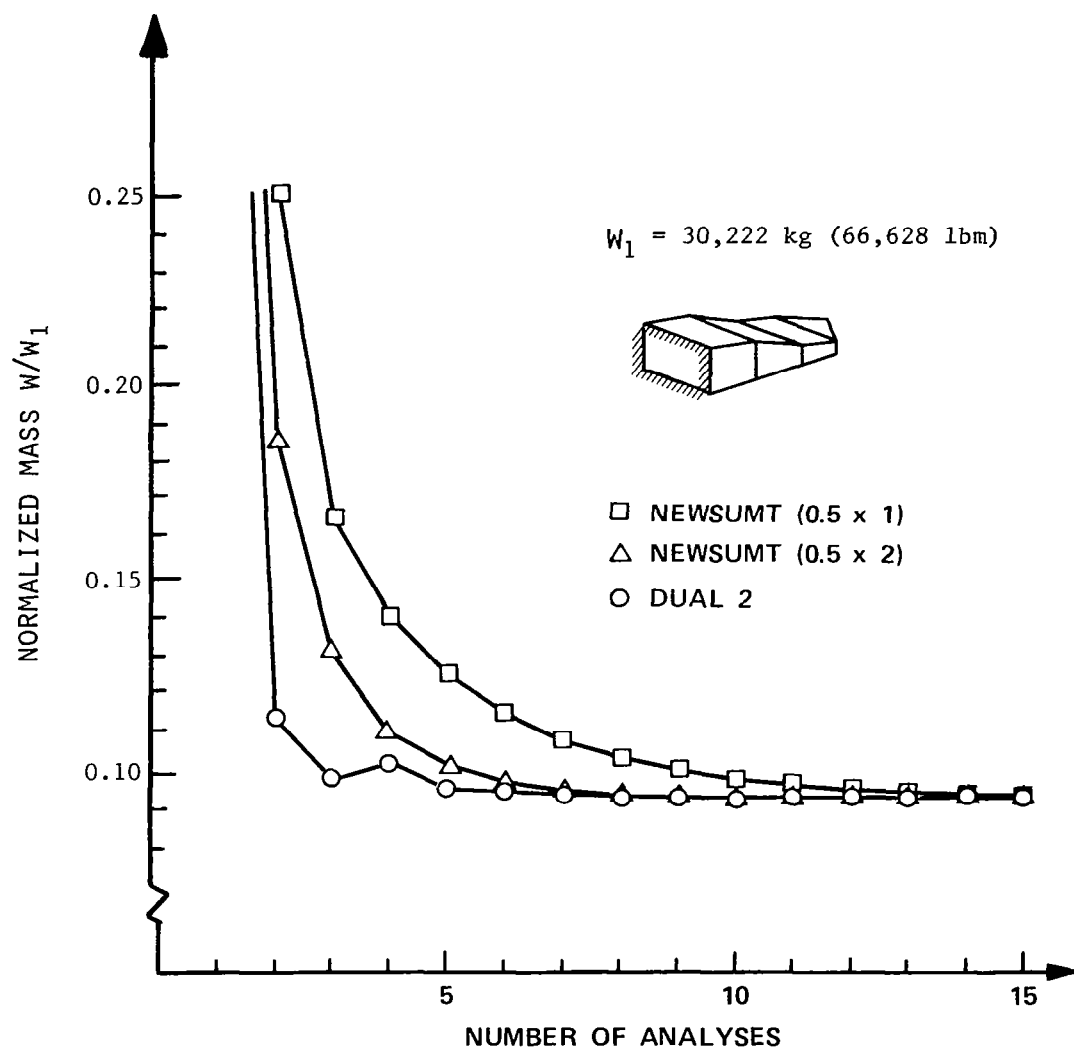


Figure 20. Iteration History for Problem 4
 63-Bar Space Truss.

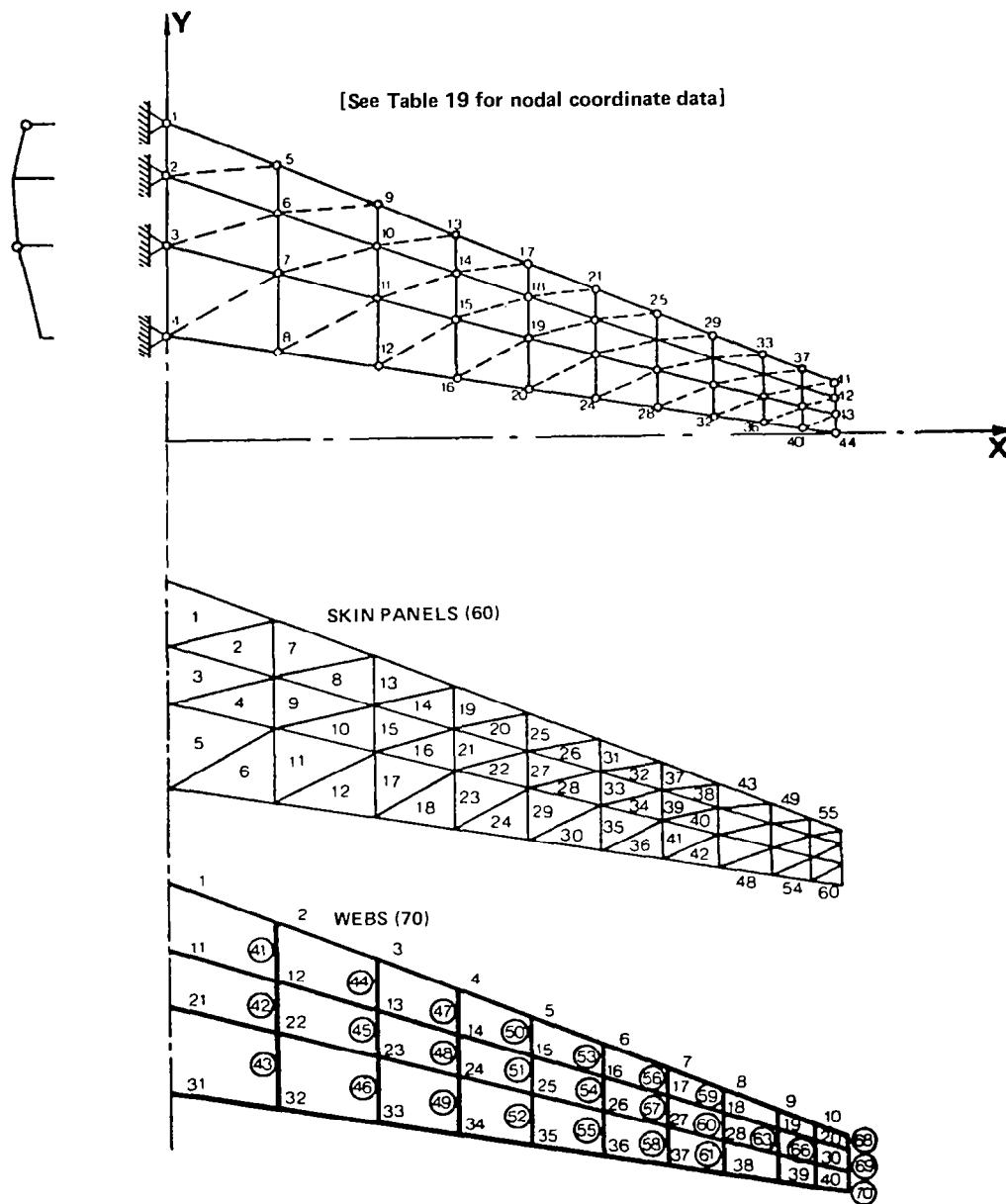


Figure. 21. Swept Wing Analysis Model (Problem 5).

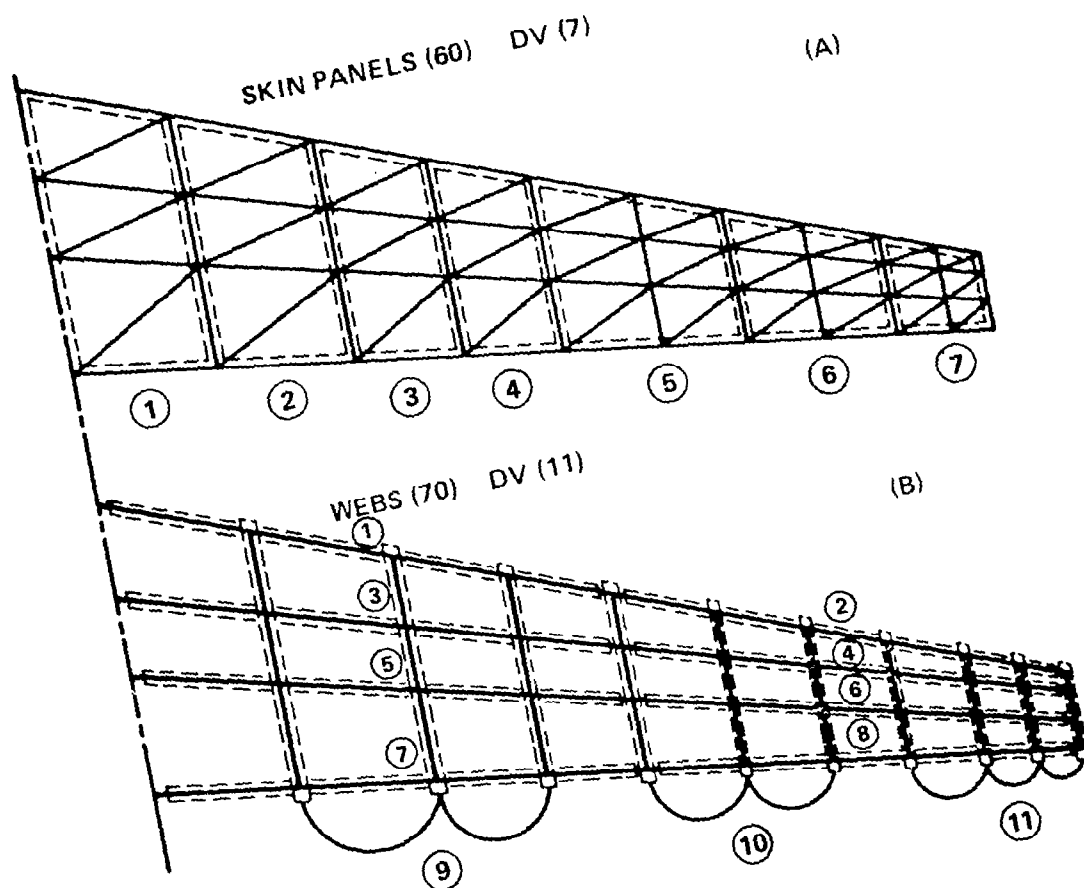


Figure 22. Swept Wing Design Model (Problem 5).

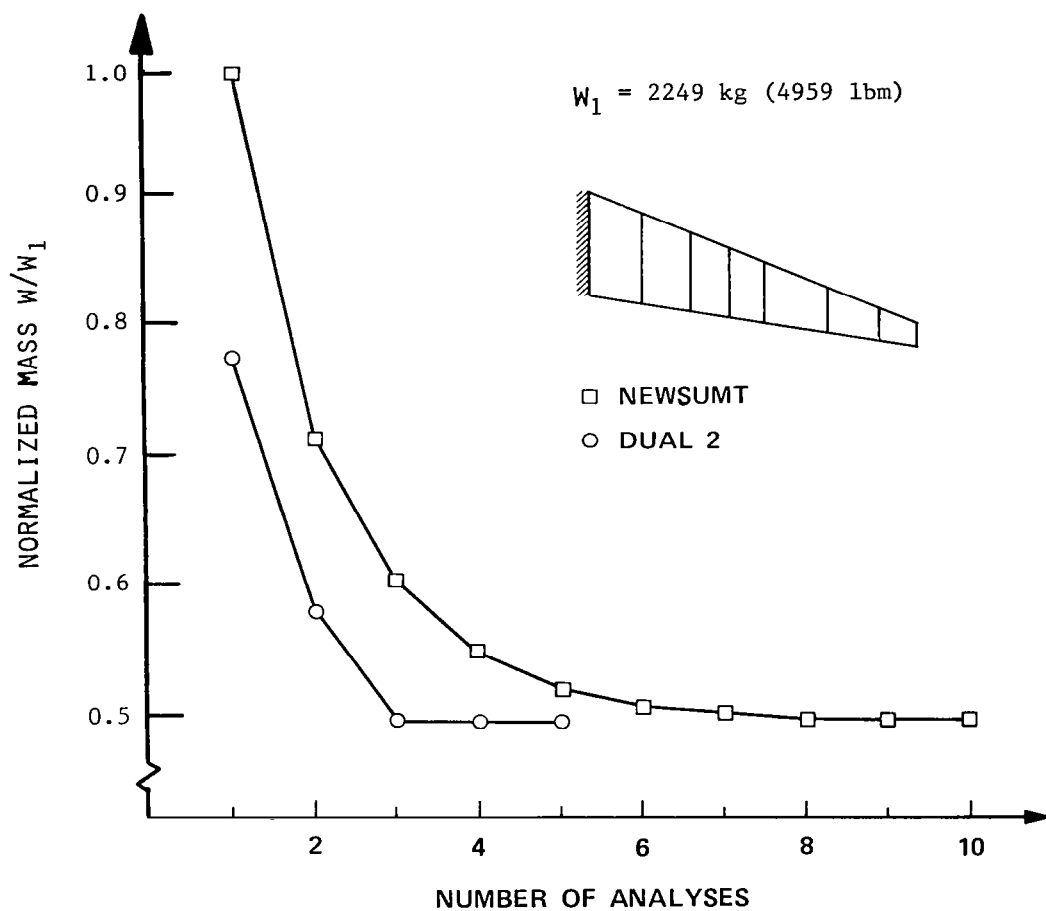


Figure 23. Iteration History for Problem 5
Swept Wing Model.

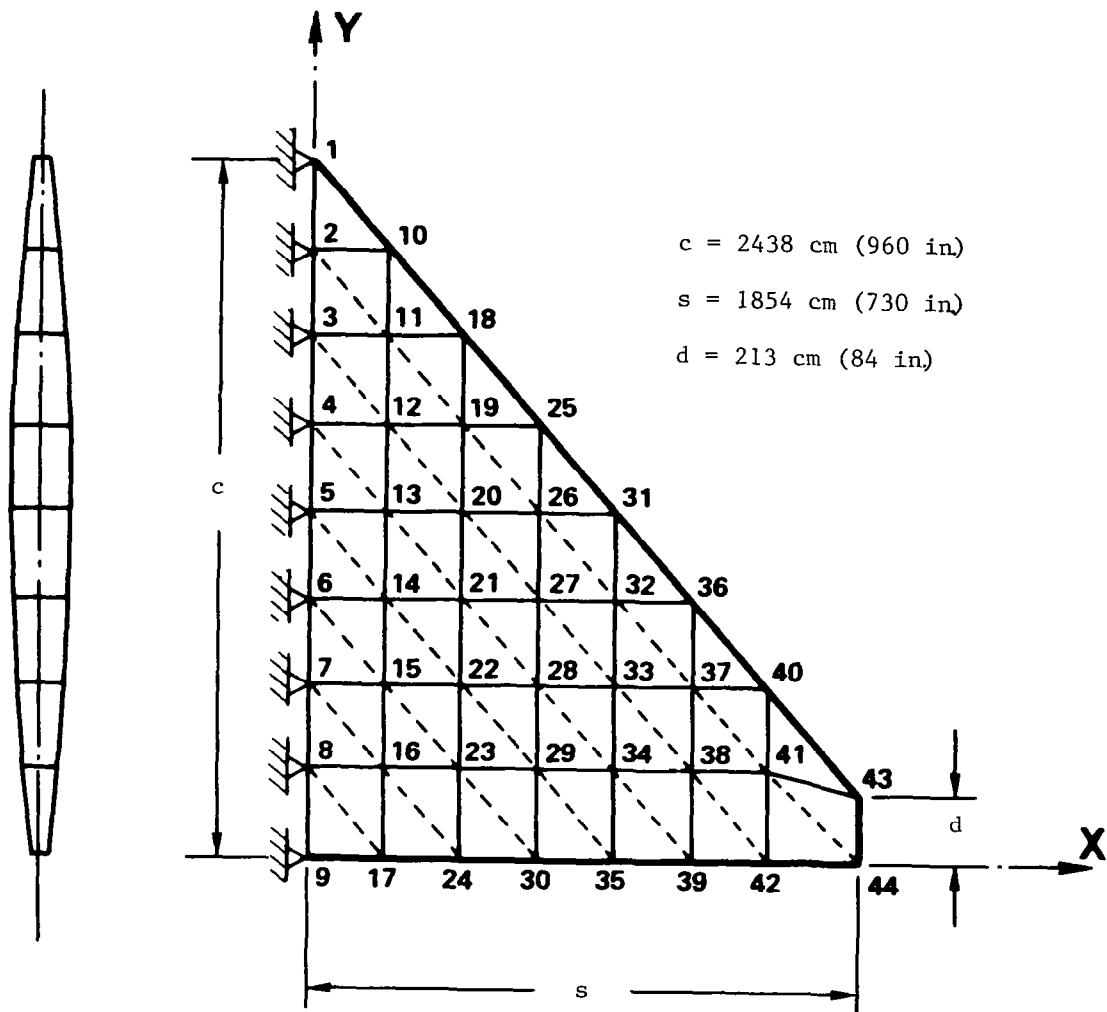


Figure 24. Delta Wing Analysis Model (Problem 6).

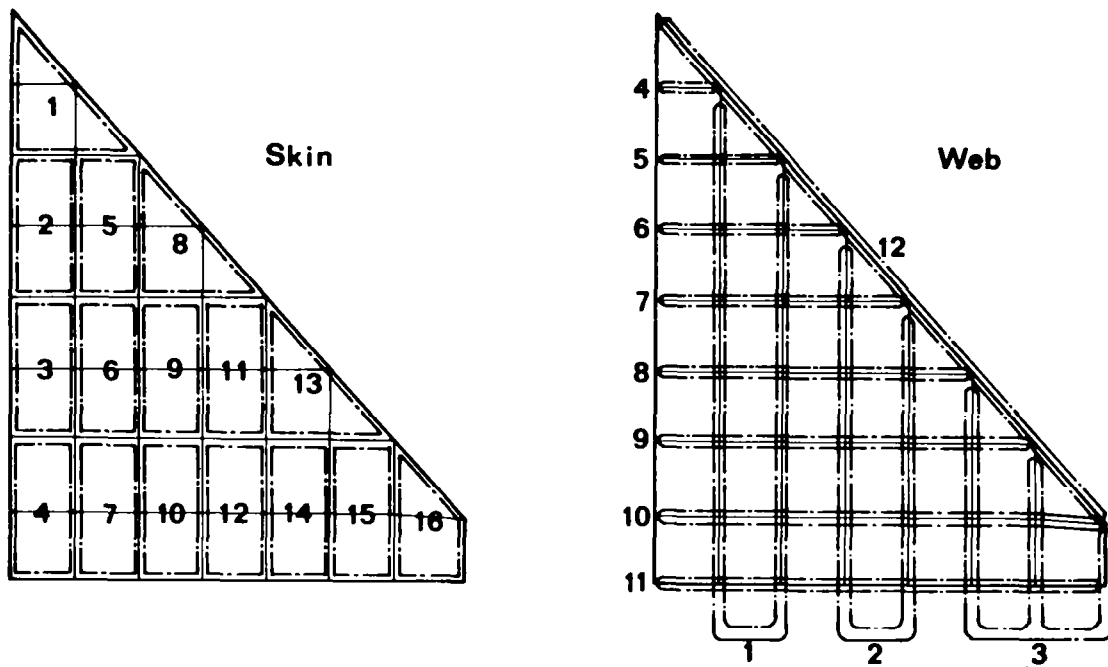


Figure 25. Delta Wing Design Model (Problem 6).

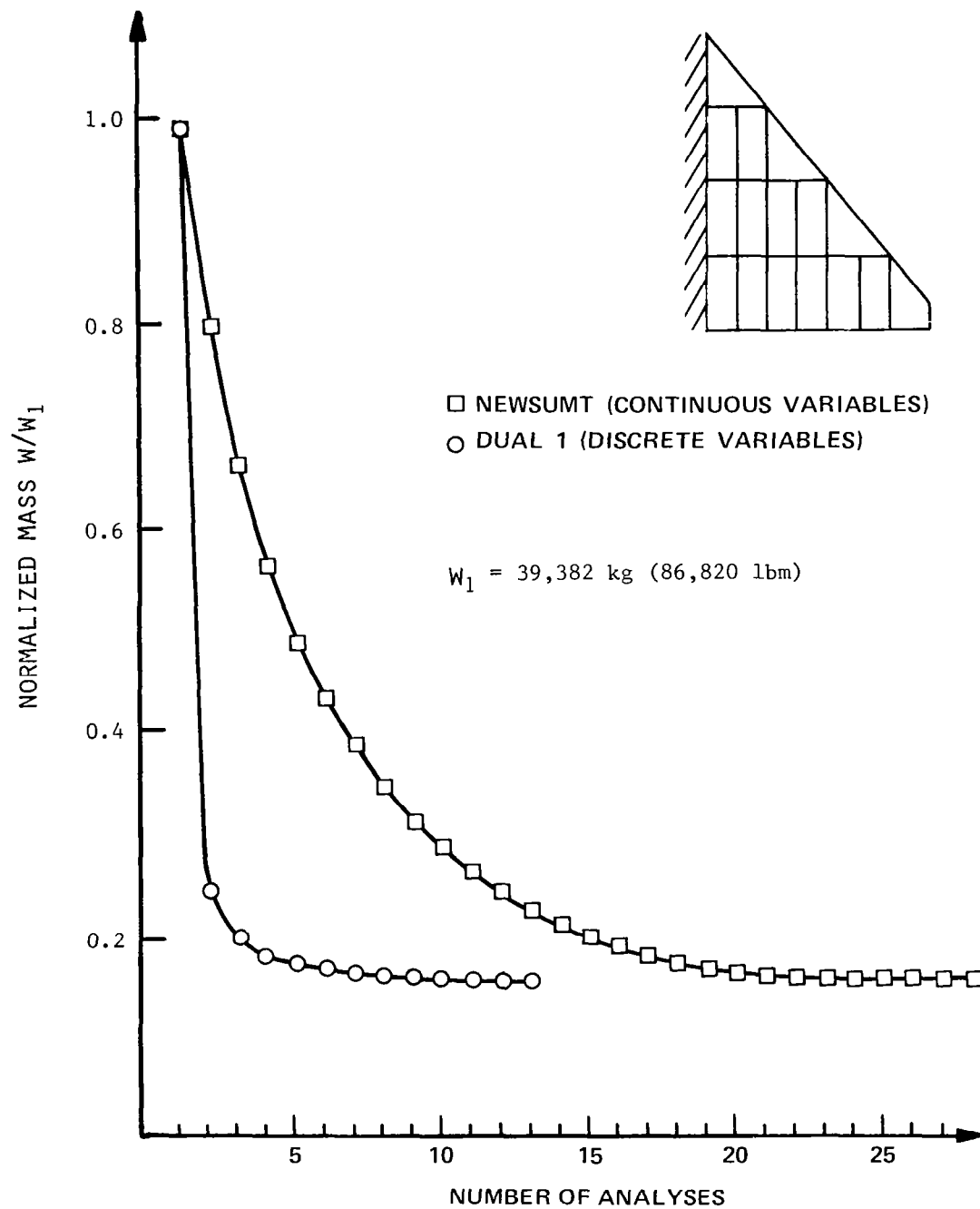


Figure 26. Iteration History for Problem 6
Delta Wing Model.

1. Report No. NASA CR-3226		2. Government Accession No.		3. Recipient's Catalog No.	
4. Title and Subtitle DUAL METHODS AND APPROXIMATION CONCEPTS IN STRUCTURAL SYNTHESIS				5. Report Date December 1980	
				6. Performing Organization Code	
7. Author(s) Claude Fleury and Lucien A. Schmit, Jr.				8. Performing Organization Report No.	
				10. Work Unit No.	
9. Performing Organization Name and Address University of California, Los Angeles Los Angeles, CA 90024				11. Contract or Grant No. NSG-1490	
				13. Type of Report and Period Covered Contractor Report	
12. Sponsoring Agency Name and Address National Aeronautics and Space Administration Washington, DC 20546				14. Sponsoring Agency Code 505-33-63-02	
15. Supplementary Notes Langley Technical Monitor: J. Sobieski Progress Report					
16. Abstract Approximation concepts and dual method algorithms are combined to create a new method for minimum weight design of structural systems. Approximation concepts convert the basic mathematical programming statement of the structural synthesis problem into a sequence of explicit primal problems of separable form. These problems are solved by constructing explicit dual functions, which are maximized subject to nonnegativity constraints on the dual variables. It is shown that the joining together of approximation concepts and dual methods can be viewed as a generalized optimality criteria approach. The dual method is successfully extended to deal with pure discrete and mixed continuous-discrete design variable problems. The power of the method presented is illustrated with numerical results for example problems, including a metallic swept wing and a thin delta wing with fiber composite skins.					
17. Key Words (Suggested by Author(s)) Optimization Structures Numerical methods			18. Distribution Statement Unclassified - Unlimited Subject Category 39		
19. Security Classif. (of this report) Unclassified	20. Security Classif. (of this page) Unclassified	21. No. of Pages 222	22. Price A10		